SAPIENZA
UNIVERSITÀ DI ROMA

MECHANICAL AND AEROSPACE ENGINEERING DEPARTMENT

DOCTORATE OF PHILOSOPHY

IN AERONAUTICAL AND AEROSPACE TECHNOLOGY

Perturbation Methods and Proper Orthogonal Decomposition Analysis for Nonlinear Aeroelastic Systems

PH.D. CANDIDATE:

Marco Eugeni

ADVISOR:

Prof. Franco Mastroddi

Academic Year 2012-2013

[This page intentionally left blank]

I fly a starship across the Universe divide
And when I reach the other side
I'll find a place to rest my spirit if I can
Perhaps I may become a highwayman again
Or I may simply be a single drop of rain
But I will remain
And I'll be back again,
and again and again and again and again...

The Highwayman, Johnny Cash.

Acknowledgements

Abstract

The modern engineering deals with applications of high complexity. From a mathematical point of view such a complexity means a large number of degrees of freedom and nonlinearities in the equations describing the process. To approach this difficult problem there are two levels of simplification. The first level is a physical reduction: the real problem is represented by mathematical models that are treated in order to be studied and their solution computed. At this level we can find all the discretization techniques like Galerkin projection or Finite Element Methods. The second level is a simplification of the original problem in order to study it in an easier way: a reduced order model is advocated.

Simplification means to determine a dominant dynamics which drives the whole problem: not all the unknowns are considered independent being some of them functions of the remaining others. Two methodologies are considered in this a Thesis. The first is the Lie Transform Method based on the results of Normal Form Theory and the Center Manifold Theorem. For some conditions, called resonance or zero divisors, depending on combinations of the eigenvalues of the linearized system, the nonlinearity of the problem is reduced and a driving dynamics determined. The second is the Proper Orthogonal Decomposition (POD), which from the analysis of representative time responses of the original problem determines a subspace of state variables energetically significant spanned by the Proper Orthogonal Modes (POMs).

The main issues related to the Lie Transform Method, as for all the Normal Form based Method, is the presence of small divisors for which there is no general rules to be determined when considering nonconservative systems. In the present work, this problem is considered and some physical parameters are related to such conditions determining qualitatively what *small* means for a divisor relatively to a perturbation parameter.

Moreover, starting from the analytical results obtained the POD behavior in the neighborhood of a bifurcation point has been studied. In particular, POMs has been related to the linearized modes of the studied systems and it has been demonstrated their equivalence for systems experiencing a Hopf bifurcation. Moreover, some conditions of equivalence are addressed also in presence of static bifurcations with forcing loads. Finally, the relation

between modal activation and energy distribution has been studied and the possibility to relate POD behavior and nonlinearity (small divisors) of the response has been addressed.

Contents

v

List of Figures

List of Tables

Introduction

Objection contre la science: ce monde ne mérite pas d'être connu.

Syllogismes de l'amertume, Emil Cioran.

The technological progress requires an increasing complexity of the considered physical model. A deeper physical description is translated in a greater complexity of the mathematical description requiring powerful tools helping to work with nonlinear problems. This need has been illustrated by Von Kármán in a famous lecture at the American Mathematical Society in 1939 (see Ref. [1]) where he stressed the increasing role of mathematics in engineering and physics analysis. In the present Chapter a short overview of the nonlinear aeroelastic problem is given. For more details one can consider the Refs. [2, 3, 4].

General issues on Aeroelasticity

The term Aeroelasticity denotes the field of study concerning the interaction between the deformation of an elastic structure in a flow and the resulting aerodynamic forces. The evident multidisciplinary nature of this field can be illustrated by the Collar's triangle, Fig. 1, where it is evident that the aeroelasticity is the mutual interaction between inertial, elastic and aerodynamic forces. Generally, two categories of phenomena can be distinguished:

1. Static aeroelastic phenomena that lies outside the triangle.

2. Dynamic aeroelastic phenomena that lies within the triangle involving elastic, aerodynamic and inertial forces.

Finally, being the aeroelastic phenomena the consequence of the mutual interaction between an elastic structure and a flow, it is evident that the problem will depend, generally, on some parameters governing the state of the flow such as its unperturbed velocity or the Mach number. This parameters govern the behavior of the system influencing the stability of its solutions bringing the equilibrium from a stable condition to an unstable one. The instability phenomena are either dynamical or static:
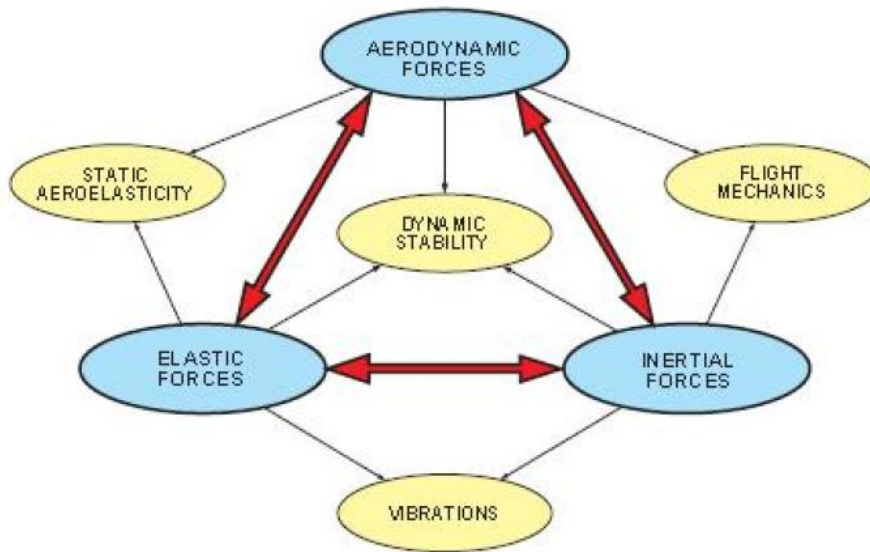
Figure 1: Collar's triangle

1. Static instability: divergence. It involves only static aerodynamics forces and elastic forces. From a mathematical point of view, it occurs when a real pole crosses the imaginary axis of the complex plane (it become positive from being negative), see Fig. 2(a).

2. Dynamical instability: flutter. It involves inertial, aerodynamical and elastic forces. From a mathematical point of view, it occurs when a pair of complex conjugate poles cross the imaginary axis of the complex plane, see Fig. 2(b), so that their real part become positive.

The first documented aeroelastic instability happened in 1916, when a bomber Handley PAGE O/400 experienced great oscillation of the tail oscillations, whereas it is famous the Tacoma bridge collapse in 1940. The studies about nonlinear effects in the aeroelastic field started in the '50s with the development of supersonic aircraft and the observation of the so called *panel flutter* phenomenon. The preloaded panels at a certain speed and altitude started to experience strong oscillation with consequent problems in the mission accomplishment (see Refs. [5] and [6]).

(a)   (b)
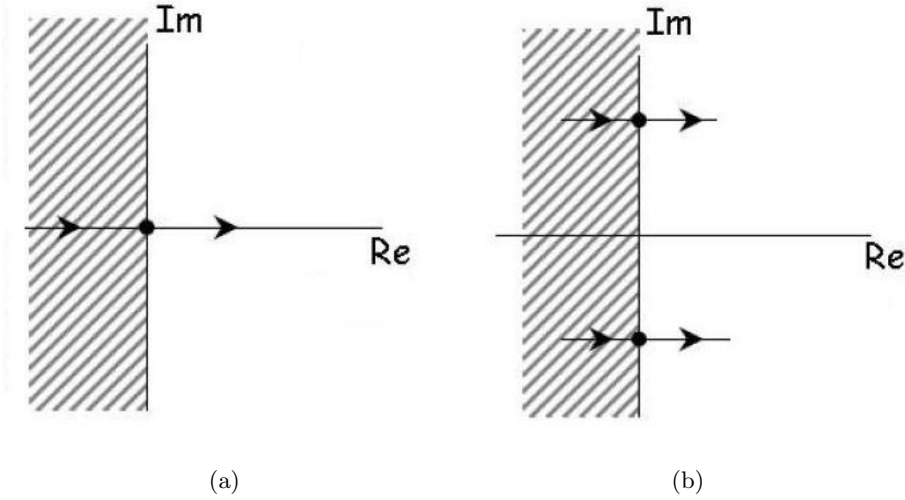
Figure 2: Spectrum behavior in presence of divergence or flutter instability phenomenum

The general formulation of the aeroelastic problem

From the mathematical point of view, the fluid-structure interaction originates from the boundary conditions that the body applies to the flow: the aerodynamic forces deform the body which will modify their self. Initially, the problem is governed by the continuum mechanics equation for fluid and solid with boundary condition at the infinity and at the border between the two different continuum types. Such conditions will be kinematic for the flow and on the surface forces for the body (see Ref. [7]). Using suitable techniques, it is possible to discretize the original partial differential equations system (see Refs. [8, 7]) to obtain, in general, a system of integro-differential equations that can be reduced increasing the state space to a system of ordinary differential equations (for more details see Ref. [2], [7] and [9]).

The general nonlinear aeroelastic problem can be written in the following form

$$\mathsf{M\ddot{y} + C\dot{y} + Ly + F(y, \dot{y}) = 0} \tag{1}$$

where the unknown vector y represent the set of generalized displacement and aerodynamic states. Observe that the problem structure given by Eq. 1 can be considered valid in both the space-continuum and space-discretized cases. The differences will be on the definitions of the operators and the problem domains. Formally, Equation 1 is analogous to the one of structural problem, but the nature of the operators is strongly different. Indeed, because of the presence of the aerodynamic terms the aeroelastic operators are no longer self-adjoint. The expression given by Eq. 1 is written in the space of generalized displacement. Sometimes it is suitable to consider the dynamics in the phase-space, where it is possible a geometric

3

interpretation of the motion:

$$\begin{cases} \dot{\mathsf{x}} = \mathcal{F}(\mathsf{x}) \\ \mathsf{x}(0) = \mathsf{x}_0 \end{cases} \tag{2}$$

where x is the vector of generalized displacement and velocities.

Comments on linear and nonlinear analysis for aeroelastic response

Real physical phenomena, as the fluid/structure interaction, are nonlinear, have an infinite number of degrees of freedom, and are governed by an infinite number of parameters (Ref. [5]). This complexity requires simplifications in order to be studied. The first step involves the definition of a mathematical model of the problem of interest: the number of degrees of freedom and parameters is reduced and fixed. Next, the obtained mathematical model is analyzed by the most suitable tools. In general, this means to cast it in canonical form (see Ref. [5, 4, 10, 11, 12, 13, 14, 15]), such as:

$$\dot{\mathsf{x}} = \mathcal{F}_U(\mathsf{x}) \tag{3}$$

where $\mathcal{F}$ is a generically nonlinear function of x and its parametric dependence from the generic flow parameter U is emphasized and $\dot{()}$ denotes differentiation with time. Equation 3 might possess an equilibrium solution $\hat{\mathsf{x}}$, that can be found for a fixed value of U such that:

$$\mathcal{F}_U(\hat{\mathsf{x}}) = 0 \tag{4}$$

The linearized dynamics in the proximity of $\hat{\mathsf{x}}$ can be studied by first rewriting Eq. 3 as:

$$\dot{\mathsf{x}} = \mathsf{A}(\mathsf{x} - \hat{\mathsf{x}}) + HOT \quad \text{with} \mathsf{A} := D\mathcal{F}(\mathsf{x})|_{\mathsf{x}=\hat{\mathsf{x}}} \tag{5}$$

and next by neglecting the contribution of higher order terms (HOT). Thus, three level of dynamical model fidelity can be considered (with decreasing fidelity order):

- **Fully nonlinear description**. It consists of considering the aeroelasitic model defined by Eq. 3 (including structural as well aerodynamic nonlinear description) to be numerically solved by direct time domain simulation.

- **Statically** nonlinear and **dynamically** linear description. The static solution $\hat{\mathsf{x}}$ is evaluated taking into account all the nonlinear effects in Eq. 5 and then by studying the linearized dynamics in the neighborhood of the equilibrium solution as given by Eq. 5 without the HOT.

- **Statically** linear and **dynamically** linear description. The static solution is evaluated avoiding to take into account the nonlinear part of $\mathcal{F}_U$. Moreover, the dynamics around such a fixed point is studied only by the linear part of Eq. 5.

Dealing with complexity

The nonlinear description of aeroelasticity requires a large computational effort in order to be studied. To deal with this complex problem in this work two different approaches are considered: a Normal Form based method (such as the considered Lie Transform Method) and the Proper Orthogonal Decomposition. The basic ideas of both methods is the identification of a fundamental dynamics (a dominant subset of whole system parameters) driving the whole process. The Normal Form obtain such a "core" dynamics via some conditions, called resonances or zero-divisors, which are related to the linearized systems in the neighborhood of the considered equilibrium (see Refs. [16, 17, 18, 19, 20]). The Proper Orthogonal Decomposition working on the time-response of the systems determines the most "energetic" basis of representation of the problem: this means that the non-energetic components can be disregarded and considered slaved to the components. In the following, some historical and bibliographic remarks are given about the cited topics.

Perturbation Methods

As shown previously the aeroelastic dynamics is usually represented by a set of equations depending on one or more parameters. This means that the study of the dynamics and in particular of the stability properties of the solutions depends on such parameters is crucial. In particular, when some "control parameter" crosses a critical value in Eq. 3, then the fixed equilibrium solution can lose its stability properties and new stable solutions arise. This phenomenon, from a mathematical point of view, corresponds to a driving dynamics associated to the unstable eigenvalues of the linearized systems (see Chapter 1.5) and a *perturbation approach* based on the idea of building the new solution as the old one plus a small correction appear a suitable mathematical tools. This means to consider the solution of the form $x(t) = x_e + \epsilon x_1 + o(\epsilon)$ where ϵ is a small parameter called perturbation parameter and the convergence is guarantee to x_e for $\epsilon \to 0$.

This method is a member of the family of "averaging" method (see Refs. [21, 22, 23]). In this Thesis, the considered method will be based on the Lie Transform (see Secs. 1.5 and 2 and Refs. [24, 25, 26]), which gives the possibility of analyze in the most direct way the dynamics showing the inner mathematical process that brings to some interesting behavior.

From a mathematical point of view, a direct perturbation methods (*regular perturbation methods*) deals with the problem of *secular terms* by the form $t \sin \omega t$ causing the explosion of the solution,*i.e.*, $\epsilon x_1 = O(x_e)$. This can be avoided by considering *singular perturbation methods* (see Refs. [27, 28, 29, 27]), where some procedure are introduced in order to avoid secular terms.

Specifically, the Lie Transform Method looks for a coordinates transformation that yields

to a simpler form of the original problem. It will be shown that this transformation is related to the presence of some zero-divisors condition (see Chapters 1.5 and 2), which are equivalent to avoid the presence of secular terms (see Refs. [28, 29, 30]). The obtained transformed systems gives a simpler dynamics that can be studied in an easier way with respect to the original problem. Moreover, having analytical expression of the solution allows us to gain interesting information about its behavior, as described in Chapters 5 and App. A.

Proper Orthogonal Decomposition

The Proper Orthogonal Decomposition, also known as Principal Component Analysis, is a powerful multivariate statistical method which has been widely used in engineering areas to capture the dominant components or modes of a dynamical system. This method can be applied to extract the dimension information from an embedded attractor (see Refs. [31, 32]) or to identify subspaces (modes) to which orbits, *i.e.*, the system responses, are constrained, see Refs. [33, 34, 35]. Originally, this method has been applied in the engineering area of turbulent flow analysis by Holmes, et al., in Ref. [36], where it has been used to extract coherent structures from turbulent velocity fields. In structural vibration areas, POD is used to relate the Proper Orthogonal Modes (POMs) to the Linear Modes (LMs), see Ref [37, 38, 39, 40].

The Proper Orthogonal Modes form an orthogonal basis, and this means that the possibility to identify some intrinsic features of the observed dynamics, as LMs, are related to the nature of such a geometry. In particular, if a systems is characterized by nonorthogonal eigen-dynamics, as a highly damped system or an aeroelastic system, there is no possibility to identify the full intrinsic geometry. Otherwise, it is possible to identify the dominant part of the intrinsic geometry as the one where the greatest part of the response is embedded.

In nonlinear dynamics, the LMs have still a relevant role being the tangent space at the equilibrium point to the invariant manifold. Moreover, via POD is still possible to identify the dimension of the considered attractors (see Ref. [31]) and then to reduce the order of the original problem in order to study a lower dimensional dynamics. In Chapter 4, it will be shown that in presence of a Hopf bifurcation, the POMs description and the LMs description are equivalent (see Ref. [41]). Moreover, some conditions of equivalence in presence of static bifurcation with forcing loads are given. In Chapter A the effect of modal discretization on the energy distribution is studied.

Outline of the Thesis

This Thesis describes the outcome of a three year period of research and study. It consists of a sinthesis among the publications and congress acts produced by the author with his advisor Prof. Franco Mastroddi, and of the outcome of his visiting period at Duke University with the research group of Prof. Earl H. Dowell. The core of the work is the study of behavior of the Proper Orthogonal Decomposition analysis when a nonlinear response are considered and the system is characterized by a non-orthogonal geometry. Indeed, in presence of a non-self adjoint operator (like in presence of fluid/structure interaction) the eigenvectors are no longer real and no longer orthogonal and the relation between eigengeometry and POD objects is no longer straightforward as in presence of self adjoint systems which are well analyzed in literature (see Ref. [40, 38]). Moreover, attention is given to the search of analytical solutions with perturbation methods and the problem of small divisors considered. This document can be divided in three parts:

1. The behavior of nonlinear systems is presented together with some tools of analysis, and in particular the Normal Form method based on the Lie Transform is presented together with the problem of small and zero divisors, a key issue in the study of systems' integrability. Moreover, the eigengeometry of systems characterized by imaginary eigenvectors and eigenvalues is presented.

2. The Lie Transform method is applied in order to obtain analytical solutions for nonlinear systems experiencing a bifurcation of equilibrium in presence of forcing loads. This example give the possibility to analyze the ideas of zero and small divisors giving also a qualitative measure of the term *small* with respect to the perturbation parameter.

3. The Proper Orthogonal Decomposition method and its relation with Linearized Modes is studied via the analytical results obtained by the Lie Transform method. In particular, some conditions of equivalence between Linearized Modes and Proper Orthogonal Modes are obtained. Moreover, the possibility of using POD as a nonlinearity measure is addressed. Finally, a study of the effect of the modal decomposition on the energy distribution is given.

Part I

Nonlinear Dynamics: General Issues

Chapter 1

General issues on dynamical systems

Some issues on the theory of differential equations from the viewpoint of the local geometrical approach are presented following the approach proposed by Holmes and Guckenheimer in Ref. [42]. For a detailed analysis one can refer to Hirsch and Smale in Ref. [43] and Arnold in Ref. [44]. In particular, the basic properties of autonomous systems of ordinary differential equations are considered with particular attention to the geometrical interpretation of the dynamics in the phase space.

1.1 Existence and Uniqueness of Solutions

Let us consider system of differential equations of the form:

$$\frac{d\mathsf{x}}{dt} := \dot{\mathsf{x}} = \mathcal{F}(\mathsf{x}) \tag{1.1}$$

where $\mathsf{x} = \mathsf{x}(t) \in \mathbb{R}^N$ is a vector valued function of an independent variable (usually the time) and $\mathcal{F} : U \to \mathbb{R}^N$ is a smooth function defined on some subset $U \subseteq \mathbb{R}^N$. In the following, we will say that the *vector field* $\mathcal{F}$ generates the *flow* $\phi_t : U \to \mathbb{R}^N$, where $\phi_t(\mathsf{x}) = \phi(\mathsf{x}, t)$ is a smooth function defined for all x in U and $t \in (a, b) \subseteq \mathbb{R}$ and ϕ is said to satisfies Eq. 1.1 in the sense that:

$$\frac{d}{dt} \left(\phi(\mathsf{x}, t) \right) |_{t=\tau} = \mathcal{F}(\phi(\mathsf{x}, \tau)) \quad \forall \mathsf{x} \in U, \ \ \tau \in I \tag{1.2}$$

It is relevant to note that the flow satisfies the group properties:

$$\begin{aligned} \phi_0 &= \mathsf{I} \\ \phi_{t+s} &= \phi_t \circ \phi_s \end{aligned} \tag{1.3}$$

Systems of the above form where the time do not appear explicitly are called *autonomous*. One of the more interesting features of the dynamical systems in the phase-space is the possibility to study their behavior through geometry. Indeed, their solutions will represent curves in the general N-dimensional space where the problem is defined. If one consider an initial condition for Eq. 1.1

$$\mathsf{x}(0) = \mathsf{x}_0 \in U \tag{1.4}$$

which means to seek a solution $\phi(\mathsf{x}_0, t)$ such that

$$\phi(\mathsf{x}_0, 0) = \mathsf{x}_0 \tag{1.5}$$

it is possible to interpret a solution of Eq. 1.1 as a trajectory, or orbit in the phase-space based on x_0 defined by the function $\phi(\mathsf{x}_0, \cdot) : I \to \mathbb{R}^N$. In the differential equations systems properties study, it is interesting to consider family of such curves more than a single one and hence to study the global behavior of the flow $\phi_t : U \to \mathbb{R}^N$ defined for all points $\mathsf{x} \in U$. In the following, it will be introduced, in particular, the concept of invariant spaces and manifolds composed of solution curves (see Refs. [42, 44, 45]). From the above consideration, it is possible to consider Eq. 1.1 as an application which maps the points of U in points of the Euclidean space $\mathbb{R}^N$. Particular importance have the subsets of initial conditions which are characterized by invariance with respect to the vector field generating the flow.

Before to start the analysis, it is important to analyze under which hypotheses the existence and the uniqueness of solution is guarantee:

Theorem of existence and uniqueness 1.1.1 *Let $U \subseteq \mathbb{R}^N$ be an open subset of real Euclidean space (or of a differentiable manifold M), let $\mathcal{F} :\to \mathbb{R}^N$ be a continuously differentiable map and let $\mathsf{x}_0 \in U$. Then there is some constant $c > 0$ and a unique solution $\phi(\mathsf{x}_0, \cdot) : (-c, c) \to U$ satisfying the differential equation $\dot{\mathsf{x}} = \mathcal{F}(\mathsf{x})$ with initial condition $\mathsf{x}(0) = \mathsf{x}_0$.*

Observe, that in general the above Theorem ensures the existence of a solution only for a finite time: it is only local.

Important class of solutions of a differential equation are the so called *Fixed Points* or *Zeroes*. Indeed, from a practical point of view, they represent reference configuration of the studied problem modeled as a system of differential equations. An equilibrium solution of Eq. 1.1 is such that:

$$\begin{cases} \mathsf{x} = \mathsf{x}_e \\ \mathcal{F}(\mathsf{x}_e) = 0 \end{cases} \tag{1.6}$$

From Equation 1.6 it is given that the zeroes of the vector fields represent fixed point in the phase-space. For a given initial condition, the state will either converge to an equilibrium

point (asymptotic stability) or remain in a neighborhood of it depending on the initial condition (simple stability), or will leave indefinitely the equilibrium (instability) (see Ref. [43]).

1.2 Linear Systems

Let us consider a linear dynamical system whose vector field in Eq. 1.1 is defined as $f(x) = Ax$, $x \in \mathbb{R}^n$, which can be rewritten as

$$\frac{d\mathsf{x}}{dt} = \mathsf{A}\mathsf{x} \quad \forall \mathsf{x} \in \mathbb{R}^N \tag{1.7}$$

where A is a $N \times N$ matrix with constant coefficients. Together with Eq. 1.7 one has to consider the initial condition $\mathsf{x}(0) = \mathsf{x}_0$, thus the solution of the problem given by Eq. 1.7 is the flow $\phi_t(\mathsf{x}_0) = \mathsf{x}(\mathsf{x}_0, t)$. Note, that the existence and uniqueness Theorem guarantees that such a unique solution will hold at all the times, things that is not always true for general nonlinear systems where a global existence of solutions can not be guaranteed.

It can be demonstrated (see Refs. [42, 43]) that the solution of Eq. 1.7 is

$$\mathsf{x}(\mathsf{x}_0, t) = e^{t\mathsf{A}}\mathsf{x}_0 \tag{1.8}$$

where $e^{t\mathsf{A}}$ is the $N \times N$ matrix obtained by exponentiating A. For our purpose in the study of differential systems is more convenient to seek for a solution obtained by linear superposition of N linearly independent solutions $\{\mathsf{x}^i(t)\}$:

$$\mathsf{x}(t) = \sum_{j=1}^{N} c_j \mathsf{x}^j(t) \tag{1.9}$$

where the "weight" c_j are determined by the initial conditions.

Equation 1.11 introduces the idea that the dynamics of a linear system can be decomposed in the sum of motions in some subset of $\mathbb{R}^N$. In particular, it is convenient to choose these sub-sets so that they are invariant with respect to A. This means that every element of such invariant subset is a solution of the formal problem:

$$\mathsf{A}\mathsf{v} = \lambda\mathsf{v} \tag{1.10}$$

where the solutions $\mathsf{v}^i \in \mathbb{C}^N$ are called the eigenvectors of A whereas the associated number λ_i are called eigenvalues. Equation 1.10 shows the invariance property of the eigenvectors: if the dynamics start in such a subspace, it will remain in it. [1]

---

[1]The meaning of Eq. 1.10 is that it exists some direction of the state-space where the effect of the operator A on a generic vector is only a scaling factor λ.

If the operator A has N linearly independent eigenvectors v^j, $j = 1, ..., n$, then one can take as a basis for the space of solutions the functions

$$\mathsf{x}^j(t) = e^{\lambda_j t} \mathsf{v}^j \tag{1.11}$$

For the applications presented in this work, it is a relevant case the presence of $N/2$ couples of complex conjugate eigenvalues λ_i and λ_{i+1}, such that $\lambda_i = \bar{\lambda}_{i+1} = \alpha_j + j\omega_j$, associated with $N/2$ couples of eigenvectors v^i and v^{i+1} such that: $\mathsf{v}^i = \mathsf{v}_R + j\mathsf{v}_I = \bar{\mathsf{v}}_{i+1}$. In this case, one has:

$$\mathsf{x}^j(t) = e^{\alpha_j t} \left(\mathsf{v}_R \cos \omega_j t - \mathsf{v}_I \sin \omega_j t \right)$$
$$\mathsf{x}^{j+1}(t) = e^{\alpha_j t} \left(\mathsf{v}_R \sin \omega_j t + \mathsf{v}_I \cos \omega_j t \right) \tag{1.12}$$

If the geometrical multiplicity is greater than the algebraic one, there are less eigenvectors than N; in this case, one has to consider the generalized eigenvectors as described for example in Hirsch and Smale (Ref. [43]) or Braum (Ref. [46]).

1.2.1 Geometrical remarks on eigenspaces and Jordan Canonical Form in ODE's systems solving

The Jordan Canonical Form of a square linear operator is a triangular matrix J similar to A which has a structure as close as possible to a diagonal matrix. In particular, if A is diagonalizable J will be diagonal. This means that considering a differential system of the form given by Eq. 1.7 it will be easier to solve it if the Jordan Canonical Form is determined, this providing the maximum level of decoupling of the problem. In general, the structure of J will depend on the geometrical and algebraic multiplicity of the eigenvalues of the operators A (see Ref. [43]). The present work (being presented only a brief summary about the solution of differential equations systems via the geometrical methods) will consider only cases with a geometrical multiplicity equal to the algebraic one.

Let us consider the operator $\mathcal{T} : U \to U$, where for the sake of simplicity we can consider $U = \mathbb{R}^N$. Let $U_1, ..., U_r$ be subspaces of U. One says that U is the direct sum of them if $\forall \mathsf{x} \in U$ it is possible to write:

$$\mathsf{x} = \mathsf{x}_1 + ... + \mathsf{x}_r \quad \mathsf{x}_i \in U_i, \quad i = 1, ..., r \tag{1.13}$$

This is denoted by

$$U = U_1 \oplus ... \oplus U_r \tag{1.14}$$

Let $\mathcal{T}_i : U_i \to U_i$, $i = 1, ..., N$ be operators. One say that $\mathcal{T}$ is the direct sum of the $\mathcal{T}_i$'s if $U = U_i \oplus ... \oplus U_n$, each U_i is invariant under $\mathcal{T}$, that is, $\mathcal{T}(U_i) \subset U_i$ and $\mathcal{T}(\mathsf{x}) = \mathcal{T}_i(\mathsf{x})$ if

$x \in U_i$. Such a situation can be denoted by writing $\mathcal{T} = \mathcal{T}_1 \oplus ... \oplus \mathcal{T}_N$. If $\mathcal{T}_j$ has the matrix A_j in some basis for each U_j, then by taking the union of the basis elements of the U_j to obtain a basis for U, $\mathcal{T}$ has the matrix:

$$A = diag\{A_1, ...A_N\} = \begin{pmatrix} A_1 & & \\ & \ddots & \\ & & A_N \end{pmatrix} \tag{1.15}$$

This means that the matrices A_i are placed together diagonally as indicated, all other entries in A being zero. Equation 1.15 suggests that to obtain the Jordan Canonical form of the considered operators one has to choose a suitable basis of every U_i.

Let us find some subsets of $\mathbb{R}^N$ which is invariant under A. From a mathematical point of view this means to find the solution of

$$Av = \lambda v \tag{1.16}$$

which in general has N solution. Using the eigenvectors of A as a basis allows to recast the problem in a diagonal form. In particular, it can be demonstrated that if Q is a matrix whose columns are the eigenvectors of A, then:

$$J = Q^{-1}AQ = diag\{\lambda_1, ..., \lambda_n\} \tag{1.17}$$

Equations 1.17 implies that the system given by Eq. 1.7 can be cast in diagonal form

$$\begin{aligned} \dot{y} &= Q^{-1}AQ \quad x = Qy \\ J &= Q^{-1}AQ \end{aligned} \tag{1.18}$$

with solutions given by Eq. 1.11: $x(t) = c_j e^{\lambda_j t} v^j$ with c_j determined by the initial conditions. Assuming that geometrical and algebraic multiplicity are equal, the result showed above in general require the complexification of the state problem which means that in general Eq. 1.18 is not real. It is interesting to analyze what happens when the system has complex conjugate eigenvalues and then complex conjugate eigenvectors (see Ref. [7]).

1.3 Flows and Invariant Subspaces

The flow e^{tA} in Equation 1.8 can be regarded as a mapping from $\mathbb{R}^N$ to $\mathbb{R}^N$: $\forall x_0 \in \mathbb{R}^N$, it follows that $x(x_0, t) = e^{tA}x_0 \in \mathbb{R}^N$. This statement means that the flow e^{tA} contains global information about the set of all solutions of Eq. 1.7 since such an expression for the solution holds in all the space $\mathbb{R}^N$. In the set of all solutions generated by $\phi_t = e^{tA} : \mathbb{R}^N \to \mathbb{R}^N$ there is a subsets that plays a special role: all the solutions lying in the linear subspaces spanned

by the eigenvectors (see Eq. 1.10 and Secs. 1.3.1 and 1.2.1). These subspaces, as shown in the previous Sections, are invariant under ϕ_t and the following properties hold (considering, for sake of simplicity only the case of real eigenvectors and eigenvalues):

$$\begin{aligned} \mathsf{A}\mathsf{v}^j &= \lambda_j \mathsf{v}^j \\ \mathsf{x}(c\mathsf{v}^j, t) &= c\mathsf{v}^j e^{\lambda_j t} \qquad c \in \mathbb{R} \end{aligned} \tag{1.19}$$

In an analogous way, in presence of complex eigenvectors and eigenvalues Eq. 1.19 still holds with the only difference that the invariant space is given by the $span\{\mathrm{Re}(\mathsf{v}^j), \mathrm{Im}(\mathsf{v}^j)\}$. One can divide the subspaces for the flow using the nature of the associated eigenvalues:

- The stable subspace, $E^s = span\{\mathsf{v}^1, ..., \mathsf{v}^{n_s}\}$.

- The unstable subspace, $E^u = span\{\mathsf{u}^1, ..., \mathsf{u}^{n_u}\}$.

- The center subspace, $E^c = span\{\mathsf{w}^1, ..., \mathsf{w}^{n_c}\}$.

where v^i are the n_{n_s} eigenvectors whose eigenvalues have negative real part, u^j are the n_{n_u} eigenvectors whose eigenvalues have positive real part and w^p are those whose eigenvalues have zero real parts. Note that, $n_s + n_u + n_c = N$. The solutions lying in E^s are characterized by exponential decay, those lying in E^u by exponential growth, and those lying in E^c by neither growth or decay.

1.3.1 Complex eigenvectors and associated invariant subspaces

Let be $\mathsf{A} \in L(\mathbb{R}^N, \mathbb{R}^N)$, where L denotes the space of linear operators over $\mathbb{R}^N$. The associated eigenproblem is:

$$\mathsf{A}\mathsf{w} = \lambda\mathsf{w}, \;\; \text{with } \mathsf{w} \in \mathbb{C}^N/\{0\}, \;\; \lambda \in \mathbb{C} \tag{1.20}$$

The spectrum of A is denoted by $S(\mathsf{A})$ and we suppose that its elements are distinct. The operator A is real and this implies that, if $\lambda \in S(\mathsf{A}) \cap \mathbb{C}/\mathbb{R}$, then $\bar{\lambda} \in S(\mathsf{A}) \cap \mathbb{C}/\mathbb{R}$ holds as well, with eigenvectors, respectively, w and $\bar{\mathsf{w}}$. In the following we will suppose that $S(\mathsf{A}) \cap \mathbb{C}/\mathbb{R} = S(\mathsf{A})$.

Writing explicitly Eq. 1.20, one has

$$\mathsf{A}(\mathsf{w}_R + j\mathsf{w}_I) = (\lambda_R + j\lambda_I)((\mathsf{w}_R + j\mathsf{w}_I)) \tag{1.21}$$

$$\begin{cases} \mathsf{A}\mathsf{w}_R = \lambda_R \mathsf{w}_R - \lambda_I \mathsf{w}_I \\ \mathsf{A}\mathsf{w}_I = \lambda_I \mathsf{w}_R + \lambda_R \mathsf{w}_I \end{cases} \tag{1.22}$$

Note that w_R and w_I are linearly independent[2]. Thus, the independent vectors w_R and w_I span a subspace $\mathcal{W}$ of dimension two in $\mathbb{R}^N$, namely a plane. Thus, the generic vector $\mathsf{v} \in \mathcal{W}$ has the form $\mathsf{v} = a\mathsf{w}_R + b\mathsf{w}_I$ with $a, b \in \mathbb{R}$. Using Eq. 1.22, one obtains

$$\mathsf{A}\mathsf{v} \;=\; \mathsf{A}(a\mathsf{w}_R + b\mathsf{w}_I) \;=\; \check{a}\mathsf{w}_R + \check{b}\mathsf{w}_I \tag{1.25}$$

where

$$\begin{cases} \check{a} \;=\; a\lambda_R + b\lambda_I \\ \check{b} \;=\; b\lambda_R - a\lambda_I \end{cases} \tag{1.26}$$

Equation 1.25 shows that $\mathcal{W}$ is invariant under A.

Note that the statements presented above also holds for the complex conjugate eigenvector $\bar{\mathsf{w}} = \mathsf{w}_R - j\mathsf{w}_I$; thus, $\bar{\mathsf{w}}$ belongs to the same subspace $\mathcal{W}$. This implies that there is a direct correspondence between a complex conjugate pair of eigenvectors (namely, eigenvalues) and the plane $\mathcal{W}$.

Let us consider a complex number $c = \rho e^{j\tilde{\theta}}$ with $\rho \in \mathbb{R}^+/\{0\}$, $\tilde{\theta} \in \mathbb{R}/2\pi k$, $k \in \mathbb{Z}$ and, without loss of generality, we can set $\rho = 1$. The complex vector $\tilde{\mathsf{w}}$ obtained by multiplying c times the vector w with $\mathsf{w}_R, \mathsf{w}_I \in \mathcal{W}$, *i.e.*, $\tilde{\mathsf{w}} = c\mathsf{w}$, is also by definition an eigenvector of the eigenproblem 1.20. Indeed, the multiplication of the generic eigenvector w by a complex constant with module equal to one and generic phase $\tilde{\theta}$ defines the following transformation in $\mathcal{W}$,

$$\tilde{\mathsf{w}} \;=\; \mathsf{w}e^{j\tilde{\theta}} = \left(\cos\tilde{\theta}\,\mathsf{w}_R - \sin\tilde{\theta}\,\mathsf{w}_I\right) + j\left(\sin\tilde{\theta}\,\mathsf{w}_R + \cos\tilde{\theta}\,\mathsf{w}_I\right) \;=\; \tilde{\mathsf{w}}_R + j\tilde{\mathsf{w}}_I \tag{1.27}$$

or

$$\tilde{\mathsf{w}}_R \;=\; \left(\cos\tilde{\theta}\,\mathsf{w}_R - \sin\tilde{\theta}\,\mathsf{w}_I\right) \tag{1.28}$$
$$\tilde{\mathsf{w}}_I \;=\; \left(\sin\tilde{\theta}\,\mathsf{w}_R + \cos\tilde{\theta}\,\mathsf{w}_I\right) \tag{1.29}$$

Equations 1.28 and 1.29 define a family of real transformations depending on the parameter $\tilde{\theta}$, *i.e.*, $\Phi_{\tilde{\theta}} : \mathcal{W} \times \mathcal{W} \mapsto \mathcal{W} \times \mathcal{W}$ that, given $(\mathsf{w}_R, \mathsf{w}_I)$, yields $(\tilde{\mathsf{w}}_R, \tilde{\mathsf{w}}_I)$. It is relevant to observe that this transformation preserves the property that both $(\mathsf{w}_R, \mathsf{w}_I)$ and $(\tilde{\mathsf{w}}_R, \tilde{\mathsf{w}}_I)$ are real and

---

[2]Indeed, if this were not true, there would exist a $\tau \in \mathbb{R}/\{0\}$ such that $\mathsf{w}_I = \tau\mathsf{w}_R$ as shown in the following. From Eq. 1.22

$$\begin{cases} \mathsf{A}\mathsf{w}_R \;=\; (\lambda_R - \tau\lambda_I)\mathsf{w}_R \\ \mathsf{A}\mathsf{w}_I \;=\; (\lambda_I/\tau + \lambda_R)\mathsf{w}_R \end{cases} \tag{1.23}$$

Equating the Eqs. 1.23 one has the condition

$$\lambda_I(1 + \tau^2)\mathsf{w}_R \;=\; 0 \tag{1.24}$$

which is not possible by hypothesis, this demonstrating the linearly independence of w_R and w_I.

imaginary parts of complex vectors solutions of the eigenproblem 1.20 and corresponding to the same eigenvalues.

In particular, the parameter $\tilde{\theta}$ can be chosen such that $\tilde{\mathsf{w}}_R$ and $\tilde{\mathsf{w}}_I$ be orthogonal. Indeed, imposing the condition $\tilde{\mathsf{w}}_R \cdot \tilde{\mathsf{w}}_I = 0$ and using Eqs. 1.28 and 1.29, one obtains

$$\left(\tan \tilde{\theta}_\perp\right)^2 \mathsf{w}_R \cdot \mathsf{w}_I + (\mathsf{w}_I \cdot \mathsf{w}_I - \mathsf{w}_R \cdot \mathsf{w}_R) \tan \tilde{\theta}_\perp - \mathsf{w}_R \cdot \mathsf{w}_I = 0. \tag{1.30}$$

The above equation in the unknown angle $\tilde{\theta}_\perp$ allows to determine an orthogonal basis $\tilde{\mathsf{w}}_{R_\perp}$ and $\tilde{\mathsf{w}}_{I_\perp}$ on $\mathcal{W}$ such that $\tilde{\mathsf{w}}_\perp = \tilde{\mathsf{w}}_{R_\perp} + j\tilde{\mathsf{w}}_{I_\perp} = e^{j\tilde{\theta}_\perp}\mathsf{w}$. Thus, for every given couple $(\mathsf{w}_R, \mathsf{w}_I)$, there exists a particular transformation, $\Phi_{\tilde{\theta}_\perp}$, in the one parameter family of $\Phi_{\tilde{\theta}}$ that maps $(\mathsf{w}_R, \mathsf{w}_I)$ in the orthogonal direction $(\mathsf{w}_{R_\perp}, \mathsf{w}_{I_\perp})$, see Fig. 1.1. It is worth to remark that,
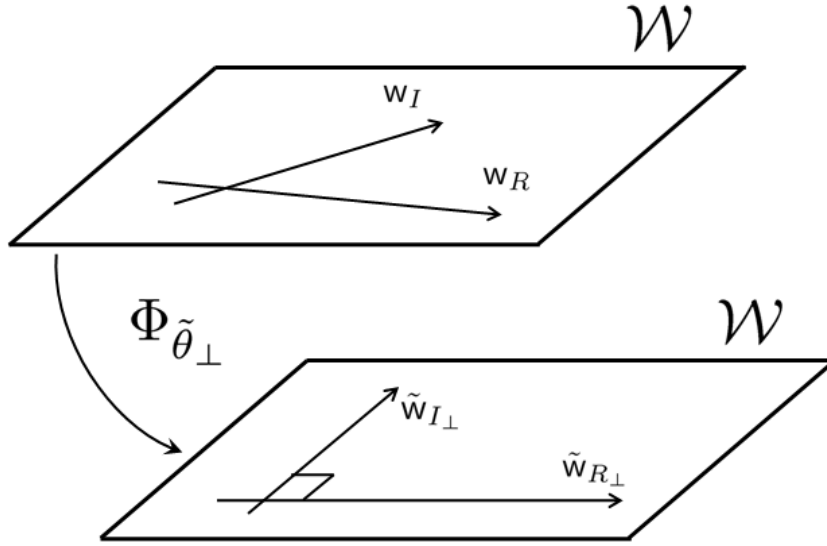
Figure 1.1: Orthogonalyzing trasnformation for vectors w_R and w_I.

even if $\tilde{\theta}_\perp$ is a function of the ordered couple $(\mathsf{w}_R, \mathsf{w}_I)$, the mutually orthogonal vectors $(\mathsf{w}_{R_\perp}, \mathsf{w}_{I_\perp})$ are unique.

It is relevant to observe that this choice of the parameter $\tilde{\theta}$ is not equivalent to the Gram-Schmidt orthogonalization procedure. In fact, if we apply the Gram-Schmidt procedure to the basis $(\mathsf{w}_R, \mathsf{w}_I)$ it is not guaranteed that the new obtained orthogonal basis corresponds to the real and imaginary part of an eigenvector of the operator A with the same eigenvalue.

It is also possible to give a geometrical interpretation of the generic transformation $\Phi_{\tilde{\theta}}$ (Eqs. 1.28 and 1.29). Let us denote with $(x_{\tilde{\mathsf{w}}_R}, y_{\tilde{\mathsf{w}}_R})$ and $(x_{\tilde{\mathsf{w}}_I}, y_{\tilde{\mathsf{w}}_I})$ the generic coordinates of the tip points of the vectors $\tilde{\mathsf{w}}_R$ and $\tilde{\mathsf{w}}_I$, respectively, when applied at the origin of the reference system with unit orthogonal basis vectors $\mathsf{w}_{R_\perp}/\|\mathsf{w}_{R_\perp}\|$ and $\mathsf{w}_{I_\perp}/\|\mathsf{w}_{I_\perp}\|$ (evaluated with the previous procedure). Then, the curves described by these tip points over the subspace plane are parametrized by $\tilde{\theta}$ and are given by (see Eqs. 1.28 and 1.29 with $\tilde{\mathsf{w}}_R$ and

$\tilde{w}_I$ substituted with $\tilde{w}_{R_\perp}$ and $\tilde{w}_{I_\perp}$)

$$x_{\tilde{w}_R} = \frac{w_{R_\perp}}{\|w_{R_\perp}\|} \cdot \tilde{w}_R = \|w_{R_\perp}\| \cos \tilde{\theta} \qquad (1.31)$$

$$y_{\tilde{w}_R} = \frac{w_{I_\perp}}{\|w_{I_\perp}\|} \cdot \tilde{w}_R = -\|w_{I_\perp}\| \sin \tilde{\theta} \qquad (1.32)$$

and

$$x_{\tilde{w}_I} = \frac{w_{R_\perp}}{\|w_{R_\perp}\|} \cdot \tilde{w}_I = \|w_{R_\perp}\| \sin \tilde{\theta} \qquad (1.33)$$

$$y_{\tilde{w}_I} = \frac{w_{I_\perp}}{\|w_{I_\perp}\|} \cdot \tilde{w}_I = \|w_{I_\perp}\| \cos \tilde{\theta}. \qquad (1.34)$$

The above relations show that the vector-tip points describe the same ellipse as $\tilde{\theta}$ varies with principal axes equal to $\|w_{R_\perp}\|$ and $\|w_{I_\perp}\|$ on the subspace plane $\mathcal{W}$, as shown in Fig. 1.2.
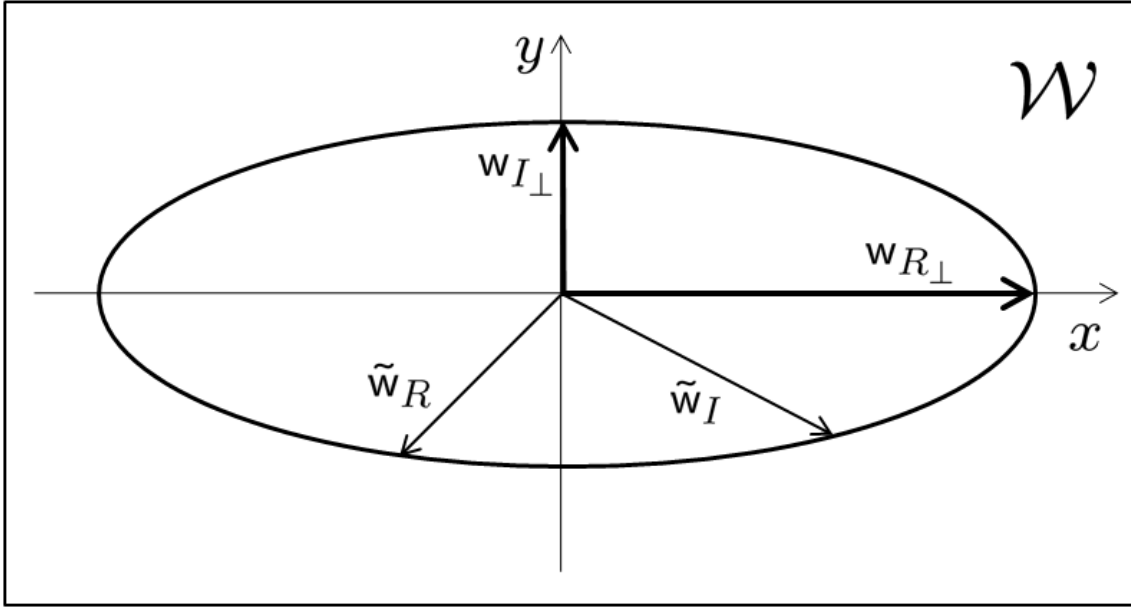
Figure 1.2: Geometrical interpretation of the transformations family $\Phi_{\tilde{\theta}}$.

1.4   The Nonlinear System

In Section 1.1, it has been shown that for a smooth vector field $\mathcal{F}(x)$, the solution of the nonlinear problem given by Eq. 1.1 together with the condition $x(0) = x_0$ is unique and defined at least in some neighborhood $t \in (-a, a)$ of $t = 0$. Thus, it is possible to define only a local flow $\phi_t : \mathbb{R}^N \to \mathbb{R}^N$ mapping x_0 to $x(x_0, t)$ but it is not possible to give a general shape of it as in the linear case. Usually, in the application, the dynamics represents the behavior of some kind of physical problem in the neighborhood of some reference state. This means that is very common to start the study of the dynamics by finding the fixed

points, *i.e.*, the equilibrium, of Eq. 1.1. Once found such equilibria, the first step is to study the *linearized* dynamics around them. Let us consider how the nonlinear problem and the linearized associated one relate.

Let us suppose to have found a fixed point $\hat{x}$ so that $\mathcal{F}(\hat{x}) = 0$. The associated linear system is:

$$\dot{\xi} = D\mathcal{F}(\hat{x})\xi \quad \xi \in \mathbb{R}^N \tag{1.35}$$

where $D\mathcal{F} = [\partial f_i / \partial x_j]$ is the Jacobian matrix containing the first partial derivatives of the considered vector field evaluated at the equilibrium point and $x = \hat{x} + \xi$, $|\xi| \ll 1$. The solution of Eq. 1.35 is defined as the linearized flow

$$D\phi_t(\hat{x})\xi = e^{tD\mathcal{F}(\hat{x})}\xi \tag{1.36}$$

Finally, observe that the properties of stability of the equilibrium $\hat{x}$ with respect to the linearized flow can be studied observing the spectral properties of the matrix $D\mathcal{F}(\hat{x})$ by following the procedure outlined in Secs. 1.3.1 and 1.2.1.

Being the theory of linear differential systems and the study of their stability properties well known and tractable in closed form, the following theorem is fundamental in the theory of nonlinear differential equations:

The Nonlinear System 1.4.1 *If $D\mathcal{F}(\hat{x})$ has no zero or purely imaginary eigenvalues then there is a homeomorphism* h *defined on some neighborhood U of $\hat{x} \in \mathbb{R}^N$ locally taking orbits of the nonlinear flow ϕ_t of Eq. 1.1, to those of the linear flow $e^{tD\mathcal{F}(\hat{x})}$ of Eq. 1.35. The homeomorphism preserves the sense of orbits and can also be chosen to preserve parametrization by time.*

The above theorem, called Hartman-Grobman, expressed the fundamental result that to study the stability of a fixed point of a nonlinear system is sufficiently to study its linearization about such a fixed point. Observe that a fixed point associated with a Jacobian without zero or purely imaginary eigenvalues is called hyperbolic or nondegenerate (in the sense of Hartman-Grobman Theorem), whereas it is called a center.

The concept of invariant subspaces can be extended in the nonlinear case considering the so called *invariant manifold*. How such invariant spaces relate to the linear ones is expressed by the following Center Manifold Theorem:

Center Manifold Theorem for Flows 1.4.1 *Let $\dot{x} = \mathcal{F}(x)$ with $\mathcal{F} \in C^r$ vanishing in $\hat{x}$ and let* A $= D\mathcal{F}(\hat{x})$. *Divide the spectrum of* A *into three parts σ_s, σ_c, σ_u with*

$$\text{Re}\lambda = \begin{cases} < 0 \text{ if } \lambda \in \sigma_s \\ = 0 \text{ if } \lambda \in \sigma_c \\ > 0 \text{ if } \lambda \in \sigma_u \end{cases}$$

Let the generalized eigenspaces of σ_s, σ_c, σ_u be E^s, E^c, E^u, respectively. Then there exist C^r stable and unstable invariant manifold W^u and W^s tangent to E^u and E^s at $\hat{x}$ and a C^{r-1} center manifold W^c tangent to E^c in $\hat{x}$. The manifolds are invariant under $\mathcal{F}$. Moreover, W^u and W^s are unique, but W^c need not be.

It is interesting to note that, in general, it is always possible to define our problem in such a way that the considered equilibrium point coincides with the origin,*i.e.*, $\hat{x} = 0$. This is possible by a change of coordinates: $q = x - \hat{x}$. Moreover, the above fundamental result will be considered in the next Sections being the basis for the study of the nonlinear dynamics and, in particular, the Center Manifold Theorem permits to consider to extend the idea of *modes* in the nonlinear case. Indeed, in the nonlinear problem, it is not possible to consider the solution as a superimposition of independent solutions along certain invariant subspaces of problem space (defined by the eigenvectors of the state matrix) but the existence of invariant manifolds W permits to extend the concept of *mode*, at least in local way. Indeed, it will be shown that exists some dominant sets that lead the dynamics of the process. For a deep analysis of nonlinear modes, it is possible to refer to the fundamental work by Rosenberg, Ref. [47] or to the works of Shaw and Pierre (Ref. [48]) or Vakakis (Ref. [49]).

1.4.1   Asymptotic Behavior

In the previous Sections, we considered only linear/linearized systems that, at large times, collapse on a fixed point. In general, a nonlinear systems can present a more various behavior with harmonic, quasi-harmonic of chaotic solutions: such solutions differently from a fixed point are long term behavior of the dynamics, the orbits will tend to such subset of the space. Moreover, such special sets will be invariant with respect to the flow. It is possible to define an invariant set S for a flow ϕ_t on $\mathbb{R}^N$ as a subset of the whole space such that:

$$\phi_t(x) \in S \ \ \forall x \in S, \ \ \forall t \in \mathbb{R} \tag{1.37}$$

Of course, the stable and unstable manifold of a fixed point are example of invariant sets, as well as an harmonic solution (remember that the invariant manifolds are made of solutions orbits).

A closed invariant set $A \subset \mathbb{R}^N$ is called an attracting set if there is some neighborhood U of A such that $\phi_t(x) \in U$ for $t \geq 0$ and $\phi_t(x) \to A$ as $t \to +\infty$ for all $x \in A$. Of course, the domain of attraction of A is given by $\bigcup_{t \geq 0} \phi_t(U)$ and it will coincide with the stable manifolds of A. Analogously, it is possible to define a repelling set as an attracting set for $t < 0$. The concepts of attracting set permits to expand the idea of solution to the one of long term dynamics understanding the solution as a limit behavior of the system which tends to it called attractors. Finally, let us consider from a geometrical point of view, how a

harmonic, quasi-periodic and chaotic system behavior. A harmonic solution is characterized by the presence of commensurable frequencies, see Fig. 1.3, whereas in the presence of a quasi-periodic solution the frequencies are uncommensurable. This means that from a geometrical view point, the orbit will lie on a torus, see Fig. 1.4 . For a chaotic behavior, it means that the system solution tends to a so called strange attractors, which characterized by a large difference between solutions (both lying in such an attracting set) generated by nearby initial conditions. An example of the Rössler strange attractor is presented in Fig. 1.5. For a deeper analysis of chaotic behavior in nonlinear systems, the reader can refer to the work of Tabor (Ref. [23]).
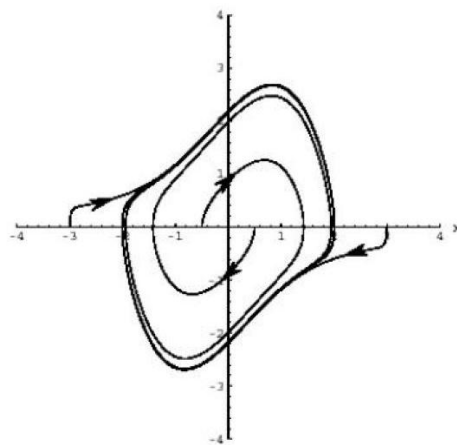
Figure 1.3: Periodic ortbit
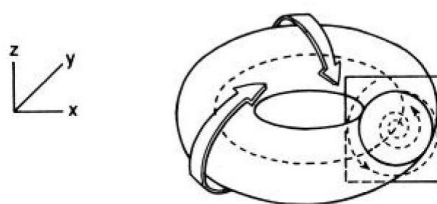
Figure 1.4: A Quasi-periodic orbit will lie on a Torus

1.5   The bifurcation of Equilibrium

In the application, the consider dynamical systems represent via a mathematical model some physical problem. Usually, a real problem depends on various parameters influencing its behavior and in particular its solutions properties. Indeed, depending on the values
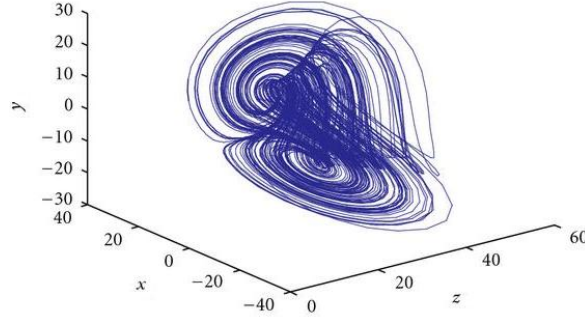
Figure 1.5: Strange attractor of Rössler

of control parameters, the equilibrium should be stable or unstable and harmonic, quasi-harmonic or chaotic behavior could arise. In this Chapter some issues about the bifurcation of nonlinear systems and the methods to study such a class of problem are given. For a deeper analysis refer to Refs. [19, 44, 42, 23].

1.5.1 An introductory example about bifurcation of equilibrium

Let us consider a system with polynomial nonlinearities (Refs. [50] and [51])

$$\ddot{x} + x + \dot{x}[-\mu + c_1(x^2 + \dot{x}^2) + c_2(y^2 + \frac{1}{\omega_y^2}\dot{y}^2)] = 0 \tag{1.38}$$

$$\ddot{y} + \omega_y^2 y + \dot{y}[\delta - c_3(x^2 + \dot{x}^2)] = 0 \tag{1.39}$$

with c_1, c_2, c_3, δ real and positive whereas $\mu \in \mathbb{R}$.

Equations 1.38 can be cast in first order form:

$$\dot{\mathsf{z}} = \mathsf{A}\mathsf{z} + \mathsf{f}_{nl}(\mathsf{z}) \tag{1.40}$$

where $\mathsf{z}^T = \{\dot{x}\ \dot{y}\ x\ y\ \}$ and

$$\mathsf{A} = \begin{bmatrix} \mu & 0 & -1 & 0 \\ 0 & -\delta & 0 & -\omega_y^2 \\ 1 & 0 & 0 & 0 \\ 0 & 1 & 0 & 0 \end{bmatrix} \tag{1.41}$$

$$\mathsf{f}_{nl}(\mathsf{z}) = \begin{Bmatrix} 0 \\ 0 \\ \dot{x}[c_1(x^2 + \dot{x}^2) + c_2(y^2 + \alpha^2\dot{y}^2)] \\ -\dot{y}[c_3(x^2 + \dot{x}^2)] \end{Bmatrix} \tag{1.42}$$

The equilibrium solution, $z = 0$, is stable until $\mu < 0$. If $\mu > 0$ a Limit Cycle Oscillations (LCO) arises. In particular assuming that

$$x(t) = X \cos(t + \phi_x), \ y(t) = Y \cos(\omega_y t + \phi_y) \tag{1.43}$$

one obtains the bifurcation equations

$$X(-\mu + c_1 X^2 + c_2 Y^2) = 0 \tag{1.44}$$

$$Y(\delta - c_3 X^2) = 0 \tag{1.45}$$

From Equations 1.44-1.45 it appears that for $\mu < 0$ the equilibrium solution is possible whereas for $\mu > 0$ a LCO appears with, assuming $Y = 0$ (see Refs. [50] and [51]), $X = \sqrt{\frac{\mu}{c_1}}$. It is clear that $\mu = 0$ represent an equilibrium bifurcation point for the considered dynamical system. Moreover, substituting $X = \sqrt{\frac{\mu}{c_1}}$ in Eq. 1.45 one obtains

$$Y(\delta - c_3 \frac{\mu}{c_1}) = 0 \tag{1.46}$$

If the following relation holds

$$\mu = \frac{\delta c_1}{c_3} = \mu_c \tag{1.47}$$

Equation 1.46 is satisfied without the condition $Y = 0$. This means that also the Y mode is activated for $\mu > \mu_c$. The new solution will be:

$$
\begin{aligned}
X &= \sqrt{\frac{\delta}{c_3}} \\
Y &= \sqrt{\frac{\mu - \mu_c}{c_2}}
\end{aligned}
\tag{1.48}
$$

where it is shown that all the terms in Eq. 1.43 are active. Moreover, if $\omega_y \in \mathbb{N}$ it will be observed a harmonic LCO otherwise a quasi-periodic behavior is expressed by the system. Finally, it is possible to summarize the behavior of Eq. 1.38:

- $X = 0, Y = 0$ for $\mu \leq 0$

- $X = \sqrt{\frac{\mu}{c_1}}, Y = 0$ for $0 < \mu \leq \mu_c, \mu_c = \frac{\delta c_1}{c_3}$

- $X = \sqrt{\frac{\mu}{c_1}}, Y = \sqrt{\frac{\mu - \mu_c}{c_2}}$ for $\mu \geq \mu_c$

showing that the parameter μ influences the behavior of the system causing the loss of stability of the unperturbed state with the arrising of a LCO which changes its nature for $\mu > \mu_c$. For a deeper analysis of such a system consider Ref. [51].

1.5.2   Some issues about Bifurcation Problems

Let us consider an ordinary differential equations system depending on a k-dimensional parameter μ:

$$\dot{\mathsf{x}} = \mathcal{F}_\mu(\mathsf{x}) = \mathcal{F}(\mu, \mathsf{x}); \; \mathsf{x} \in \mathbb{R}^n, \;\; \mu \in \mathbb{R}^k. \tag{1.49}$$

where all the equilibria satisfies the condition

$$\mathcal{F}_\mu = 0 \tag{1.50}$$

The Implicit Function Theorem (see Ref. [43]) states that varying the paramenters μ the equilibria described by Eq. 1.50 will be described by smooth function in μ as long as the relation $x_{eq}(\mu)$ will be biunivocal. When there is not a biunivocal relation between equilibrium and parameters the so called bifurcation of equilibrium happens: different solutions coincide for different set of parameters.

A typical example is what happens in aeroelasticity with the flutter phenomenon. If the flow velocity is larger than a certain threshold, the unperturbed solution is no longer stable and a LCO arises. In this case, one will speak about a dynamical bifurcation but are possible also static bifurcation and a lot of different mechanisms can characterize a bifurcation process. For a deep analysis of such a problem one can consider Ref. [42, 19, 44, 52]. In this work two kind of bifurcations will be considered. The first is called Hopf bifurcation and it is a dynamical process, whereas the second one is a static process and it is called pitchfork bifurcation. The statical or dynamical nature of the process will depend on the behavior of the spectrum of the linearized system as shown in the next section.

1.5.3   Consequences of Center Manifold Theorem

The existence of invariant manifolds stated by the Center Manifold Theorem has important consequence in the study of nonlinear systems in the neighborhood of bifurcation points. Indeed, the cited theorem implies that (see Ref. [42]) the system Eq. 1.49 is locally topologically equivalent to

$$\begin{aligned} \dot{\mathsf{v}} &= \mathsf{f}(\mathsf{v}) \\ \dot{\mathsf{y}} &= -\mathsf{y} \qquad (\mathsf{v}, \mathsf{y}, \mathsf{z}) \in W^c \times W^s \times W^u \\ \dot{z} &= \mathsf{z} \end{aligned} \tag{1.51}$$

at the bifurcation point, $i.e.$, for $\mu = \mu_c$.

Let us consider, for the sake of simplicity, that the unstable manifold is empty. Moreover, let us assume that the linear part is block diagonal:

$$\begin{aligned} \dot{\mathsf{v}} &= \mathsf{B}\mathsf{v} + \mathsf{f}(\mathsf{v}, \mathsf{y}) \\ \dot{\mathsf{y}} &= \mathsf{C}\mathsf{y} + \mathsf{g}(\mathsf{v}, \mathsf{y}) \end{aligned} \tag{1.52}$$

where $(\mathsf{v}, \mathsf{y}) \in \mathbb{R}^n \times \mathbb{R}^m$ and B and C are $n \times n$ and $m \times m$ matrices, respectively. The eigenvalues of B have zero real parts whereas the ones of C have negative real parts. The center manifold is tangent at the equilibrium to the space E^c so there is a local graph

$$W^c = \{(\mathsf{v}, \mathsf{y}) \| \mathsf{y} = \mathsf{h}(\mathsf{v})\} \qquad \mathsf{h}(0) = D\mathsf{h}(0) = 0 \tag{1.53}$$

where it has been assumed that the considered equilibrium point coincides with the origin of the space and $\mathsf{h} : U \to \mathbb{R}^m$ is defined in some neighborhood of $\mathsf{x} = 0$. Equation 1.53 means that the following relation hold along W^c:

$$\dot{\mathsf{v}} = \mathsf{B}\mathsf{v} + \mathsf{f}(\mathsf{v}, \mathsf{h}(\mathsf{v})) \tag{1.54}$$

Finally, Equations 1.54 indicates that the existence of the Center Manifold permits to reduce the effective dimension of the problem, *i.e.*, the number of equations. From a practical point of view Eq. 1.54 can be related to the possibility to extend the modal superimposition to nonlinear problems (see Ref. [48]).

1.6 Static and Dynamic Bifurcation

In this Section some issues about simple bifurcation of equilibria are given. In particular, it will be considered, one example of static bifurcation where the origin losses its stability and become unstable, and two new fixed point stable solution arises (Pitchfork Bifurcation), and a dynamic bifurcation where the origin losses its stability and a stable limit cycle arises.

1.6.1 Pitchfork Bifurcation

At the bifurcation point, the stability of the trivial equilibrium changes, and a new pair of equilibria (related by symmetry) appears to one side of the bifurcation point, see Fig. 1.6. It can be demonstrated via Normal Forms analysis that all the system experiencing such kind of bifurcation are topologically equivalent to the equation (on the center manifold, see Ref. [42]):

$$\dot{x} = \mu x - x^3 \tag{1.55}$$

Observing Equation 1.55 one can observe that for $\mu \leq 0$ only the trivial solution is possible, whereas for $\mu > 0$, two new solutions appear $x = \pm\sqrt{\mu}$. Finally, the sign of the term x^3 determines the nature of the bifurcation: when it is positive, the bifurcation is subcritical, supercritical otherwise. Note that, considering a static bifurcation, the spectrum of the linearized system, evaluated in the trivial solution, has a zero eigenvalue which is going to be positive.
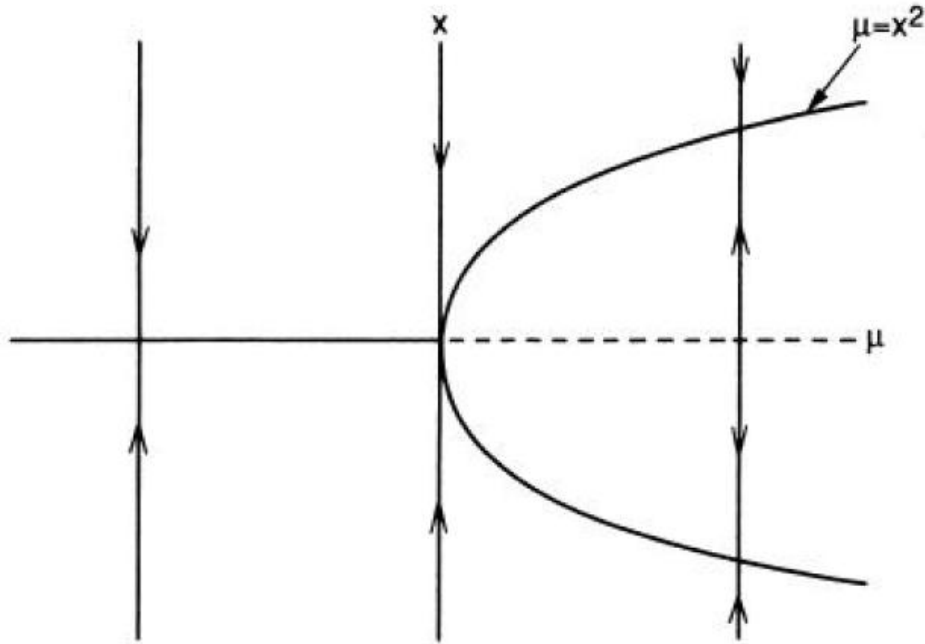
Figure 1.6: Supercritical Pitchfork Bifurcation Diagram

1.6.2 Hopf Bifurcation

The linearized system in the considered equilibrium point has a pair of purely complex conjugate eigenvalues which are going to have positive real part. It can be demonstrated (see Ref. [42]) that all the system experiencing a Hopf-type bifurcation are equivalent to the one given by Eq. 1.56 (in polar coordinates $(r, \theta) \in \mathbb{R} \times \mathbb{R}/mod\pi$:

$$\begin{cases} \dot{r} = (d\mu + ar^2)r \\ \dot{\theta} = (\omega + c\mu + br^2) \end{cases} \tag{1.56}$$

If $a \neq 0$, $b \neq 0$ the condition $r = cost$ representing a LCO gives that these solutions lie along the parabola $\mu = -ar^2/d$. If $a > 0$ the bifurcation is called supercritical and after the bifurcation point one has an unstable equilibrium point and a stable LCO, see Fig. 1.7. Otherwise, the bifurcation is called subcritical: before the bifurcation point the stability of equilibrium is conditioned (with the stability margin defined by an unstable LCO) and after the bifurcation point only an unstable equilibrium exists, see Fig. 1.8.
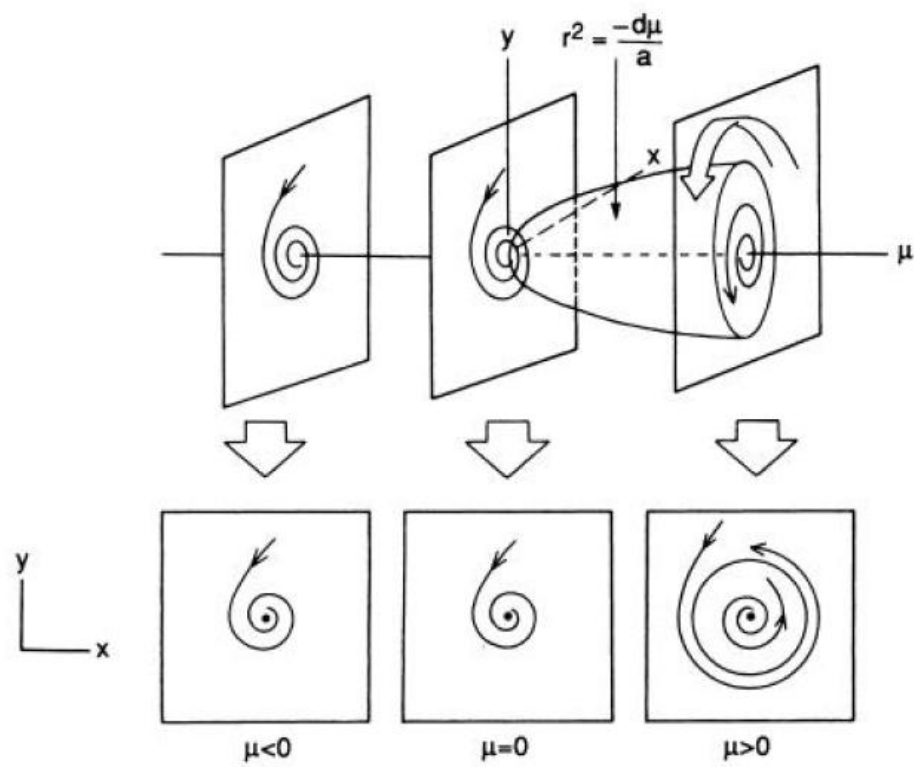
Figure 1.7: Supercritical Hopf Bifurcation Diagram
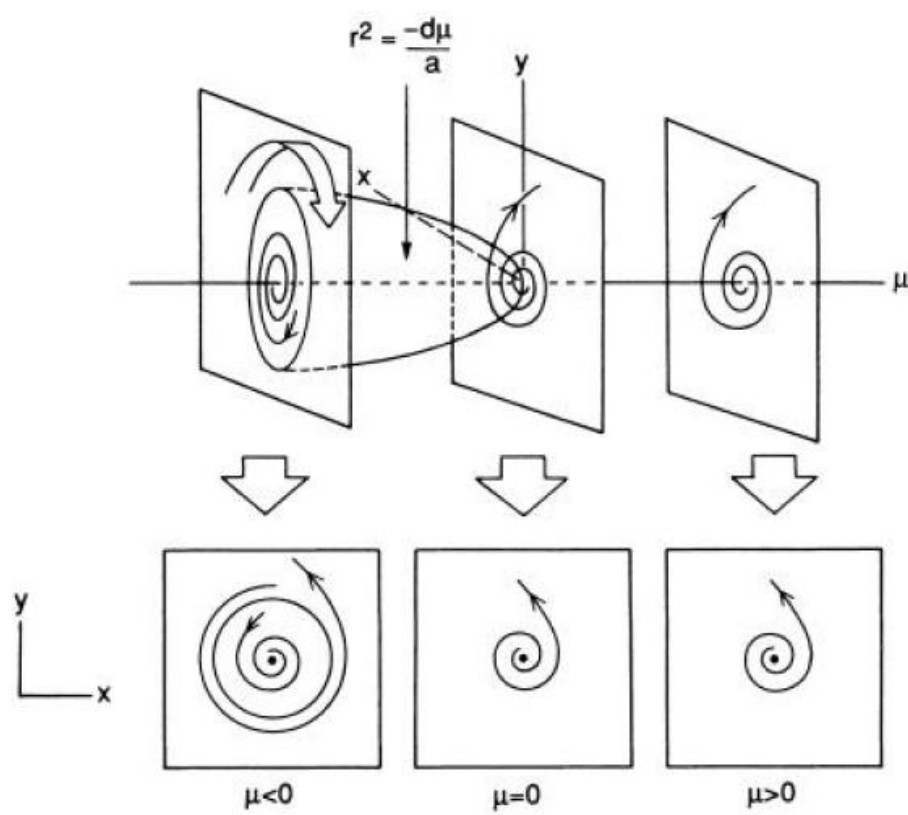
Figure 1.8: Subcritical Hopf Bifurcation Diagram

Chapter 2

Flows near a bifurcation point: analytical methods

In Chapter 1.5 some issues about the properties of dynamical systems in the neighborhood of a bifurcation point have been given. Indeed, it has been shown that in the neighborhood of a fixed point exists a smooth transformation that map our system in a more simple one with the same properties of the original one. In particular, in presence of purely imaginary eigenvalues will be the part of the system associated to them to carry the dynamics. In this Chapter some issues about the technical tools which provide the basis for the qualitative study of flows near bifurcation point will be given. In particular, the methods that permit to simplify the system on the Center Manifold will be analyzed. This method are based on finding additional coordinate transformations which reduce the complexity of the system written on the center manifold: such resulting vector fields are called *normal forms*. The idea of introducing successive coordinate transformation in order to simply the expression of a general problem forms the basis of the Kolmogorov-Arnold-Moser (KAM) theory (see Refs. [23, 53, 54]) for Hamiltonian systems.

2.1 Normal Forms

In the proximity of a fixed point, the Center Manifold Theorem permits us to restrict our attention to the flow within the center manifold. Moreover, one can try to simplify the expression of the vector field on the center manifold introducing successive coordinates transformations obtaining the so called *normal form* of the vector field. This idea is the base of the Kolmogorov-Arnold-Moser (KAM) (see Refs. [23, 53, 54]) theory for Hamiltonian systems and in this work some results about nonconservative systems will be presented. Such a methodology works well with the presence of polynomial nonlinearities. We will consider

vector fields of the form $\mathcal{F}(\mathsf{x}) = \mathsf{A}\mathsf{x} + \mathsf{f}(\mathsf{x})$ with $\mathsf{f}_i(\mathsf{x})$ a vector of polynomials of order k in the state variables x_i. Note also that the polynomial structure of the nonlinear terms implies that we are assuming that in the neighborhood of the considered equilibrium it is possible to expand the flow in Taylor's series.

Let us consider the system

$$\dot{\mathsf{x}} = \mathcal{F}(\mathsf{x}) \tag{2.1}$$

with an equilibrium at $\mathsf{x} = 0$, *i.e.*, $\mathcal{F}(0) = 0$. The main idea behind normal form is to find a coordinate change $\mathsf{x} = \hat{\mathsf{h}}(\eta)$ with $\hat{\mathsf{h}}(0) = 0$ such as the system becomes as simple as possible, *i.e.*, linear in the best case. One has:

$$\dot{\mathsf{q}} = (D\hat{\mathsf{h}}(\eta))^{-1} \mathcal{F}(\hat{\mathsf{h}}(\eta)) \tag{2.2}$$

In the best case Eq. 2.2 will be linear. In term of power series, one can reduce the complexity of the problem by finding a sequence of coordinate transformation $\hat{\mathsf{h}}_1, \hat{\mathsf{h}}_2, ...$ which remove terms of increasing order from Eq. 2.2. In general, it will not be possible to reduce the original system to a linear one: some *essential* nonlinearities will remain.

Let us assume that $\mathsf{A} = D\hat{\mathsf{h}}(0)$ has distinct eigenvalues $\lambda_1, ..., \lambda_n \in \mathbb{C}$ and that the system has been brought to a diagonal form of the linear part:

$$\dot{\mathsf{x}} = \Lambda\mathsf{x} + \mathsf{g}(\mathsf{x}) \tag{2.3}$$

with $g_i = o(|\mathsf{x}|)$ in the origin. Let us consider the quasi-identical transformation:

$$\mathsf{x} = \hat{\mathsf{h}}(\eta) = \eta + \mathsf{h}(\eta) \tag{2.4}$$

Now, Equation 2.2 has the form:

$$\dot{\eta} = (\mathsf{I} + D\mathsf{h}(\eta))^{-1} \mathcal{F}(\eta + \mathsf{h}(\eta)) \tag{2.5}$$

Denoting with g_i^k the terms of g_i of degree k one has:

$$\dot{\eta}_i = \lambda_i \eta_i + \lambda_i P_i(\eta) + g_i^k(\eta) - \sum_{j=1}^{N} \frac{\partial h_i}{\partial \eta_i} \lambda_j \eta_j \tag{2.6}$$

The unknowns $h_i(\eta)$ can be chosen in order to eliminate the k-degree terms $g_i^k(\eta)$:

$$\lambda_i h_i(\eta) - \sum_j \frac{\partial h_i}{\partial \eta_i} \lambda_j q_j = -g_i^k(\eta) \tag{2.7}$$

To solve Eq. 2.7 one can observe that it is linear in the coefficient of h and that h_i is the monomial $\eta_1^{a_1} \cdots \eta_n^{a_n}$:

$$\frac{\partial h_i}{\partial \eta_i} \lambda_j \eta_j = a_j \lambda_j h_i$$

$$(\lambda_i - \sum_j a_j \lambda_j) h_i = -g_i^k(\eta) \tag{2.8}$$

Finally, from Eqs. 2.7 the solution of Eq. 2.8 is:

$$h_i = -\frac{g_i^k}{\lambda_i - \sum_j a_j \lambda_j} \tag{2.9}$$

Equation 2.9 gives the condition to chose h in order to eliminate the nonlinearities of order k. Observe that this is possible only if *none of the sums* $\lambda_i - \sum_j a_j \lambda_j$ is zero when the terms $a_1,...,a_n$ are nonnegative integers with $\sum_j a_j = k \geq 2$. If this is true for any order the transformation, by iterating the transformation given by Eq. 2.4, this yields to a diffeomorphism, which maps the initial nonlinear problem to a linear one. In particular, the normal form in the neighborhood of an hyperbolic fixed point coincides with the form cited by the Hartman's Theorem.

2.2 Perturbation Methods

In the previous Section, the possibility to simplify the dynamics in the neighborhood of a bifurcation point using the Center Manifold Theorem has been addressed with particular attention to systems with polynomial nonlinearities. Now, the problem is considered from a practical point of view developing the theoretical results (that ensure some possibility) in such a way to obtain effective results. In particular, let us consider weakly nonlinear systems depending on a parameter that influence the stability of the unperturbed state. This means that can be regarded as a linear problem *perturbed* by *small* nonlinear terms.

This means that, in general, our problem will be of the form:

$$\dot{\mathsf{x}} = \mathsf{A}(\mu)\mathsf{x} + \epsilon\mathsf{f}(\mathsf{x};\mu) \tag{2.10}$$

where the vector of nonlinear terms, f, has polynomial elements, μ is the general control parameter and ϵ is a small parameter. Assuming that the real part of some eigenvalue (or couple of eigenvalues) of A change its sign for $\mu = 0$ it is possible to write (assuming A analytical in the control parameter):

$$\mathsf{A}(\mu) = \mathsf{A}(0) + \epsilon\frac{\partial\mathsf{A}}{\partial\mu}\Big|_{\mu=0} + o(\epsilon) = \mathsf{A}_0 + \epsilon\mathsf{A}_1 + o(\epsilon) \tag{2.11}$$

where it has been assumed

$$\mu = 0 + \epsilon + o(\epsilon) \tag{2.12}$$

Then, Equations 2.10 becomes:

$$\dot{\mathsf{x}} = \mathsf{A}_0\mathsf{x} + \epsilon[\mathsf{A}_1 + \mathsf{f}(\mathsf{x};0)] + o(\epsilon) \tag{2.13}$$

where also the coefficient of polynomials f_i has been expanded in a Mac Laurin's series. Observe that Eq. 2.13 represents a perturbation of the problem at its stability margins.

2.2.1 Lie Transform Method

The main idea beyond the Normal Forms method is to simplify the studied problem by eliminating the non-essential nonlinearities by a suitable nonlinear transformation of the coordinates. In this Section the method based on the Lie Transform will be presented (see Refs. [25, 24, 22, 30]). Such a method use a transformation of the flow in a power series of a small parameter ϵ (see Eq. 2.13).

Let us assume that Eq. 2.13 has been cast in diagonal form by using the eigenbasis associated to A_0. Moreover, for the sake of simplicity, only odd nonlinearities up to the third order will be considered.

$$\dot{\mathsf{q}} = \Lambda_0 \mathsf{q} + \epsilon \left(\check{\mathsf{A}}_1 \mathsf{q} + \mathsf{f}(\mathsf{q}) \right) + O(\epsilon^2) \quad \epsilon \ll 1 \tag{2.14}$$

where

$$\mathsf{f}_i(\mathsf{q}) = \sum_{p,q,r=1}^{N} \gamma_{ipqr} q_p q_q q_r \tag{2.15}$$

The Lie Transform method is applied by introducing a near-identity transformation $\mathsf{q} = \eta + \epsilon \mathsf{h}(\eta) + O(\epsilon^2)$ where the function vector $\mathsf{h}(\cdot)$ is the unknown that defines the transformation. The unknown is chosen in order to simplify the problem of Eq. 2.14 giving a simpler form:

$$\dot{\eta} = \Lambda_0 \eta + \epsilon \left(\check{\mathsf{A}}_1^{ess} \eta + \mathsf{f}^{ess}(\eta) \right) \tag{2.16}$$

where it is indicated that only the *essential* (or resonant) contributions to the system response are considered. Now, a criterion to identify the essential terms and disregard the unessential ones is left to choose.

Indeed, it can be demonstrated (see Ref. [19]), that, at the ϵ order the functions h_i are solution of the equation:

$$\sum_{n=1}^{N} \lambda_n y_n \frac{\partial h_j}{\partial q_n} - \lambda_j h_j = \sum_{s=1}^{N} \check{\mathsf{A}}_{1_{js}} q_s + \sum_{p,q,r=1}^{N} \gamma_{jpqr} q_p q_q q_r \tag{2.17}$$
$$j = 1, ..., N$$

If we assume that

$$h_j = \sum_{s=1}^{N} h_{ns}^{(1)} \eta_s + \sum_{p,q,r=1}^{N} h_{npqr}^{(2)} \eta_p \eta_q \eta_r \tag{2.18}$$

and substituting Eq. 2.18 in Eq. 2.17 we obtain:

$$h_j = \sum_{s=1}^{N} \frac{\eta_s}{\lambda_s - \lambda_j} + \sum_{p,q,r=1}^{N} \frac{\eta_p \eta_q \eta_r}{\lambda_p + \lambda_q + \lambda_r - \lambda_j} \tag{2.19}$$

Observing Eq. 2.19, that determines the transformation given in Eq. 2.17, it is clear that only the terms such that

$$\lambda_s - \lambda_n \quad \neq \quad 0 \quad \forall\, n, s = 1, ..., N \tag{2.20}$$

$$\lambda_p + \lambda_q + \lambda_r - \lambda_n \quad \neq \quad 0 \quad \forall\, n, p, q, r = 1, ..., N \tag{2.21}$$

can be eliminated, being non-essential to the process: the remaining ones are obtained by solving Eq. 2.16. Then the solution of Eq. 2.14 is:

$$q_n = \eta_n + \epsilon \left\{ \sum_{s=1}^{N} \frac{\eta_s}{\lambda_s - \lambda_n} + \sum_{p,q,r=1}^{N} \frac{\eta_p \eta_q \eta_r}{\lambda_p + \lambda_q + \lambda_r - \lambda_n} \right\} \tag{2.22}$$

Part II

Analytical Methods: Applications

Chapter 3

Longterm Dynamical Analysis via Normal Form

In the present Chapter, the dynamic response of harmonically forced systems experiencing a postcritical bifurcation will be analyzed via a singular perturbation analysis by analyzing the influence of the physical coefficients on the nonlinear behavior of the response. For this purpose, the model of a beam and of a finite plate forced by a vertical dynamic excitation and subject to an axial static buckling are considered. This physical model is able to represent a variety of response scenarios (see Refs. [55, 56, 57, 58, 59, 60]) and, in particular, they give an interesting opportunity to analyze the concept of small divisors (see Ref. [19]), which is an analytical issue in the perturbation approach. Specifically, the considered partial differential models are reduced via a Galerkin projection on a suitable functional basis to a system of nonlinear forced and coupled oscillators of Duffying-equation type. Indeed, the dynamical behavior of such a isolated nonlinear oscillator has been analyzed in the work of Holmes and Marsden (Ref. [42]) and also by Szemplinska-Stupnika et al. (see Ref. [61]). The Normal Form method is here applied to the coupled system of nonlinear oscillators in order to reduce the problem to a simpler form defined by the resonances conditions. Analyzing how different parameters work in the resonance conditions a physical interpretation of small divisors involved in such a condition is given. In particular, the role of damping is outlined.

3.1 Longterm dynamics of a forced beam

The static behavior of forced beam partial differential equation and the stability properties of its solutions have been recently studied in Refs. [62, 63, 64, 65], whereas its global behavior has been analyzed in Refs. [66, 67, 68]. The effect of an harmonic axial load on system internal resonance is studied in Ref. [69]. In the present work the partial differential equation

of an extensible beam with harmonic transversal load and constant axial load is studied via a perturbation approach based on the Normal Form method (see Refs. [70, 30, 16, 71]) after a space discretization of the original partial differential problem on the modal basis of the structural operator. For more informations about the influence of the number of modes used to discretized the original space-continuum system see Refs. [72, 73].

3.1.1   Governing Equations

Let us consider the dimensional hinged-hinged beam equation, for the sake of simplicity without space-distributed forcing load (see Refs. [65]):

$$\rho_m h \partial_{\tau\tau} w + c \partial_\tau w + D \partial_{x^* x^* x^* x^*} w + \left(N - \frac{EA}{2a} \int_0^a [\partial_x^* w]^2 dx^* \right) \partial_{x^* x^*} w = 0 \tag{3.1}$$

$$w(0,\tau) = w(a,\tau) = \partial_{x^* x^*} w(0,\tau) = \partial_{x^* x^*} w(a,\tau) = 0 \tag{3.2}$$

$$w(x^*, 0) = w_0 \tag{3.3}$$

$$\partial_\tau w(x^*, 0) = \dot{w}_0 \tag{3.4}$$

where a is the length of the beam, ρ_m is the mass per unit length of the beam, $x^* \in [0, a]$ is the dimensional coordinate, c is the damping coefficient, τ is the dimensional time, E is the Young modulus, D is the bending stiffness, A and I are the cross-section area and the moment of inertia of the beam respectively.

Defining the dimensionless time $t = \tau (D / \rho_m h a^4)^{1/2}$ one obtains the dimensionless partial differential equation governing the bending dynamics of a Von Kàrmàn beam:

$$\partial_{tt} u + \delta \partial_t u + \partial_{xxxx} u + \left(R - \frac{1}{2} \int_0^1 [\partial_x u]^2 dx \right) \partial_{xx} u = f \tag{3.5}$$

$$u(0,t) = u(1,t) = \partial_{xx} u(0,t) = \partial_{xx} u(1,t) = 0 \tag{3.6}$$

$$u(x,0) = u_0 \tag{3.7}$$

$$\partial_t u(x,0) = \dot{u}_0 \tag{3.8}$$

where

$$x := \frac{x^*}{a} \qquad \bar{r} = \sqrt{I/A} \qquad u = \frac{w}{\bar{r}}$$

$$R := \frac{N_e a^2}{D} \qquad \delta := \frac{ca^2}{\sqrt{\rho_m h D}}$$

where $u : [0,1] \to \mathbb{R}$, $f : (0,1) \times \mathbb{R}^+ \to \mathbb{R}$ is the vertical load distribution, $R \in \mathbb{R}$ is the axial load acting in the reference configuration (assumed to be positive when the beam is compressed) and $\delta > 0$ is a damping parameter.

3.1.2   ODEs reduction via Galerkin method

The partial differential Equation 3.5 can be reduced to an infinite number of nonlinear ordinary differential equations by projection on a suitable functional basis. Using the eigenfunctions of the self-adjoint structural operator ∂_{xxxx}, it is possible to diagonalize the linear part of the ordinary differential equations system. Indeed, projecting Eq. 3.5 on the complete and orthonormal functional basis $\{\phi^n\} = \{\sqrt{2}\sin(n\pi x)\}$, $n \in \mathbb{N}$, one obtains:

$$\ddot{z}_n + \delta\dot{z}_n + \Omega_n^2 z_n + g_n = f_n(t) \tag{3.9}$$

where the overdots denotes derivative with respect to the dimensionless time t and

$$\Omega_n^2 := \pi^4 n^4 - \pi^2 n^2 R \tag{3.10}$$

whereas the term g_n collects the nonlinear cubic terms

$$g_n := \sum_{p,q,r\in\mathbb{N}} c_{npqr} z_p z_q z_r \tag{3.11}$$

$$c_{npqr} := \frac{1}{2}\pi^4(np)^2\delta_{nq}\delta_{pr} = \gamma\pi^4(np)^2\delta_{nq}\delta_{pr} \tag{3.12}$$

Finally, substituting Eq. 3.12 in Eq. 3.11 one obtains:

$$g_n := \sum_{p,q,r\in\mathbb{N}} c_{npqr} z_p z_q z_r = \gamma n^2 z_n \sum_{p\in\mathbb{N}} \left(\pi^2 p z_p\right)^2 \tag{3.13}$$

Observing that the set $\mathbb{A} = \{\pi, 2\pi, 3\pi...\}$ is numerable with the same cardinality of $\mathbb{N}$, the obtained equations can be rewritten in a simpler form:

$$\ddot{z}_m + \delta\dot{z}_m + m^2(m^2 - R)z_m + \gamma m^2 z_m \sum_{p\in\mathbb{A}} (pz_p)^2 = f_m(t) \tag{3.14}$$

$$m \in \mathbb{A}$$

Assuming that $\exists\, N$ such that for $m > N$ the modal contribution is negligible, the initial P.D.E. problem can be converted in a finite dimensional system of ordinary differential equations. Observing Eq. 3.14 it appears that a qualitative study of the considered system can be done considering $m \in \mathbb{A}/mod(\pi)$ reducing the symbols present in the analysis. Of course, a quantitative study of the problem would require the use of the real values of equations coefficients.

3.1.3   Static behavior of extensible beam equation

The longterm dynamics of Eq. 3.5 has been studied in depth in numerous papers. Referring to Ref. [62], it is possible to establish general condition for the existence of steady solutions

for the considered problem. Moreover, it is possible to prove the existence of a global attractor of Eq. 3.5 that coincides with the unstable manifold of the set of the stationary states, see Ref. [68].

Let us consider Eq. 3.5 without forcing terms:

$$\partial_{xxxx}u + \left(R - \frac{1}{2} \int_0^1 [\partial_x u]^2 dx \right) \partial_{xx}u = 0 \tag{3.15}$$

$$u(0) = u(1) = \partial_{xx}u(0) = \partial_{xx}u(1) = 0 \tag{3.16}$$

Assuming that $u = z_n \phi^n, \forall$ fixed $n \in \mathbb{A}$ one obtains from Eq. 3.15:

$$\sqrt{\lambda_n} z_n (\sqrt{\lambda_n} - R + \gamma \sqrt{\lambda_n} z_n^2) = 0 \tag{3.17}$$

where $\{\lambda_n = n^4\}$ is the set of eigenvalues associated to each eigenfunction ϕ^n of the structural operator, *i.e.*, $\partial_{xxxx}\phi^n = \lambda_n \phi^n$.

Equation 3.17 has only the trivial solution, $z_n = 0$, if and only if $R < \sqrt{\lambda_n}$.

If $R \geqslant \sqrt{\lambda_n}$ (buckling relation) there are also the symmetric solutions:

$$z_n = \pm \sqrt{\frac{R - \sqrt{\lambda_n}}{\gamma \sqrt{\lambda_n}}} = \pm \sqrt{\frac{R - n^2}{\gamma n^2}} \tag{3.18}$$

$$\tag{3.19}$$

$\forall n$ such as $\sqrt{\lambda_n} < R$. This means that there are $2K + 1$ solutions with $K = \bar{n}/\pi$, $\bar{n}$ being the larger integer $n \in \mathbb{A}$ verifying the buckling relation (For further details see Refs. [62, 65]).

3.1.4 One-mode approximation: the Duffing forced and damped equation

A one mode approximation of Eq. 3.14 yields to a Duffing type equation with a damping and a forcing term.

$$\ddot{z} + \delta \dot{z} + (1 - R)z + \gamma z^3 = f(t) \tag{3.20}$$

Let us suppose that the forcing load is harmonic: $f(t) = \mathbf{F} \cos \Omega t$.

The associated static problem (with $\mathbf{F} = 0$) has only the unperturbed stable solution $z = 0$ if $R \leq 1$, otherwise there exists three solutions $z = 0$ (unstable) and $z = \pm \sqrt{\frac{R-1}{\gamma}}$ (stable). The dynamical behavior of Eq. 3.20 is various and can present harmonic solutions and even chaotic motion. The aim of this section is to analyze these different motions.

Equation 3.20 has a set of fixed points. If the forcing load is small in amplitude, $\mathbf{F} = o(\epsilon)$ $\epsilon \ll 1$, the response can be built as a static part plus a dynamical one represented by an oscillation of the same frequency of the load. This involves to write the solution of Eq. 3.20 as:

$$z = z_0 + \epsilon^p z_1(t) \quad \epsilon \ll 1 \ p \geq 1 \tag{3.21}$$

This means that the dynamics develops a harmonic motion around a fixed point.

If the amplitude of the forcing load increases to a larger magnitude, it will not be possible to decompose the static and the dynamic contribution to build the response.

Let us consider a same order interaction between the nonlinear terms and the forcing load: $\mathtt{F} = \epsilon^{3/2}F$, $(R-1) = \epsilon\beta$. Equation 3.20 can be rewritten by imposing $z = \sqrt{\epsilon}\,x$, as:

$$\ddot{x} + \delta\dot{x} = \epsilon(\beta x - \gamma x^3 + F\cos\Omega t) \tag{3.22}$$

The forcing terms can be rewritten using the Euler formulae as the summation of two new state variables:

$$
\begin{aligned}
F\cos\Omega t &= \frac{F}{2}\left(e^{j\Omega t} + e^{-j\Omega t}\right) = \hat{F}\left(x_3 + x_4\right) \\
\hat{F} &= \frac{F}{2} \\
x_{3,4} &= e^{\pm j\Omega t}
\end{aligned}
\tag{3.23}
$$

Finally, $x_{3,4}$, are solutions of two new ODEs:

$$\dot{x}_{3,4} = \pm j\Omega\, x_{3,4} \tag{3.24}$$

Equations 3.22 and 3.24 can be recast in an extended phase-space form:

$$\dot{\mathsf{y}} = \mathsf{A}_0\mathsf{y} + \epsilon\left(\mathsf{A}_1\mathsf{y} - \mathsf{f}_{nl}(\mathsf{y})\right) \tag{3.25}$$

where

$$
\mathsf{A}_0 = \begin{bmatrix} 0 & 1 & 0 & 0 \\ 0 & -\delta & 0 & 0 \\ 0 & 0 & j\Omega & 0 \\ 0 & 0 & 0 & -j\Omega \end{bmatrix}
\tag{3.26}
$$

$$
\mathsf{A}_1 = \begin{bmatrix} 0 & 0 & 0 & 0 \\ \beta & 0 & \hat{F} & \hat{F} \\ 0 & 0 & 0 & 0 \\ 0 & 0 & 0 & 0 \end{bmatrix}
\tag{3.27}
$$

$$
\mathsf{f}_{nl}(\mathsf{y}) = \begin{Bmatrix} 0 \\ \gamma y_1^3 \\ 0 \\ 0 \end{Bmatrix} \Rightarrow f_{nl_i}(\mathsf{y}) = \gamma_{ijkl}y_j y_k y_l
\tag{3.28}
$$

$$
\mathsf{y} = \begin{Bmatrix} x \\ \dot{x} \\ x_3 \\ x_4 \end{Bmatrix}
\tag{3.29}
$$

The phase-space form allows us to use suitable techniques to build approximated solutions. Finally, the whole system can be rewritten using the eigenbasis associated to the state matrix A_0

$$\mathsf{q} = \Lambda_0 \mathsf{q} + \epsilon \left(\check{\mathsf{A}}_1 \mathsf{q} - \check{\mathsf{f}}_{nl}(\mathsf{q}) \right) \tag{3.30}$$

where

$$\Lambda_{0ij} = \lambda_i \delta_{ij} \tag{3.31}$$
$$\lambda_1 = 0$$
$$\lambda_2 = -\delta$$
$$\lambda_{3,4} = \pm j\Omega$$

with

$$\mathsf{A}_{0ij} u_j = \lambda_i u_i \tag{3.32}$$

$$y_i = u_i^{(p)} q_p \tag{3.33}$$

and

$$u_i^{(p)} \check{f}_p(\mathsf{q}) = \gamma_{ijkl} u_j^{(r)} u_k^{(m)} u_l^{(n)} q_r q_n q_m \tag{3.34}$$

Small divisor solution: perturbation approach

An artificial perturbation parameter has been introduced. It can be identified with the increment in the Taylor expansion of the stiffness $(R - 1) = 0 + \beta\epsilon + O(\epsilon^2)$, where the condition $\beta > 0$ corresponds to a post buckling behavior. Then Eq. 3.25 can be solved in the neighborhood of the origin through a small divisors approach as the Lie-Transform method, see Ref. [16], that is equivalent to perform a Normal Form Analysis, see Ref. [71] and [19]. Since the present analysis being interested in a supercritical bifurcation, it is assumed $\beta > 0$.

Normal Forms solution of one-dimensional Duffing Equation

Let us consider Equation 3.25: the right and left eigenvectors matrices are, respectively,

$$
\mathsf{U} = \left\{
\begin{array}{cccc}
1 & 1 & 0 & 0 \\
0 & -\delta & 0 & 0 \\
0 & 0 & 1 & 0 \\
0 & 0 & 0 & 1
\end{array}
\right\}
\tag{3.35}
$$

$$
\mathsf{L} = \left\{
\begin{array}{cccc}
\delta & 1 & 0 & 0 \\
0 & 1 & 0 & 0 \\
0 & 0 & 1 & 0 \\
0 & 0 & 0 & 1
\end{array}
\right\}
\tag{3.36}
$$

then projecting on such basis one obtains:

$$
\dot{q}_1 = \frac{\epsilon}{\delta} \left\{ \beta q_1 + \beta q_2 + \hat{F} q_3 + \hat{F} q_4 - \gamma \left(q_1 + q_2 \right)^3 \right\}
\tag{3.37}
$$

$$
\dot{q}_2 = -\delta q_2 + \frac{\epsilon}{\delta} \left\{ -\beta q_1 - \beta q_2 - \hat{F} q_3 - \hat{F} q_4 + \right.
$$

$$
\left. + \gamma \left(q_1 + q_2 \right)^3 \right\}
\tag{3.38}
$$

$$
\dot{q}_3 = j\Omega q_3
\tag{3.39}
$$

$$
\dot{q}_4 = -j\Omega q_4
\tag{3.40}
$$

Now it is possible to apply the Normal Form procedure showed above. The only resonance conditions are

$$
\lambda_i - \lambda_i = 0 \quad i = 1, ..., 4
\tag{3.41}
$$

$$
\lambda_1 - \lambda_1 + \lambda_1 + \lambda_1 = 0
\tag{3.42}
$$

$$
\lambda_2 - \lambda_2 + \lambda_1 + \lambda_1 = 0
\tag{3.43}
$$

This means that the system given by Eq. 3.37-3.40 can be transformed as (see Sec. 2.2.1):

$$
\dot{\eta}_1 = \frac{\epsilon}{\delta} \left\{ \beta u_1 - \gamma \eta_1^3 \right\}
\tag{3.44}
$$

$$
\dot{\eta}_2 = \left\{ -\delta - \frac{\epsilon}{\delta} \beta + \frac{3\epsilon\gamma}{\delta} \eta_1^2 \right\} \eta_2 = -\tilde{\lambda}(\|\eta_1\|^2, \epsilon)\eta_2
\tag{3.45}
$$

$$
\dot{\eta}_{3,4} = \pm j\Omega \eta_{3,4}
\tag{3.46}
$$

$$
\tag{3.47}
$$

Then the longterm behavior of the beam is given by:

$$
z(t) = \sqrt{\epsilon} x(t)
\tag{3.48}
$$

$$
x(t) = x_0 + x_\epsilon(t) + o(\epsilon)
\tag{3.49}
$$

with

$$x_0 = \sqrt{\frac{\beta}{\gamma}} \qquad (3.50)$$

$$x_\epsilon(t) = -\frac{\epsilon F}{\delta\Omega}\left(\cos\left(\Omega t - \pi/2\right) - \frac{\Omega^2}{\Omega^2 + \delta^2}\cos\left(\Omega t - \pi/2\right) - \right. \qquad (3.51)$$
$$\left. +\frac{\delta\Omega}{\Omega^2 + \delta^2}\cos\left(\Omega t\right)\right)$$

The obtained result has the form shown in Eq. 3.21. This means that under the assumed hypotheses on the order of the interactions among the linear part, nonlinear terms and forcing load the motion can be built as an oscillation around a fixed point. Moreover, it can be observed that the fixed (time-invariant) term in Eqs. 3.49-3.51 is the exact solution for the static problem of the standard buckled beam. This means that our assumptions neglect the influence of the load on the static part of solution. Finally, it can be observed that in the obtained asymptotic series, the convergence to the exact solution is guaranteed not only really by the smallness of the introduced perturbation parameter ϵ, but also by the smallness of a new parameter depending on loading and on damping. Thus, the asymptotic convergence is given by the condition

$$\frac{F}{\delta\Omega}\epsilon = O(\epsilon) \qquad (3.52)$$

This parameter will be analyzed in the following Section together with the small-divisors effects.

Integrability issues and Chaos

The solution given by Eqs. 3.49-3.51 shows the relevance of some parameters to the response and to the integrability of the problem or the smoothly dependence of solutions to system parameters.

In particular, the chosen order interaction among nonlinear terms, linear perturbation and forcing terms allows one to see the response as an oscillation of the same frequency of the forcing load around the buckled fixed point. At this point the first approximation arises by the choice of the order for the forcing load: $\mathtt{F} = O(\epsilon^{3/2})$. It is a key point that the observed motion is well predicted by the proposed approach if the assumed order of interaction is valid.

Moreover, Eq. 3.52 shows that the asymptotic behavior of the solution is guaranteed if and only if a sufficiently high damping and a sufficiently high load frequency are present. This means that the radios of convergence of our approximated solution to the real one depends, for a fixed Ω, on ϵ/δ that must satisfy the usual condition: $\epsilon/\delta \ll 1$. Observing Eq. 3.26 one can observe that $|\lambda_1 + \lambda_2| = \delta$. This means that our Normal Forms assumptions require that

the damping δ is sufficiently high. If the damping is small *i.e.*, $\delta = o(\epsilon)$, the Eqs. 3.44-3.45 are no longer valid. According to the previous observations, the damping is directly related to the presence of a small divisor and to the asymptoticity of the obtained solution and it will be directly related to the possibility of a chaotic response.

Finally, let us consider the role of the load frequency for a fixed value of damping. Observing the condition given by the Eq. 3.52 it is clear that the condition given by Eq. 3.52 is true if and only if the frequency of the response is not too low. This means that the higher the frequency of the harmonic load the better will be our approximation for a fixed ϵ. Nevertheless, a quasi-steady load will show a behavior not predictable with a zero-divisors Normal Form approach.

Figures 3.1 and 3.2 show the effect of the perturbation parameter ϵ on the perturbation solution and compare the results to those of a direct numerical solution of Eq. 3.22. The numerical solution is accurate for any ϵ while the perturbation solution is most accurate for small ϵ. The fixed parameters are:

$$\beta = 1, \quad \delta = 1, \quad F = 1, \quad \Omega = 2, \quad \gamma = 0.5 \tag{3.53}$$
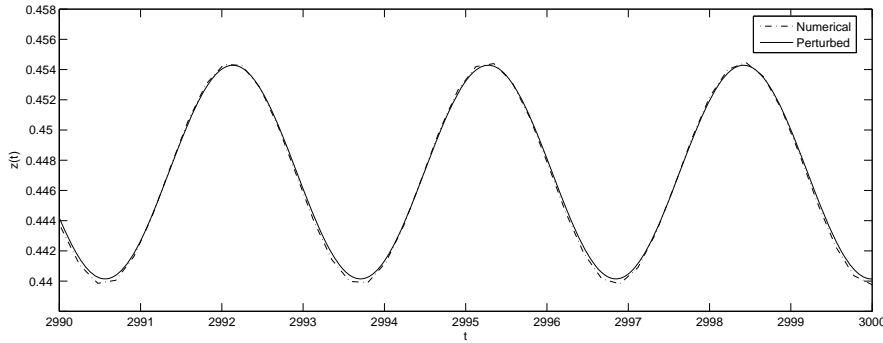
Figure 3.1: Perturbed vs Numerical solution, $\epsilon = 0.1$

Increasing the perturbation parameter, ϵ, shows that the perturbed solution and the numerical one differ as expected. It is interesting to observe that the error is both on the phase and on the static component of the solution, whereas the frequency is still very similar in both solution. This means that, in the presented examples, the solution is still of the form

$$z(t) = z_{stat} + z_{dyn}(t) \tag{3.54}$$

The error on z_{stat} is due to our hypothesis on the load order. From our assumptions, it follows that the forcing load does not influence the essential problem in the Lie Transform method. Let us next consider the effect of the damping δ. The fixed parameters are:

$$\epsilon = 0.1, \quad \beta = 1, \quad \gamma = 0.5, \quad F = 1 \tag{3.55}$$
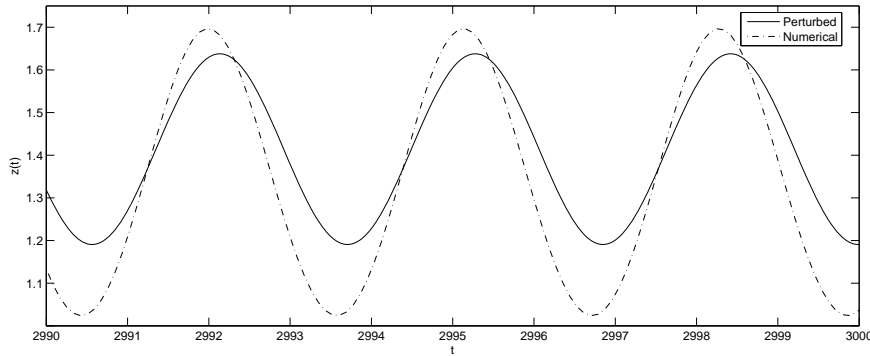
Figure 3.2: Perturbed vs Numerical solution, $\epsilon = 1$

Figures 3.3 and 3.4 show the solution for $\delta = 0.001, \Omega = 2$ and $\delta = 0.001$, $\Omega = 1$.
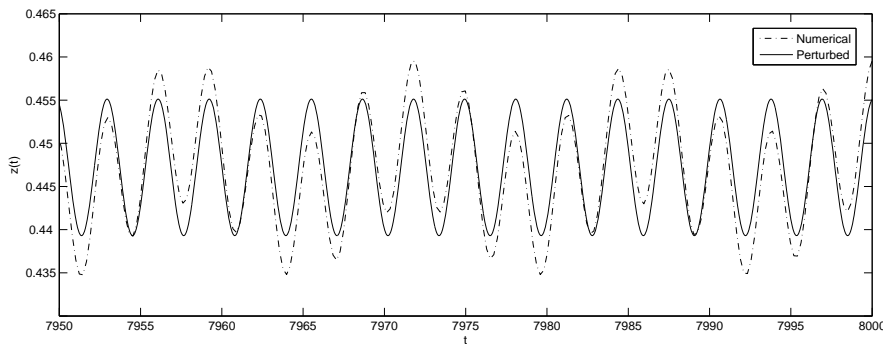
Figure 3.3: Perturbed vs Numerical solution, $\delta = 0.001$ $\Omega = 2$

If the damping is sufficiently small, then the solution is no more an asymptotic expansion, thereby losing its validity. Moreover, we can observe the effect of the load frequency having a smoothing effect on the solution delaying the chaoticity of the response (compare Fig. 3.3 and Fig. 3.4). Equation 3.51 shows that for increasing Ω, the detrimental effect of a small damping δ on the asymptoticity of the solution decreases. [1]

Let us next consider the effect of the load order of magnitude. The Figure 3.5 and 3.6 show the response for $F = 50$ and $F = 500$ respectively. The fixed parameters are:

$$\epsilon = 0.1, \quad \beta = 1, \quad \delta = 1, \quad \gamma = 0.5, \quad \Omega = 2 \tag{3.56}$$

By increasing the load, the structure of the solution, $z(t) = z_{stat} + z_{dyn}(t)$, changes. In particular, in Fig. 3.5 the error is only in the static component of the response, whereas

---

[1]This can be shown observing that Eq. 3.52 depends on the quantity $1/\delta\Omega$ for a fixed F.
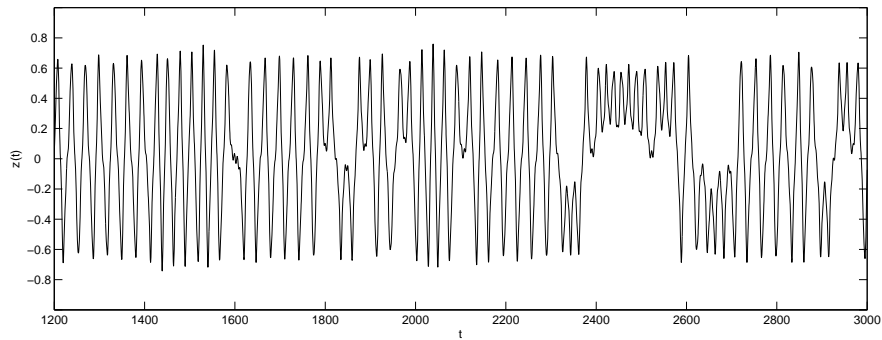
Figure 3.4: Perturbed vs Numerical solution, $\delta = 0.001 \; \Omega = 1$
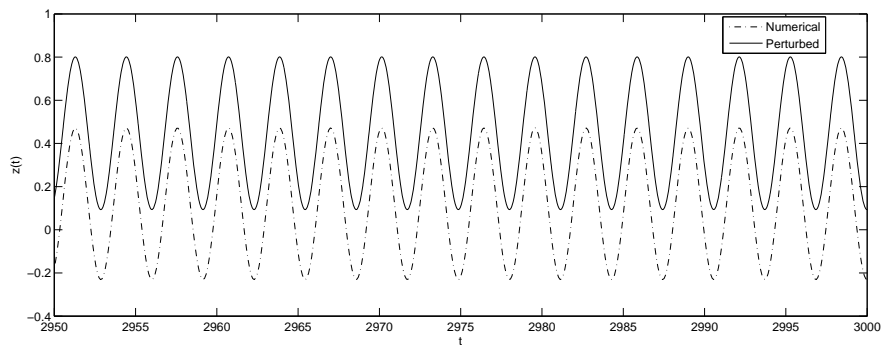
Figure 3.5: $F = 50$
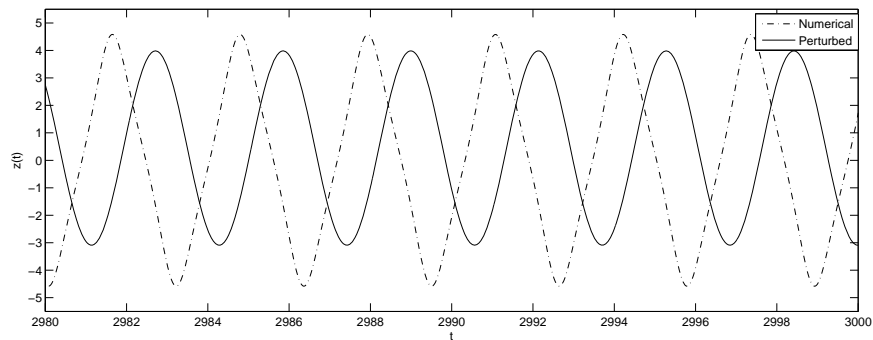
Figure 3.6: Perturbed vs Numerical solution, $F = 500$

in Fig. 3.6 the oscillation is around the origin and there is a phase shift with respect to the perturbation solution. Otherwise, the frequency is the same. The discrepancy shown in Fig. 3.5 is due to the fact that the effect of the load (even if its average is zero) cannot be neglected in computing z_{stat} (as our Normal Form assumptions do).

Quasi-Steady forcing load: a small divisor case

In the previous Section we observed that a quasi-steady load cannot be represented via the zero divisor approach that we chose. Indeed, a slow frequency load means that $\Omega = o(\epsilon)$. This means that the supposed asymptotic behavior of Eq. 3.51 given by condition in Eq. 3.52 is not true. Therefore, it is necessary to take into account the presence of a small divisor. Remembering that $\lambda_1 = 0$, the small divisor condition to consider is $|\lambda_1 - \lambda_{3,4}| = o(\epsilon)$, where $\lambda_1 = 0$ and $\lambda_{3,4} = \pm j\Omega$. From the physical point of view this means that the interaction among inertial and forcing load can not be disregarded. Then, the "essential" system is (remember Sec. 2.2.1):

$$\dot{\eta}_1 = \frac{\epsilon}{\delta}\left(\beta\eta_1 + F\cos\Omega t - \gamma\eta_1^3\right) \tag{3.57}$$

$$\dot{\eta}_2 = \left(-\delta - \frac{\epsilon}{\delta}\beta + \frac{3\epsilon\gamma}{\delta}\eta_1^2\right)\eta_2 = -\tilde{\lambda}(\|\eta_1\|^2, \epsilon)\eta_2 \tag{3.58}$$

where the forcing load is written explicitly. The solution of Eq. 3.57 can be obtained by numerical integration, whereas for times sufficiently large $\eta_2 \to 0$. Finally, substituting in Eq. 2.22 the solution of the whole problem is:

$$z(t) = \sqrt{\epsilon}\eta_1(t) + \tag{3.59}$$
$$+\epsilon\sqrt{\epsilon}\left(-\frac{\beta}{\delta^2}\eta_1(t) + \frac{\gamma}{\delta^2}\eta_1^3(t) - \frac{\Omega}{\delta}\frac{F}{\Omega^2 + \delta^2}\cos(\Omega t - \pi/2)\right.$$
$$\left.-\frac{F}{\Omega^2 + \delta^2}\cos(\Omega t)\right)$$

Observing Eq. 3.59 it is possible to note that the quantity ϵ/δ must be small. Moreover, the obtained solution for $F \to 0$ tends to Eq. 3.49.

The comparison between numerical and perturbed solution is presented in Fig. 3.7 where

$$\epsilon = 0.1, \quad \beta = 1, \quad \delta = 1, \quad \gamma = 0.5, \quad \Omega = 0.01, \quad F = 1 \tag{3.60}$$

Figure 3.7 shows a good qualitative agreement between the numerical and perturbed solutions. The region of the main error is enlarged in Fig. 3.8 which corresponds to the change of direction of the loading.

In Figures 3.9 and 3.10, the effect of the load order is analyzed.

One can observe that by increasing the load the induced error between the perturbed and numerical solution increases slowly with respect to the example with a not small forcing frequency. This is due to the fact that the forcing load appears in the reduced (essential) system.
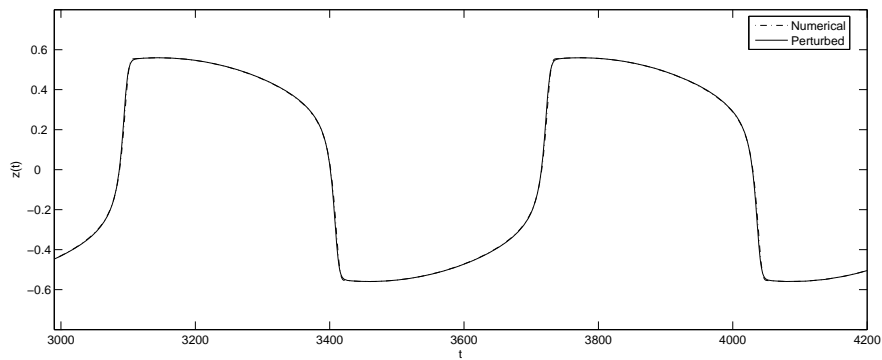
Figure 3.7: Perturbed vs Numerical solution, quasi-static forcing load
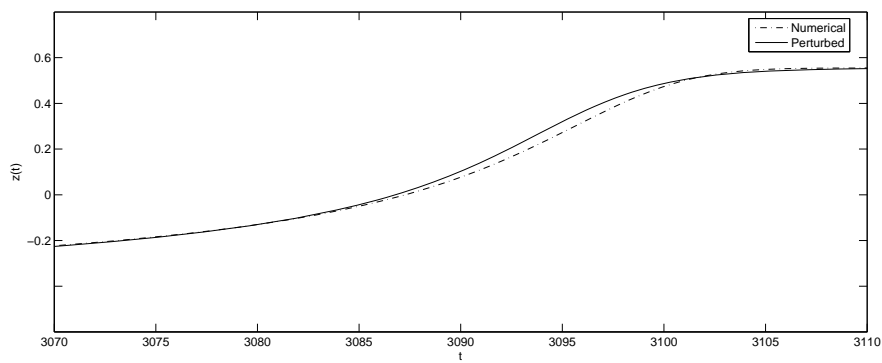
Figure 3.8: Perturbed vs Numerical solution: quasi-static forcing load.
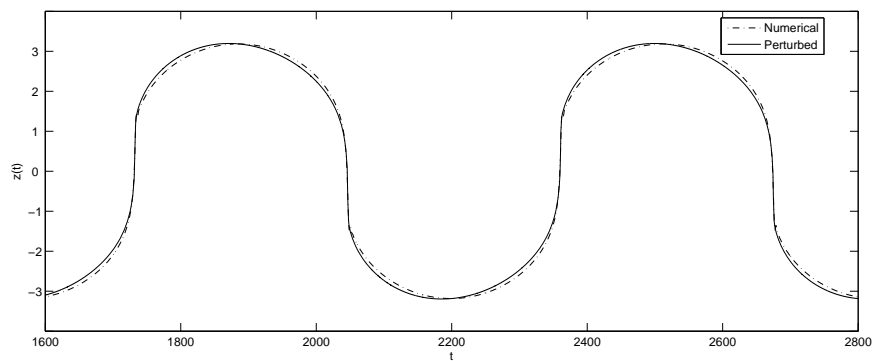
Figure 3.9: Perturbed vs Numerical solution, $F = 500$
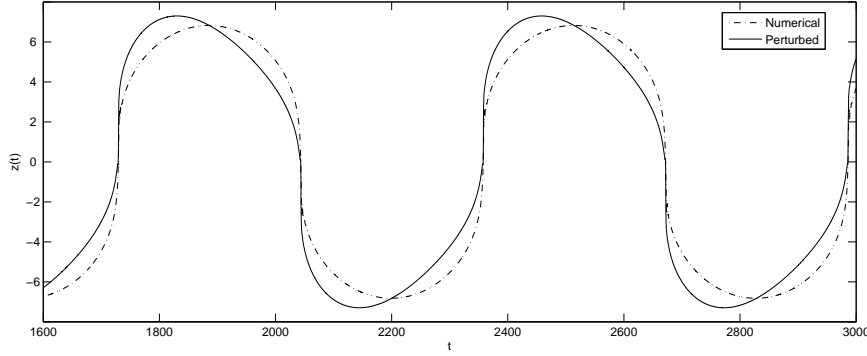
Figure 3.10: Perturbed vs Numerical solution, $F = 5000$

3.1.5 Normal Form of N coupled nonlinear oscillators

In the previous Sections, the problem of a one-mode buckled and forced beam has been considered. In the following the problem of a N-mode approximation will be addressed and the problem of small divisors and its physical meaning analyzed in this new context.

Let us consider Eqs. 3.14 representing the coupling of N nonlinear oscillators: $dim(\mathbb{A}) = N$. The system given by Eqs. (3.14) can be rewritten in a phase-space form introducing this change of variables:

$$\dot{z}_i = v_i \tag{3.61}$$

$$\dot{v}_i = -\delta v_i + i^2(R - i^2)z_i - \gamma i^2 z_i \sum_{p \in \mathbb{A}} (p\, z_p)^2 + \tag{3.62}$$

$$+ \frac{F_i}{2}(q_{i+1} + q_{i+2})$$

$$\dot{q}_{i+1} = j\Omega_i q_{i+1} \tag{3.63}$$

$$\dot{q}_{i+2} = -j\Omega_i q_{i+2} \tag{3.64}$$

$$i \in \mathbb{A} = \{1, ..., N\}$$

Observing Eqs. 3.61-3.64, we can conclude that our beam PDE equation is transformed into $4N$ equations lying in orthogonal planes and that are coupled only by the nonlinear cubic term. Now assuming that $(R - i^2) = i^2\epsilon\hat{\beta}_i + i^2(R_0 - i^2)$ where $\hat{\beta}_i = i^2\beta_i$ (in particular, $\beta = \hat{\beta}_1$), $R_0 = 1$, $z_i = \sqrt{\epsilon}x_i$, $v_i = \sqrt{\epsilon}x_{i+1}$ and $\mathtt{F}_i = \epsilon^{3/2}F$ the above equations can be

rewritten as:

$$\dot{x}_i = x_{i+1} \tag{3.65}$$

$$\dot{x}_{i+1} = -\delta x_{i+1} - i^2(R_0 - i^2)x_i + \epsilon[\hat{\beta}_i x_i - \gamma i^2 x_i \sum_{p \in \mathbb{A}} (p\,x_i)^2 + \tag{}$$

$$+ \quad \hat{F}(q_{i+2} + q_{i+3})] \tag{3.66}$$

$$\dot{q}_{i+2} = j\Omega_i q_{i+2} \tag{3.67}$$

$$\dot{q}_{i+3} = -j\Omega_i q_{i+3} \tag{3.68}$$

$$i \in \mathbb{A} = \{1, ..., N\}$$

The linear part of every i-th system can be transformed in a diagonal form using the transformations:

$$x_i = \xi_i + \bar{\xi}_i \tag{3.69}$$

$$x_{i+1} = \lambda_i \xi_i + \bar{\lambda}_i \bar{\xi}_i \tag{3.70}$$

For $i = 1$ we obtain the same Equations analyzed in Sec. 3.1.4 with the difference of a nonlinear terms involving all the other coordinates. Whereas, the other Equations are:

$$\dot{\xi}_i = \lambda_i \xi_{i+1} - \frac{\epsilon}{2j\omega_i}[\hat{\beta}_i \xi_i + \hat{\beta}_i \bar{\xi}_i - \gamma i^2 \xi_i \sum_{p \in \mathbb{A}} p^2 \left(\xi_p + \bar{\xi}_p\right)^2 + \tag{}$$

$$+ \quad \hat{F}(q_{i+2} + q_{i+3})] \tag{3.71}$$

$$\dot{\bar{\xi}}_i = \bar{\dot{\xi}}_i \tag{3.72}$$

$$\dot{q}_{i+2} = j\Omega_i q_{i+2} \tag{3.73}$$

$$\dot{q}_{i+3} = -j\Omega_i q_{i+3} \tag{3.74}$$

$$i \in A = \{2, ..., N\}$$

where $j\omega_i = \Im m\{\lambda_i\} = \lambda_{I_i} = \Im m\{-\frac{\delta}{2} + \sqrt{\frac{\delta^2}{4} + i^2(R_0 - i^2)}\}$ $i > 1$.

The spectrum of the linear parts of the studied systems is made in the bifurcation point $R = 1$ by $\lambda_1 = 0$, $\lambda_2 = -\delta$, $\lambda_{i+1} = \bar{\lambda}_i$. Thus, the resonance conditions are:

$$\lambda_1 + \lambda_1 = 0 \tag{3.75}$$

$$\lambda_i + \lambda_1 + \lambda_1 - \lambda_i = 0 \tag{3.76}$$

Then applying the Normal Form procedure one obtains:

$$\dot{\eta}_1 = \frac{\epsilon}{\delta}\left(\beta\eta_1 - \gamma\eta_1^3\right) \tag{3.77}$$

$$\dot{\eta}_2 = \left(-\delta - \frac{\epsilon}{\delta}\beta + \frac{3\epsilon\gamma}{\delta}\eta_1^2\right)\eta_2 =$$

$$= -\tilde{\lambda}(\|\eta_1\|^2, \epsilon)\eta_2 \tag{3.78}$$

$$\dot{\eta}_i = \left(\lambda_i + \epsilon\hat{\beta}_i + \frac{3\epsilon\gamma_i}{2j\omega_i}\right)\eta_i = -\tilde{\lambda}(\|\eta_1\|^2, \epsilon)\eta_i \tag{3.79}$$

$$\dot{\bar{\eta}}_i = \bar{\dot{\eta}}_i \tag{3.80}$$

$$\dot{q}_{i+2} = j\Omega_i q_{i+2} \tag{3.81}$$

$$\dot{q}_{i+3} = -j\Omega_i q_{i+3} \tag{3.82}$$

$$i \in A = \{2, ..., N\}$$

The solution of Eq. 3.77 has been given in Sec. 3.1.4, whereas $\eta_2 = 0$ for sufficiently large times. Then substituting in Eq. 2.22 the results of Eqs. 3.77, 3.79 and the explicit expression for the forcing loads (see Eqs. (3.81)-3.82), one obtains the solution of the beam equation discretized with N modes:

$$z_1 = \sqrt{\epsilon}\sqrt{\frac{\beta}{\gamma}} - \frac{\epsilon F}{\delta}\sqrt{\epsilon}\left(\frac{1}{\Omega}\cos\left(\Omega t - \pi/2\right)\right.$$
$$\left. -\frac{\Omega}{\Omega^2 + \delta^2}\cos\left(\Omega t - \pi/2\right) - \frac{\delta}{\Omega^2 + \delta^2}\cos\left(\Omega t\right)\right) \tag{3.83}$$

$$z_i = -\epsilon\sqrt{\epsilon}\frac{F_i}{\omega_i}\left(\frac{\Omega_i}{(\Omega_i - \omega_i)^2 + \lambda_{R_i}^2}\cos(\Omega_i t)+\right.$$
$$\left. +\frac{|\lambda_i|}{(\Omega_i - \omega_i)^2 + \lambda_{R_i}^2}\sin(\Omega_i t - \angle\lambda_i)\right) \tag{3.84}$$

with $i = 2, ..., N$ and

$$\lambda_i = \lambda_{R_i} + j\lambda_{I_i} = \lambda_{R_i} + j\omega_i = \left(\lambda_{R_i}^2 + \lambda_{I_i}^2\right)e^{j\angle\lambda_i} = |\lambda_i|e^{j\angle\lambda_i}$$

From Equations 3.83-3.84, one can observe that the results for the N-dimensional problem, under the assumed hypothesis on the order of interaction between the equation's terms, are similar to the ones for $N = 1$. The motions still remains as an oscillation around a fixed point. This oscillation is characterized by a finite number of frequencies Ω_i. Note that in the explained case resonance is not considered. If a resonance is present this means that one has to consider the forcing load in the equations of normal forms but that (under the assumed hypotheses of terms interaction) without a coupling within different modes (at the considered order) as analyzed in Ref. [71].

The motion along the stable modes $z_i(t)$ must be *small* and of order $\epsilon^{3/2}$. Equations 3.84

show that the response is small if and only if the following relation is true (remember that the resonances are not considered):

$$\frac{F_i}{\omega_i} = O(1) \tag{3.85}$$

This means that not only the forcing load can cause a strong nonlinear response, as expected, but also the presence of low frequencies. The condition $\omega_i \ll 1$ means that $|\lambda_i - \bar{\lambda}_i| = |\lambda_i - \lambda_{i+1}| \ll 1$: new resonance conditions appear and our Normal Form is not longer valid. The solution for the critical mode has been already studied in Sec. 3.1.4. In Figures 3.11-3.12 the perturbed solution for the $N = 2$ is presented and compared with the numerical one. The fixed parameters are assumed to be:

$$\epsilon = 0.1 \quad \beta = 1 \quad \beta_2 = 1 \quad \delta = 1 \quad \gamma = 0.5 \quad \Omega_1 = 1$$

$$\Omega_2 = 2 \quad \omega_2 = 3.369 \quad F_{1,2} = 1 \tag{3.86}$$

The comparison in Figs. 3.11-3.12 shows a good qualitative agreement between the numer-
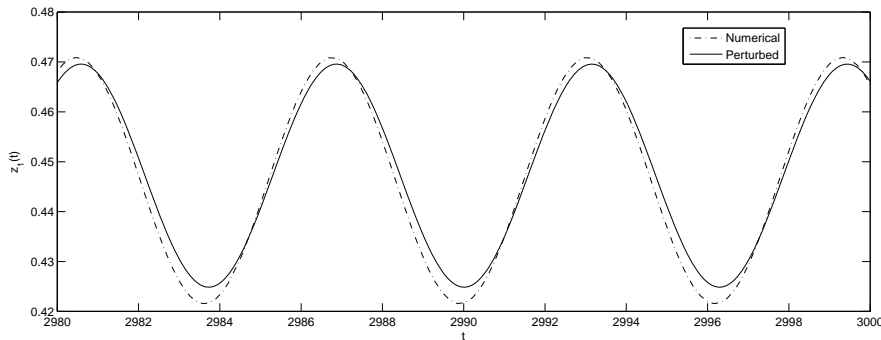
Figure 3.11: Comparison between perturbed and numerical solution along the generic 1-th unstable mode

ical solution and the one obtained via Normal Form.

Let us consider a resonant load: $\omega_2 = \Omega_2 = 3.369$ with the others parameters equal to those of the previous example. In Figures 3.13-3.14 the comparison between numerical and perturbed solutions is shown. In particular, one can observe that the effect of the resonance is compensated by the presence of high damping. Indeed, observing Eqs. 3.83-3.84 it appears that the higher the damping the smaller are the high order terms in the asymptotic expansion (note that λ_{R_i} is proportional to the damping for a stable mode).

To underline the role of damping let us consider a case with low damping and resonant
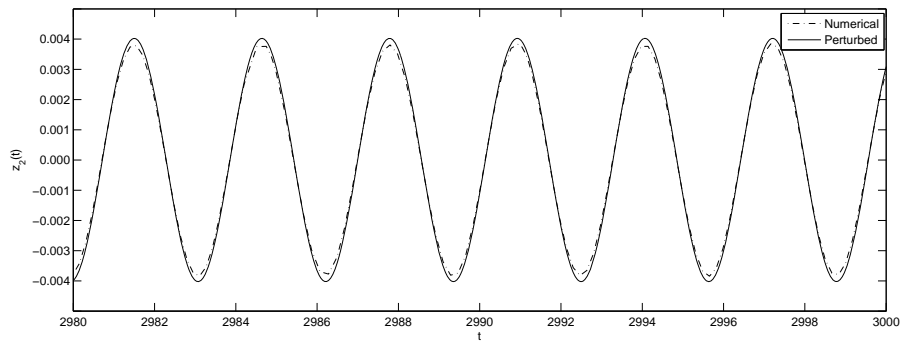
Figure 3.12: Comparison between perturbed and numerical solution along the generic 2-th stable mode
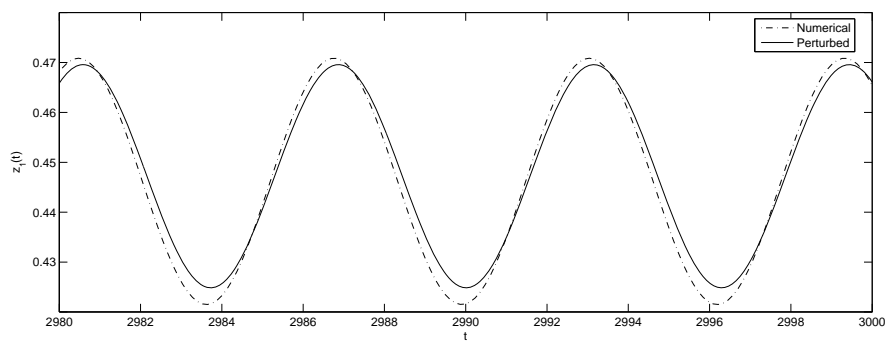
Figure 3.13: Comparison between perturbed and numerical solution along the generic 1-th unstable mode, resonant case.
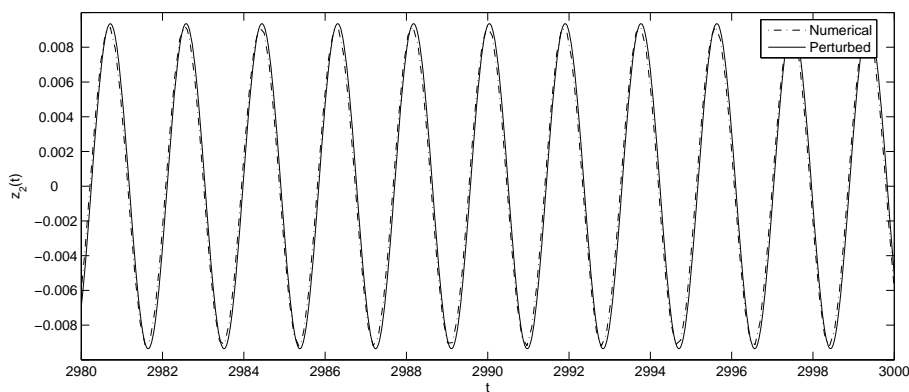
Figure 3.14: Comparison between perturbed and numerical solution along the generic 2-th stable mode, resonant case.

load:

$$\epsilon = 0.1 \quad \beta = 1 \quad \beta_2 = 1 \quad \delta = 0.1 \quad \gamma = 0.5 \quad \Omega_1 = 1$$

$$\Omega_2 = \omega_2 = 3.406 \quad F_{1,2} = 1 \tag{3.87}$$

In Figure 3.15 it is shown the comparison between the numerical and perturbed solution for the motion along the stable mode and a discrepancy between numerical and perturbed solution can be observed being no longer true the conditions that ensures Eq. 3.84 to be an asymptotic expansion. Finally, recalling Eq. (3.84) one can observe the necessity that
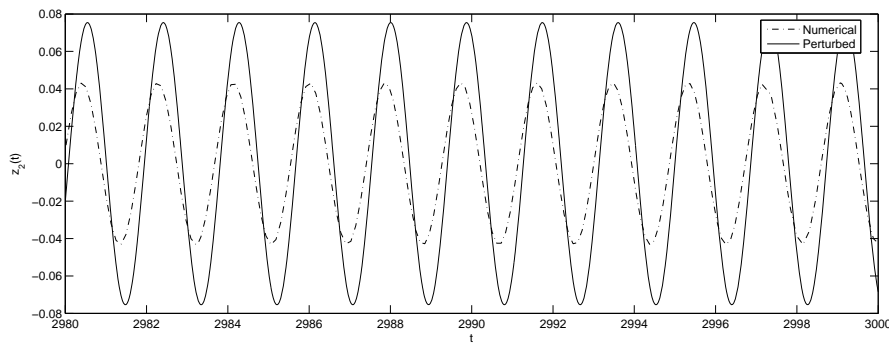
Figure 3.15: Comparison between perturbed and numerical solution along the generic 2-th stable mode, resonant case with low damping.

$$\frac{F_i}{\omega_i} = O(1) \tag{3.88}$$

The condition on the load has been already analyzed, then let us consider what role ω_i plays. The eigenfrequency depends on the stiffness (and thus on the axial load) and on the damping. If the axial load is sufficient the mode experiences a static bifurcation, $\omega_i = 0$ and the Normal Form assumptions are no longer valid. If the damping is too large the studied mode is associated to a real negative eigenvalues and again our Normal Form is no longer valid. From the above results it is interesting to stress that again the damping plays an important role in the small divisor, although implicitly.

3.1.6 Concluding Remarks

The dynamic response of a harmonically forced beam experiencing a pitchfork bifurcation have been studied through a space-discretization and then a singular perturbation approach based on Normal Form method. The obtained system of ordinary differential equation can be considered integrable if there exists a continuous dependence between the solution and the parameters present in the equations. This implies that, using a perturbation approach, the asympoticity of the series representing the solution is guaranteed. This statement is related

to the absence of zero or small divisors in the obtained asymptotic expansion and this is a key issue in the perturbation approach and well stressed by the Normal Form method used in this paper. The performed analysis, original contribution of such a thesis, have emphasized the role of the damping in the presence of a weakly chaotic response for weak forcing load. Indeed, the smaller the damping the smaller is the magnitude of forcing harmonic loads that cause chaotic responses. Moreover, the role of the load frequency has been investigated for the quasi-steady case (low frequency) and an analytical solution has been obtained. Finally, it is relevant to observe that the obtained found solutions, obtained as asymptotic series, allows to give some quantitative consideration about the small divisors. Indeed, the role of damping and load frequency as small divisors has been studied and a quantitative estimation of their smallness given.

3.2 Longterm dynamics of a two dimensional Von Kármán panel

In Sec. 3.1 the longterm dynamics of a one-dimensional continuum system has been analyzed. In this Section the analysis is extended to a two-dimensional forced system with aeroelastic terms and both structural and aerodynamical nonlinearities. For this purpose, the problem of a plate subjected to a biaxial compressive load and to a supersonic flow together with a transversal harmonic load has been investigated (Ref. [6]). The effects of the relevant physical parameters have been studied in order to investigate how they relate with the zero and small divisors concept (see Ref. [44]) in the Normal Form reduction method (see Ref. [42]) extending the results of Sec. 3.1. As in the previous Section, the partial differential equation governing the behavior of the panel is studied via a perturbative approach based on the Normal Form method (see Refs. [27, 21, 74, 16, 71]) after a space discretization of the original partial differential problem. Specifically, a Galerkin projection on aS suitable functional basis is used to obtain a system of nonlinear forced and coupled oscillators. The simplified system is defined by satisfying the so-called resonance conditions (Ref. [44, 16]). A physical interpretation of some small divisors is given and, in particular, the role of damping is also investigated.

3.2.1 Governing Equation and Boundary Conditions

Let us consider the equilibrium of an elastic rectangular panel simply supported and exposed to one side to a supersonic flow with unperturbed velocity U. We shall employ the usual Kirchhoff-Love hypothesis for the nonlinear theory of elastic plates, which assumes that the deflections of the shell are of comparable magnitude with the plate thickness h, but small

compared with its edge lengths a and b. The partial differential equations governing the considered physical problem are (see Ref. [6]):

$$\rho h w_{,\tau\tau} + \rho h \delta w_{,\tau} + D\nabla^2\nabla^2 w = \phi_{,yy}w_{,xx} + \phi_{,xx}w_{,yy} - 2\phi_{,xy}w_{,xy} + f + p - p_\infty \tag{3.89}$$

$$\frac{1}{Eh}\nabla^2\nabla^2\phi = (w_{,xy})^2 - w_{,xx}w_{,yy} \tag{3.90}$$

$$\nabla^2\nabla^2(\cdot) = (\cdot)_{,xxxx} + (\cdot)_{,yyyy} + 2(\cdot)_{,xxyy} \tag{3.91}$$

where $w(x, y, t)$ is the vertical displacement, δ is the damping coefficient, ρ is the material density of the panel, E the Young modulus, $p - p_\infty$ is the differential pressure load on the panel surface as given by the aerodynamic loads, ϕ the Airy's stress function defined by the following relations:

$$N_x = \phi_{yy} \quad N_y = \phi_{xx} \quad N_{xy} = -\phi_{xy} \tag{3.92}$$

which implies that the in-plane equilibrium equation

$$N_{x,x} + N_{xy,y} = 0 \quad N_{yx,x} + N_{y,y} = 0 \quad N_{yx} = N_{xy} \tag{3.93}$$

are automatically satisfied. The considered panel is simply supported, or

$$w\mid_{x=0} = w_{xx}\mid_{x=0} = 0 \quad w\mid_{x=a} = w_{xx}\mid_{x=a} = 0 \tag{3.94}$$

$$w\mid_{y=0} = w_{yy}\mid_{y=0} = 0 \quad w\mid_{y=b} = w_{yy}\mid_{y=b} = 0 \tag{3.95}$$

The initial condition are given by

$$w(x, y, 0) = \bar{w} \quad w_{,t}(x, y, 0) = \bar{\bar{w}} \tag{3.96}$$

The boundary condition for Eq. 3.90 can be imposed "on the average" (see Ref. [6]). In particular, assuming that

$$\phi(x, y, t) = \phi_1(x, y, t) + \frac{1}{2}(N_x y^2 + N_y x^2 - 2N_{xy}xy). \tag{3.97}$$

where $\phi_1(x, y, t)$ is somea particular solution of Eq. 3.90 "zero on average", on the boundary of the physical domain and N_x, N_y, N_{xy} are the average forces along the edges of the plate:

$$\frac{1}{b}\int_0^b \phi_{,yy}\mid_{x=0} dy =: N_x \tag{3.98}$$

$$\frac{1}{a}\int_0^a \phi_{,xx}\mid_{y=0} dx =: N_y \tag{3.99}$$

$$\frac{1}{a}\int_0^a \phi_{,xy}\mid_{y=0} dx =: N_{xy} \tag{3.100}$$

Finally, the gas pressure on one side of the panel can be modeled using the Piston Theory (see Ref. [6, 75]). Retaining three terms of the expansion one obtains:

$$\rho h w_{,tt} + (\rho h \delta + \frac{\gamma p_\infty}{a_\infty})w_{,t} + D\nabla^2\nabla^2 w + \gamma p_\infty M w_{,x} + \frac{\gamma(\gamma+1)p_\infty M^2}{4}w_{,x}^2 +$$

$$+\frac{\gamma(\gamma+1)^2 p_\infty M^3}{12}w_{,x}^3 = \phi_{,yy}w_{,xx} + \phi_{,xx}w_{,yy} - 2\phi_{,xy}w_{,xy} + f \tag{3.101}$$

where γ is the polytropic index, a_∞ is the velocity of sound in the undisturbed gas and M is the Mach number.

3.2.2 ODE's reduction via Galerkin Method and Solution of Airy's Equation

Let us assume that the space-continuum displacement can be expressed as

$$w(x, y, t) = \sum_{i,j=1}^{N_M} q_j(t) \psi^j(x, y) \tag{3.102}$$

where it is assumed that the response can be represented by the linear combination of N_M independent and orthogonal functions $\{\psi^j\}_1^{N_M}$ verifying the boundary condition given by Eq. 3.94-3.95. By Equation 3.89 one can observe that the spatial operator $\nabla^2\nabla^2$, together with the given spatial boundary condition, is self adjoint and positive. This means that its eigenfunctions (in the simply supported case here considered $\psi^{m,n}(x, y) = \sin \frac{n\pi x}{a} \sin \frac{m\pi y}{b}$) describe a system of independent and orthogonal functional basis verifying Eq. 3.94-3.95 and we can use such a functional system as a basis to represent the problem.

Let us consider the dynamic deflection in the form of only two terms of the cited basis:

$$w(x, y, t) = q_1(t) \sin \frac{\pi x}{a} \sin \frac{\pi y}{b} + q_2(t) \sin \frac{2\pi x}{a} \sin \frac{\pi y}{b} \tag{3.103}$$

Substituting Expression 3.103 in Eq. 3.90 and remembering Eq. 3.97 one has (see Ref. [6]):

$$\phi_1(x, y, t) = \frac{Eh\varphi^2}{4} \left[-q_1 q_2 \cos \frac{\pi x}{a} + \frac{q_1^2}{8} \cos \frac{2\pi x}{a} + \frac{q_1 q_2}{9} \cos \frac{3\pi x}{a} + \frac{q_2^2}{32} \cos \frac{4\pi x}{a} + \right.$$

$$\left. \frac{9q_1 q_2}{(1+4\varphi^2)^2} \cos \frac{\pi x}{a} \cos \frac{2\pi y}{b} - \frac{q_1 q_2}{(9+4\varphi^2)^2} \cos \frac{3\pi x}{a} \cos \frac{2\pi y}{b} + \frac{q_1^2 + 4q_2^2}{8\varphi^4} \cos \frac{2\pi y}{b} \right] \tag{3.104}$$

where $\varphi = a/b$. The solution for the Airy's function is:

$$\phi(x, y, t) = \phi_1(x, y, t) - \frac{1}{2}(N_x y^2 + N_y x^2) \tag{3.105}$$

Writing Equation 3.89 in the shortened form $\Gamma[w; f] = 0$, we make the requirement that it is satisfied approximately in the sense of Galerkin's method in the subspace spanned by the eigenfunctions $\{\psi^j\}_1^{N_M}$:

$$\int_0^a \int_0^b \Gamma[w; f] \psi^j dx dy = 0 \quad j = 1, ..., N_M \tag{3.106}$$

Assuming a 2-mode approximation for the vertical displacement, as given by Eq. 3.103, and for the external load $f(x, y, t) = f_1\sqrt{\frac{4}{ab}} \cos \Omega_1 t \sin \frac{\pi x}{a} \sin \frac{\pi y}{b} + f_2\sqrt{\frac{4}{ab}} \cos \Omega_2 t \sin \frac{2\pi x}{a} \sin \frac{\pi y}{b}$,

one obtains after a Galerikin projection on the basis $\{\psi^j\}_1^2$:

$$\ddot{x}_1 + g\dot{x}_1 + \omega_1^2 x_1 + K\left[-\frac{2}{3}\nu x_2 + \frac{2}{9}\nu^2(\gamma+1)x_1^2 + \frac{56}{45}\nu^2(\gamma+1)x_1^2 + \right.$$
$$\left. +\nu^3 x_2(b_{11}x_1^2 + b_{12}x_2^2)\right] + Sx_1(c_{11}x_1^2 + c_{12}x_2^2) = f_1\cos\Omega_2 t \tag{3.107}$$

$$\ddot{x}_2 + g\dot{x}_2 + \omega_2^2 x_2 + K\left[\frac{2}{3}\nu x_1 + \frac{16}{45}\nu^2(\gamma+1)x_1 x_2 + \nu^3 x_1(b_{21}x_1^2 + b_{22}x_2^2)\right] +$$
$$+Sx_2(c_{21}x_1^2 + c_{22}x_2^2) = f_2\cos\Omega_2 t \tag{3.108}$$

If both sides of the panel are exposed to the flow, the second order terms can be disregarded (Ref. [6]). Moreover, in general, it is to be expected that the effect of second-order terms will be small compared with the effect of third-order terms (see Ref. [6, 76]). Equations 3.107-3.108 become:

$$\ddot{x}_1 + g\dot{x}_1 + \omega_1^2 x_1 + K\left[-\frac{2}{3}\nu x_2 + \right.$$
$$\left. +\nu^3 x_2(b_{11}x_1^2 + b_{12}x_2^2)\right] + Sx_1(c_{11}x_1^2 + c_{12}x_2^2) = f_1\cos\Omega_2 t \tag{3.109}$$

$$\ddot{x}_2 + g\dot{x}_2 + \omega_2^2 x_2 + K\left[\frac{2}{3}\nu x_1 + \nu^3 x_1(b_{21}x_1^2 + b_{22}x_2^2)\right] +$$
$$+Sx_2(c_{21}x_1^2 + c_{22}x_2^2) = f_2\cos\Omega_2 t \tag{3.110}$$

where the equations coefficients are found in Ref. [6, 77]. Moreover,

$$x_1 = \frac{q_1}{h} \quad x_2 = \frac{q_2}{h} \quad \Omega_0 = \frac{\pi^2}{a^2}\sqrt{\frac{D}{\rho h}} \quad t = \frac{\tau}{\Omega_0}$$
$$\omega_j = \frac{\Omega_j}{\Omega_0} \quad g = \frac{1}{\Omega_0}\left(\delta + \frac{\gamma p_\infty}{\rho h a_\infty}\right) \quad \nu = M\frac{h}{a}$$
$$K = \frac{4\gamma p_\infty}{\rho h^2 \Omega_0^2} \quad S = \frac{\pi^4 E h^2}{16\rho a^4 \Omega_0^2} = \frac{3}{4}(1-\bar{\nu}) \tag{3.111}$$

with $\bar{\nu}$ the Poisson's coefficient and

$$\omega_1^2 = \left[(1+\varphi^2)^2 - \frac{a^2}{\pi^2 D}(N_x + \varphi^2 N_y)\right] \tag{3.112}$$

$$\omega_2^2 = \left[(4+\varphi^2)^2 - \frac{a^2}{\pi^2 D}(4N_x + \varphi^2 N_y)\right] \tag{3.113}$$

The system given by Eqs. 3.109-3.110 can be rewritten as

$$\mathsf{x} = \{x_1, x_2\}^{\mathrm{T}} \tag{3.114}$$

$$\ddot{\mathsf{x}} + \mathsf{C}\dot{\mathsf{x}} + (\mathsf{K} + \mathsf{A}_{\mathrm{aero}})\mathsf{x} + \hat{\mathsf{f}}_{\mathrm{nl}}(\mathsf{x}) = \hat{\mathsf{f}} \tag{3.115}$$

where

$$C = \begin{bmatrix} g & 0 \\ 0 & g \end{bmatrix} \tag{3.116}$$

$$K = \begin{bmatrix} \omega_1^2 & 0 \\ 0 & \omega_2^2 \end{bmatrix} \tag{3.117}$$

$$A_{\text{aero}} = \begin{bmatrix} 0 & -\frac{2}{3}\nu K \\ \frac{2}{3}\nu K & 0 \end{bmatrix} \tag{3.118}$$

$$\hat{f}_{\text{nl}}(x) = \left\{ \begin{array}{c} \nu^3 K (b_{11}x_2 x_1^2 + b_{12}x_3^2) + S(c_{11}x_1^3 + c_{12}x_1 x_2^2) \\ \nu^3 K (b_{21}x_1^3 + b_{22}x_1 x_2^2) + S(c_{21}x_2 x_1^2 + c_{22}x_2^3) \end{array} \right\} \tag{3.119}$$

$$\hat{f}(x) = \left\{ \begin{array}{c} f_1 \cos \Omega_1 t \\ f_2 \cos \Omega_2 t \end{array} \right\} \tag{3.120}$$

Finally, a phase-space form is obtained:

$$y = \{x_1, x_2, \dot{x}_1, \dot{x}_2\}^{\mathrm{T}}$$

$$\dot{y} = Ay + f_{\text{nl}}(y) + f \tag{3.121}$$

with

$$A = \begin{bmatrix} O & I \\ -C & -(K + A_{\text{aero}}) \end{bmatrix} \tag{3.122}$$

$$f_{\text{nl}} = \left\{ \begin{array}{c} 0 \\ 0 \\ \hat{f}_{\text{nl}} \end{array} \right\} \tag{3.123}$$

$$\bar{f} = \left\{ \begin{array}{c} 0 \\ 0 \\ \hat{f} \end{array} \right\} \tag{3.124}$$

with O is the 2×2 zero matrix.

3.2.3   Perturbative approach and stability scenarios

The presented equations represent a family of systems depending on the parameters ν and the axial loads N_x and N_y. The considered system can experience both static and dynamic bifurcation of the equilibrium solution. This means, that the trivial solution $y = 0$ become unstable and a new stable solution arises: a new fixed point (buckling) or an harmonic oscillation (flutter), see Ref. [6]. The buckling loads are all the combinations of N_x and N_y such that the right hand sides of Eqs. 3.112-3.113 are negative (independent on the value of

ν) whereas the critical value to observe the flutter is (under the hypothesis of small structural damping) $\nu^* = \frac{3}{4K}(\omega_2^2 - \omega_1^2)$ (see Ref. [6]).

Before starting a perturbative analysis, it is necessary to *order* the system's terms through a perturbation parameter linked to the physical parameter governing the bifurcation process. In the present problem one has two possibilities: the axial load (driving the static bifurcation) and the "geometrically scaled" Mach number $\nu = M\frac{h}{a}$ driving the dynamical (namely, Hopf-type) bifurcation. Let us consider the panel system in the form given by Eqs. 3.121. Expressing the general parameter governing the bifurcation process as $\mu = \mu_0 + \epsilon\mu_1 + o(\epsilon)$ with $\epsilon \ll 1$ and μ_0 the critical value of the governing parameter, the state matrix can be written as:

$$\mathsf{A} = \mathsf{A}_0 + \epsilon\mathsf{A}_1 + o(\epsilon) \tag{3.125}$$

Moreover the nonlinear term, here expressed in a general form with coefficient depending on μ, can be written as:

$$\mathsf{f}_i(\mu) = \sum_{p,q,r=1}^{N} \gamma_{ipqr}(\mu)q_pq_qq_r = \sum_{p,q,r=1}^{N} \gamma_{ipqr}(\mu_0)q_pq_qq_r + o(\epsilon) \tag{3.126}$$

Now, one has to consider the forcing load. In this work we assume to be in presence of weak forcing load interacting at the same order of the nonlinear terms:

$$\bar{\mathsf{f}} = \epsilon^{3/2}\mathsf{f} \tag{3.127}$$

Finally, scaling the response as $\mathsf{q} = \sqrt{\epsilon}\bar{\mathsf{q}}$ one obtains the following form

$$\dot{\bar{\mathsf{q}}} = \mathsf{A}_0\bar{\mathsf{q}} + \epsilon[\mathsf{A}_1 + \mathsf{f}(\mu_0) + \bar{\mathsf{f}}] \tag{3.128}$$

which is equivalent to the system given by Eq. 2.14 up to a linear transformation, *i.e.*, expressing the problem on the eigenbasis of A_0.

Static bifurcation with forcing load

Let us assume the PDE model given by Eqs. 3.89-3.90 is experiencing a static, *i.e.*, pitchfork-type, bifurcation. Let us study the structural dynamics disregarding the aerodynamic terms, $\nu = 0$, so to obtain, after the Galerikin procedure presented in Sec. 3.2.2, the following form for the two-mode panel system

$$\ddot{x}_1 + g\dot{x}_1 + \omega_1^2 x_1 + Sx_1(c_{11}x_1^2 + c_{12}x_2^2) = f_1\cos\Omega_1 t \tag{3.129}$$

$$\ddot{x}_2 + g\dot{x}_2 + \omega_2^2 x_2 + Sx_2(c_{21}x_1^2 + c_{22}x_2^2) = f_2\cos\Omega_2 t \tag{3.130}$$

where, assuming $N_y = 0$, one has:

$$\omega_1^2 = (1 + \varphi^2)^2 - \bar{N}_x \tag{3.131}$$

$$\omega_2^2 = (4 + \varphi^2)^2 - 4\bar{N}_x \tag{3.132}$$

being $\bar{N}_x = \frac{a^2}{\pi^2 D} N_x$ the dimensionless axial load. The buckling load $N_{x_{cr}}$ is such that either ω_1 or ω_2 in Eqs. 3.131-3.132 is zero. For the sake of simplicity, we can assume that the first mode will be the buckling one: $N_{x_{cr}} = (1 + \varphi^2)^2$. This is true if $\varphi < \sqrt{2}$. Equations 3.129-3.130 can be rewritten in the first order form

$$\dot{x}_i = v_i \tag{3.133}$$

$$\dot{x}_i = -gv_i - \omega_i^2 x_i - Sx_i \sum_{i=1}^{2} \left(c_{ip} x_p^2 \right)^2 + \tag{3.134}$$

$$+ \quad \frac{f_i}{2}(q_{i+1} + q_{i+2})$$

$$\dot{q}_{i+1} = j\Omega q_{i+1} \tag{3.135}$$

$$\dot{q}_{i+2} = j\Omega q_{i+2} \tag{3.136}$$

$$i = 1, 2$$

assuming that $\omega_i^2 = \omega_{0i}^2 + \epsilon \beta_i$ with ω_{0i}^2 the i-th mode frequency for a reference value of the axial load $\bar{N}_x$, $\beta_i = \frac{\partial \omega_i^2}{\partial \bar{N}_x}|_{\bar{N}_x = \bar{N}_{x_{cr}}}$ and imposing that $x_i = \sqrt{\epsilon} z_i$ with ϵ a small artificial parameter, Eqs 3.129-3.130 become:

$$\dot{z}_i = z_{i+1} \tag{3.137}$$

$$\dot{z}_{i+1} = -gz_i - \omega_{0i}^2 z_i + \epsilon[\beta_i z_i - Sz_i \sum_{p=1}^{2} c_{ip} z_p^2 + \tag{3.138}$$

$$+ \quad \frac{f_i}{2}(q_{i+2} + q_{i+3})]$$

$$\dot{q}_{i+2} = j\Omega q_{i+2} \tag{3.139}$$

$$\dot{q}_{i+3} = -j\Omega q_{i+3} \tag{3.140}$$

$$\tag{3.141}$$

where $i = 1, 2$ and the harmonic forcing loads are written via Eulero's formulae. Since system 3.129-3.130 is equivalent to the one considered in Sec. 3.1.5, it will be studied with the same approach. Using the eigenvectors-based transformations:

$$z_i = \xi_i + \bar{\xi}_i \tag{3.142}$$

$$z_{i+1} = \lambda_i \xi_i + \bar{\lambda}_i \bar{\xi}_i \tag{3.143}$$

and remembering that the resonance conditions are:

$$\lambda_1 + \lambda_1 = 0 \tag{3.144}$$

$$\lambda_j + \lambda_1 + \lambda_1 - \lambda_j = 0 \tag{3.145}$$

one obtains, by applying the Normal Form Transformation, the dominant nonlinear dynamics:

$$\dot{\eta}_1 = \frac{\epsilon}{g}\left(\beta\eta_1 - Sc_{11}\eta_1^3\right) \tag{3.146}$$

$$\dot{q}_{i+2} = j\Omega_i q_{i+2} \tag{3.147}$$

$$\dot{q}_{i+3} = j\Omega_i q_{i+3} \tag{3.148}$$

$$\tag{3.149}$$

where $\beta = -\beta_1 = 1$ and $i = 1, 2$. Finally, the solution of the problem is

$$z_1 = \sqrt{\epsilon}\sqrt{\frac{1}{Sc_{11}}} - \frac{\epsilon f_1}{g}\sqrt{\epsilon}\left(\frac{1}{\Omega_1}\cos\left(\Omega_1 t - \pi/2\right)\right.$$
$$\left. -\frac{\Omega_1}{\Omega_1^2 + g^2}\cos\left(\Omega_1 t - \pi/2\right) - \frac{\delta}{\Omega_1^2 + g^2}\cos\left(\Omega t\right)\right) \tag{3.150}$$

$$z_2 = -\epsilon\sqrt{\epsilon}\frac{f_2}{\omega_2}\left(\frac{\Omega_2}{(\Omega_2 - \omega_2)^2 + \lambda_{R_2}^2}\cos(\Omega_2 t) + \right.$$
$$\left. +\frac{|\lambda_2|}{(\Omega_2 - \omega_2)^2 + \lambda_{R_2}^2}\sin(\Omega_2 t - \angle\lambda_2)\right) \tag{3.151}$$

where $\angle\lambda_2$ indicates the phase of the complex number λ_2. By Equations 3.150-3.151 one can observe that, under the assumed hypothesis on the order of interaction between the equation's terms, the motions are harmonic oscillations around a fixed point $\sqrt{\epsilon}\sqrt{\frac{1}{Sc_{11}}}$ with the same frequencies of the forcing loads. This oscillation is characterized by a finite number of frequencies Ω_1, Ω_2. Note that in the explained case, resonance is not considered. If a resonance is present this means that one has to consider the forcing load in the equations of normal forms. The motion along the stable modes $z_i(t)$ must be *small* and of order $\epsilon^{3/2}$. Equation 3.151 shows that the response is small if and only if the following relation is true:

$$\frac{\epsilon f_1}{g\Omega_1} = O(\epsilon) \tag{3.152}$$

Equation 3.152 shows that the asymptotic behavior of the solution described by Eqs. 3.150-3.151 is guaranteed if and only if a sufficiently high damping and a sufficiently high load frequency are present. This means that the radios of convergence of our approximated solution to the real one depends, for a fixed Ω_1, on ϵ/g that must satisfy the usual condition: $\epsilon/g \ll 1$. Moreover, one can note that $|\lambda_i + \lambda_{i+1}| = g$, $i = 1, 2$. This means that our Normal Forms assumptions require that the damping g is sufficiently high. If the damping is small *i.e.*, $g = o(\epsilon)$, the Eqs. 3.150-3.151 are no longer valid. According to the previous observations, the damping is directly related to the presence of a small divisors and to the asymptoticity of the obtained solution. Finally, it is relevant to observe that our result are equivalent to those presented in Ref. [78].

In the presence of a primary resonance (this implies a quasi-steady load with $\Omega_1 = o(\epsilon)$)), the dominant dynamics equation is:

$$\dot{\eta}_1 = \frac{\epsilon}{g}\left(\beta\eta_1 + f_1\cos\Omega_1 t - Sc_{11}\eta_1^3\right) \qquad (3.153)$$

where the forcing load is written explicitly. The solution of the whole problem is:

$$z_1(t) = \sqrt{\epsilon}\eta_1(t) + \epsilon\sqrt{\epsilon}\left(-\frac{\beta}{g^2}\eta_1(t) + \frac{Sc_{11}}{g^2}\eta_1^3(t) - \frac{\Omega_1}{g}\frac{f_1}{\Omega_1^2 + g^2}\cos(\Omega_1 t - \pi/2)+ \right.$$
$$\left. -\frac{f_1}{\Omega_1^2 + g^2}\cos(\Omega_1 t)\right) \qquad (3.154)$$

whereas the expression for $z_2(t)$ is the same as in Eq. 3.151. Observing the results given by Eq. 3.154, one can find that the damping is the main factor governing the nonlinear dynamics of the system. It is interesting to analyze the structure of the obtained solution. For the chosen interaction of the dynamical terms the studied system has the form of a linear system perturbed by linear and nonlinear terms. In particular, in the linear perturbation, by the chosen order of the forcing load, there are also the forcing terms. This means that the forcing load does not influence the static part of the response, which is the same of the unperturbed case, but only the oscillations about it. Of course, increasing the perturbation (which means also to increase the load order), the stated hypotheses are no longer true. On the other hand, a quasi-steady load requires one to consider the load effect in the main equation of normal form influencing directly the response in a *nonlinear way*.

Let us consider some numerical applications and assume the following parameters:

$$\varphi = 0.3 \quad S = 0.68 \quad N_x = 1.3$$

In Figures 3.16-3.17 the comparison between the numerical solution and the perturbed solution is given for $\epsilon = N_x - N_{x_{cr}} = 0.11$. The results shown a good qualitative agreement
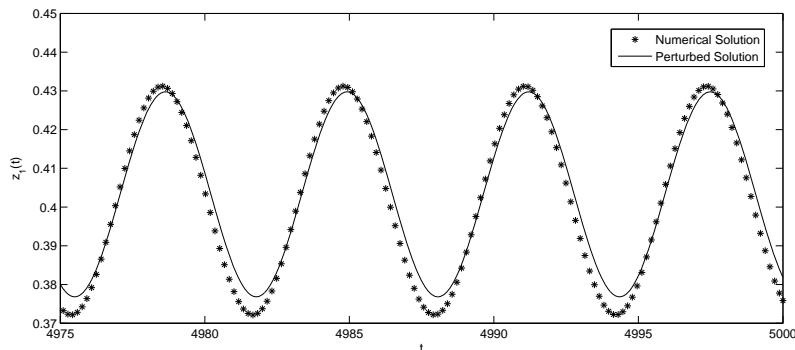
Figure 3.16: $z_1(t)$ Perturbed vs Numerical solution, $g = 1$ $\Omega_1 = 1$, $\Omega_2 = 2$, $f_1 = f_2 = 1$
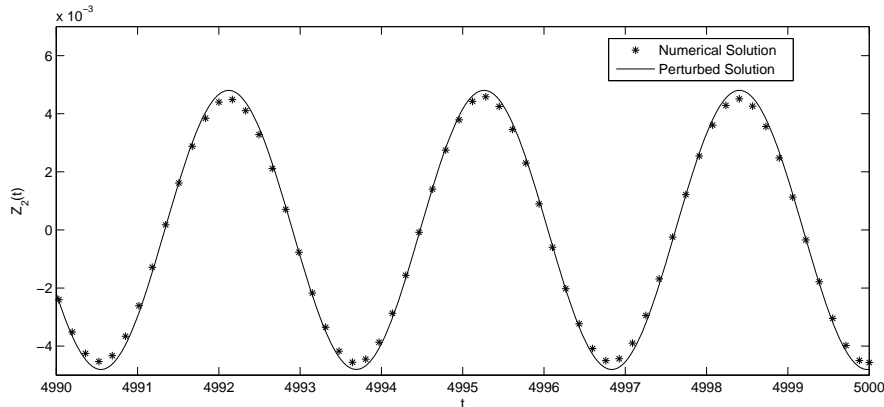
Figure 3.17: $z_2(t)$ Perturbed vs Numerical solution, $g = 1$ $\Omega_1 = 1$, $\Omega_2 = 2$, $f_1 = f_2 = 1$

between the perturbed solution and the numerical one. Moreover, the structure of the solution is the one predicted analytically showing a harmonic oscillation at frequencies $\Omega_1 = 1$ and $\Omega_2 = 2$ about a fixed point laying along the buckled mode. A small damping case[2] is
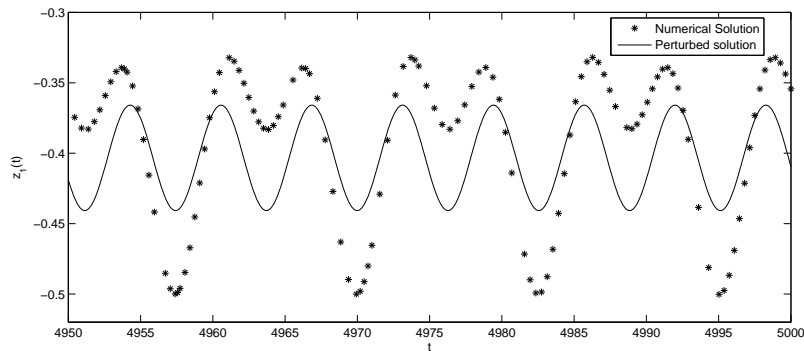
Figure 3.18: $z_1(t)$ Perturbed vs Numerical solution, $g = 0.01$ $\Omega_1 = 1$, $f_1 = 1$ $f_2 = 0$

considered in Fig. 3.18 where it is shown how the presence of a small damping influence negatively the asimptoticity of the solution for a fixed ϵ. The effect of the load amplitude is shown in Fig. 3.19, where the main error is on the static part of the response implying that it depends not only on the system parameters (axial load and nonlinear properties) but also on the forcing load amplitude. The presence of a quasi-static forcing load is presented in Fig. 3.20.

---

[2]For the sake of brevity only the motion along the critical mode has been shown.

Figure 3.19: $z_1(t)$ Perturbed vs Numerical solution, $g = 1$ $\Omega_1 = 1$, $f_1 = 100$ $f_2 = 0$
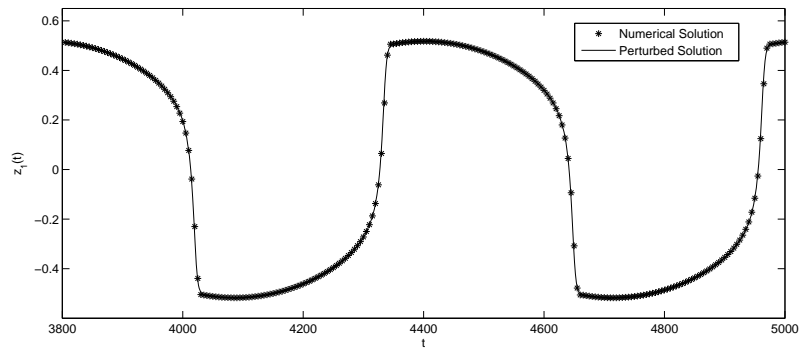
Figure 3.20: $z_1(t)$ Perturbed vs Numerical solution, $g = 1$ $\Omega_1 = 0.01$, $\Omega_2 = 2$, $f_1 = 1$, $f_2 = 1$
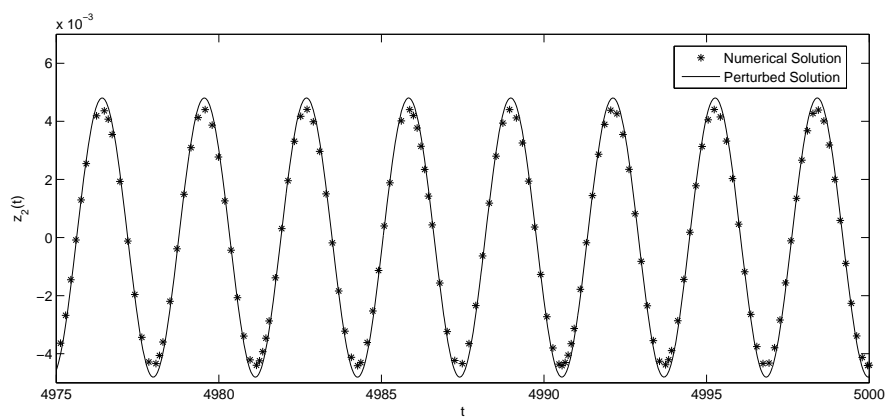
Figure 3.21: $z_2(t)$ Perturbed vs Numerical solution, $g = 1$ $\Omega_1 = 0.01$, $\Omega_2 = 2$, $f_1 = 1$, $f_2 = 1$

Hopf bifurcation with forcing load

In presence of aerodynamical load, $i.e.$, $\nu \neq 0$, the unforced system can experience a Hopf-type bifurcation for $\nu = \nu^*$. This means that the linearized system has two purely complex eigenvalues for $\nu = \nu^*$ and positive real part for $\nu > \nu^*$. Let us consider Eqs. 3.121 with the transformation

$$\mathsf{y} = \mathsf{U}\mathsf{q} \tag{3.155}$$

where the columns of U are the eigenvectors of A_0

$$\mathsf{A}_0\mathsf{U} = \mathsf{U}\mathsf{\Lambda}_0 \tag{3.156}$$

and $\mathsf{\Lambda}_0$ a diagonal matrix with the eigenvalues of A_0 as diagonal entries. For the sake of simplicity consider forcing load of the following form:

$$\mathsf{f} = \{0, 0, f_1 \cos \Omega_1 t, 0\}^{\mathrm{T}} \tag{3.157}$$

The zero-divisors conditions associated with the studied bifurcation are:

$$\lambda_i - \lambda_i = 0 \tag{3.158}$$

$$\lambda_1 + \lambda_2 + \lambda_j - \lambda_j = 0 \tag{3.159}$$

The conditions given by Eqs. 3.158-3.159 are the same that characterized an unforced system experiencing a Hopf-bifurcation (see Ref. [16]). The normal form equation is:

$$\dot{\eta}_1 = j\omega_1\eta_1 + \epsilon[\alpha_{11}\eta_1 + (\gamma_{1121} + \gamma_{1211} + \gamma_{1112})\eta_1^2\eta_2] = \beta^{(1)}\eta_1 + \gamma^{(1)}\eta_1^2\bar{\eta}_1 \tag{3.160}$$

$$\dot{\eta}_2 = \bar{\dot{\eta}}_1 \tag{3.161}$$

with

$$\alpha_{ij} = \sum_{s,p=1}^{4} U_{is}^{-1} A_{1sp} U_{pj} \tag{3.162}$$

$$\gamma_{islm} = \sum_{n,p,q,r=1}^{4} U_{jn}^{-1} c_{npqr} U_{ps} U_{ql} U_{rm} \tag{3.163}$$

where $\epsilon = \nu - \nu^*$, $\beta = -j\omega_1 - \epsilon\alpha_{11} = \beta_R + j\beta_I$, $\gamma = -\epsilon(\gamma_{1121} + \gamma_{1211} + \gamma_{1112}) = \gamma_R + j\gamma_I$. Equation 3.160 can be rewritten as

$$\dot{\eta}_1 + \beta^{(1)}\eta_1 + \gamma^{(1)}\eta_1^2\bar{\eta}_1 = 0 \tag{3.164}$$

Finally, the stationary solution, on the modal basis, is:

$$\mathsf{y} = \sqrt{\epsilon}\left(a_1 e^{\phi(t)}\mathsf{u}^{(1)} + C.C.\right) + o(\epsilon^{1/2}) \tag{3.165}$$

where

$$a_1(t \to +\infty) = \sqrt{-\frac{\beta_R^{(1)}}{\gamma_R^{(1)}}} \tag{3.166}$$

$$\phi(t \to +\infty) = t\left(-\beta_I^{(1)} + \frac{\gamma_I^{(1)}\beta_R^{(1)}}{\gamma_R^{(1)}}\right) + \frac{\gamma_I^{(1)}}{\gamma_R^{(1)}}\ln(a_1) + \phi_0 \tag{3.167}$$

With respect to Sec. 3.2.3 the solution is presented up to order $\sqrt{\epsilon}$. Indeed, in the static bifurcation it is necessary to study the motion to build the solution up to order $\epsilon^{3/2}$.

In presence of an external resonance $\Omega_1 = \omega_1$ the resonance condition

$$\lambda_1 - j\Omega_1 = 0 \tag{3.168}$$

appears. This implies that the forcing load directly influences the normal form equation:

$$\dot{\eta}_1 + \beta^{(1)}\eta_1 + \gamma^{(1)}\eta_1^2\bar{\eta}_1 = \epsilon\frac{f_1}{2}\theta e^{j\Omega_1 t} \tag{3.169}$$

where θ is the load component along the critical eigenvector. Equation 3.169 suggests that the motion will be influenced by the external load also at the $\sqrt{\epsilon}$ order:

$$\mathsf{y}(t) = \sqrt{\epsilon}\eta_1(t)\mathsf{u}^{(1)} + CC + o(\epsilon^{3/2}) \tag{3.170}$$

The results in Eqs. 3.166-3.167 and 3.170 show some interesting features of the behavior of the system under our hypotheses. Indeed, except for the resonant case, it appears that the forcing load is not necessary to represent correctly the dynamics. In particular, this means that in the observed phenomenon, the essential features are from the internal dynamics of the system: the forcing load is a nonessential term that can be disregarded in the first order analysis.

Let us consider some numerical experiments with fixed parameters:

$$\varphi = 0.30, \quad S = 0.68, \quad K = 100.50, \quad g = 0.10, \quad N_x = 1.00 \tag{3.171}$$

The critical value of the parameter ν associated to the parameters given by Eq. 3.171 is $\nu^* \cong 0.09$ and the critical frequency is $\omega_1 = 2.54$. In Figure 3.22, the comparison between numerical and perturbed solution is shown. In particular, it is possible to observe the presence of a phase shift between the exact and approximate solution. The effect of a 1 : 1 resonance is analyzed in Fig. 3.24 where one can observe that the main error of the perturbed solutions is a phase shift with respect to the numerical one. The perturbed solution given by Eq. 3.164 and the one given by Eq. 3.169, which consider the presence of the forcing load, are similar and this is due to the presence of the weight θ of the forcing load which is small in modulus. Indeed, increasing the load, *i.e.*, f_1, one can observe that the solution given by Eq. 3.169 gives a better approximation of the numerical solution (for

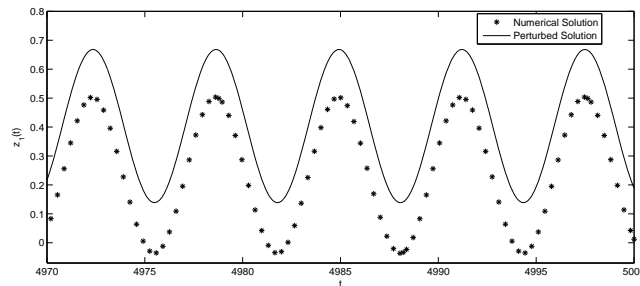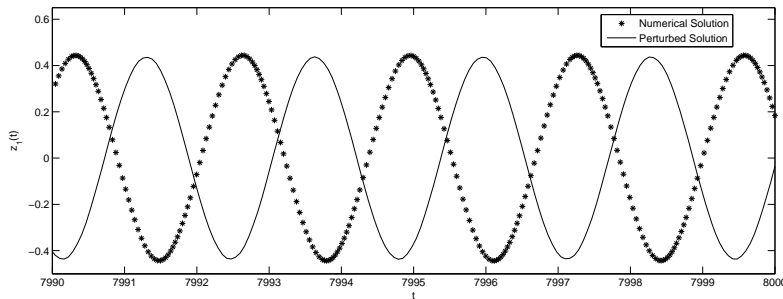**Figure 3.22:** $z_1(t)$ Perturbed vs Numerical solution, $\epsilon = 0.01$, $\Omega_1 = 1$, $f_1 = 1$
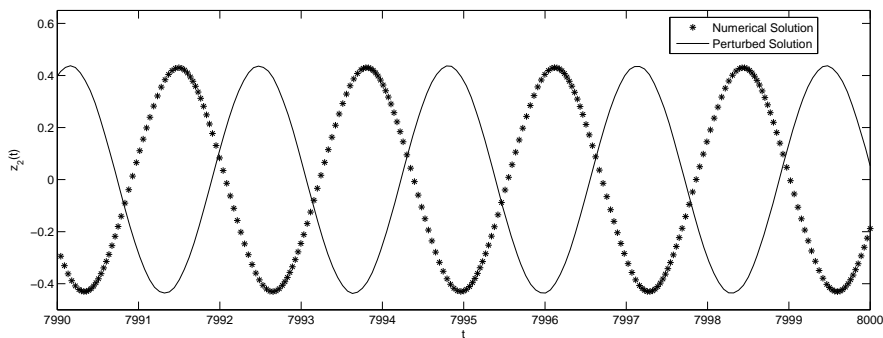
Figure 3.23: $z_2(t)$ Perturbed vs Numerical solution, $\epsilon = 0.01$, $\Omega_1 = 1$, $f_1 = 1$
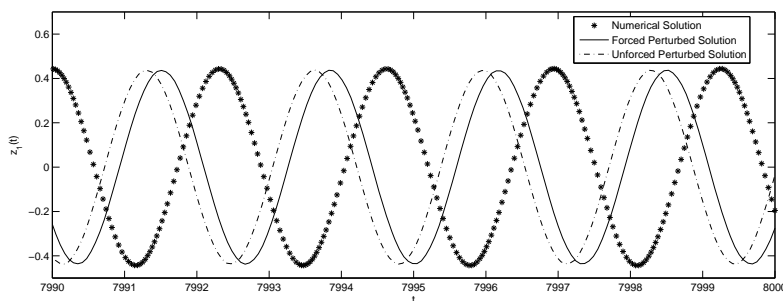
Figure 3.24: $z_1(t)$ Perturbed vs Numerical solution, $\epsilon = 0.01$, $\Omega_1 = 2.54$, $f_1 = 1$
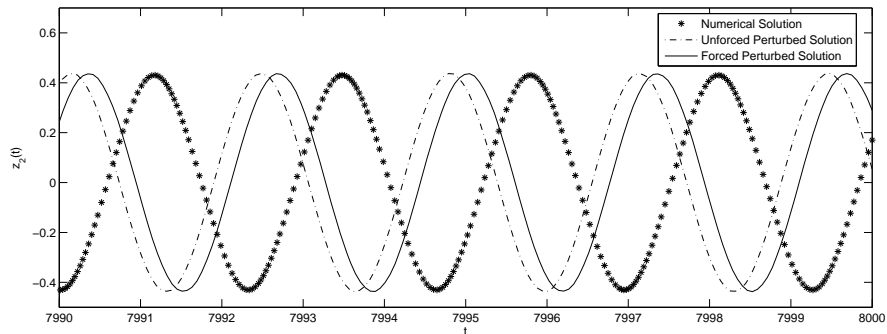
Figure 3.25: $z_2(t)$ Perturbed vs Numerical solution, $\epsilon = 0.01$, $\Omega_1 = 2.54$, $f_1 = 1$
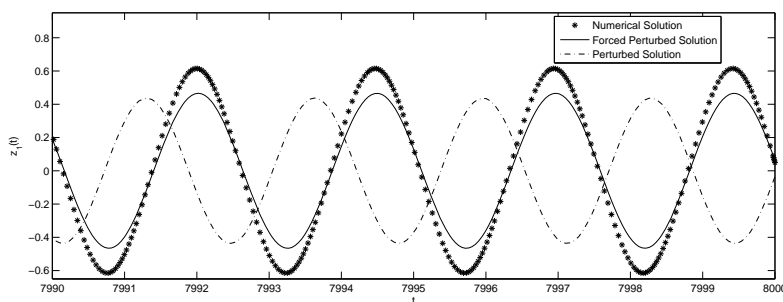
Figure 3.26: $z_1(t)$ Perturbed vs Numerical solution, $\epsilon = 0.01$, $\Omega_1 = 2.54$, $f_1 = 100$
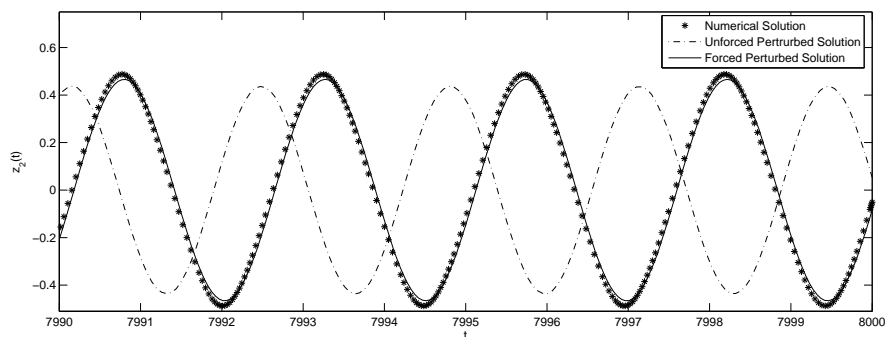
Figure 3.27: $z_2(t)$ Perturbed vs Numerical solution, $\epsilon = 0.01$, $\Omega_1 = 2.54$, $f_1 = 1$
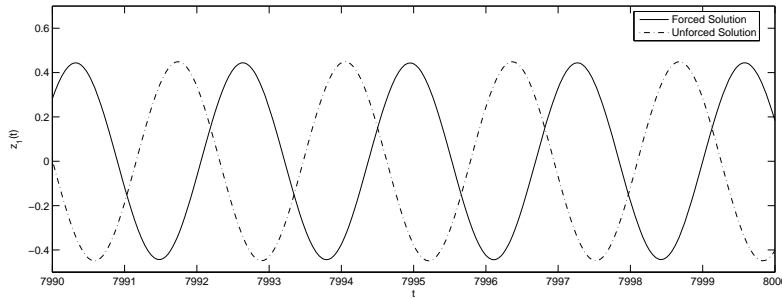
Figure 3.28: $z_1(t)$ Forced vs Unforced solution, $\epsilon = 0.01$

the same perturbation parameter), see Fig. 3.26.   Finally, in Figure 3.28 the motion along
the critical mode is compared to the numerical forced solution and the numerical unforced
solution. As emphasized above, one cane observe that, except for a phase shift, the two
solutions are similar stressing the fact that the response depends mainly on the intrinsic
nature of the system. Observe that this results is valid also in the presence of an external
resonance, if the load is small with respect to the assumed order interaction.

3.2.4   Concluding Remarks

The problem of a flat panel subjected to a biaxial compressive load and to a supersonic flow
together with a transversal harmonic load has been investigated. Thus, both structural and
aerodynamic non linear effects are included in the aeroelastic model. In particular, the effects
of some physical parameters have been studied in order to investigate how they relate with
the small and zero divisors. The zero/small divisors concepts are related to the Normal Form
reduction method, *i.e.*, to the possibility of simplification of the original problem to a more
simple one with a small number of nonlinear terms. The presence of a static bifurcation, the
role of the damping has been outlined as a small-divisor, because the resonance conditions
depend on it. Moreover, the role of the load frequency as small divisor has been stressed
in the example of quasi-steady loads. Considering a dynamical bifurcation, *i.e.*, Hopf-type,
the role of the structural modal damping is less important because of the presence of the
aerodynamic which contributes also with a damping term. Indeed, not considering the case
with a resonant external load, the only important (zero) divisors are the one associated with
the presence of a purely imaginary pair: the normal form analysis of such a system is the
same as the one performed for an unforced case. Moreover, the forcing load is weighted
with a small parameter representing the projection of the load on the critical eigenvector:
in the presence of a 1 : 1 external resonance the results are similar to the ones without
resonance. The analysis described above has shown that in presence of a weakly loaded

dynamical system the dynamics of the problem (near a bifurcation point) is driven by the parameters characterizing the system and not by the load.

It is interesting to analyze the reasons that lead to the present results. The starting point is the nature of the ordering of the terms in the perturbation parameter. In particular, the system has been written as a linear part (with at least one eigenvalue with zero-real part) and a perturbation made of linear and nonlinear terms. Writing the external load via the Euler's formulae and assuming its amplitude of order $\epsilon^{3/2}$ gives the problem the expression shown in Eq. 2.14, where in the dynamical equations the load appears as a linear perturbation of the linear part and the spatial form is described by two autonomous equations (see Eqs. 3.139-3.140 for example). The obtained geometry of the system in the state-space implies that the "physical dynamics" is orthogonal to the "load space", *i.e.*, they are related only by higher order terms in the perturbation parameters. Then the eigengeometry of the physical problem is not influenced by the external load. Consequently, to first order, the asymptotic solution is not influenced by the presence of the external load and it is the same as that the unforced problem. Otherwise, the load can influence the solution via the presence of small or zero divisors. Note that there is not a geometrical coupling in this case and the presence of the load in the Normal Form equations is only necessary in order to guarantee the "asymptotic" nature of the solution series.

3.3 Final remarks about the longterm dynamics analysis via Normal Form Method

The Normal Form reduces a nonlinear problem to a form which is as close as possible to that of a linear problem (linearized Hartman form), by identifying a diffeomorphism that eliminates the non essential nonlinearities. The essential problem is defined by the resonance conditions, whose depend on the problem, *i.e.*, of the observed bifurcation, and on the parameters appearing in the equations that can be related to physical entity present in the physical model. This means, that it gives information on what it is important to consider in a fixed bifurcation phenomenon, which is represented in a general form by its associated normal form and which is linked with the representation of the physical problem. Roughly speaking, the obtained results permit one to identify which physical parameters of the system are important to evaluate in order to obtain a correct assessment of the behavior of the physical problem characterized by Pitchfork and Hopf types bifurcation. In particular, in the presence of Limit Cycle Oscillations (namely, Hopf bifurcations), it has been shown that it is important to evaluate the flow state and the aerodynamic and structural properties more than the external load, whereas in presence of buckling (namely, pitchfork bifurcation)

the new equilibrium position will depend only on the structural properties and the axial buckling load, while the vertical harmonic load will influence only the motion about such a position,*i.e.*, displacement amplitude and frequency.

Part III

Proper Orthogonal Decomposition

Chapter 4

Proper Orthogonal Decomposition analysis of dynamics

The Proper Orthogonal Decomposition (POD), also known as Karhunen-Loève Decomposition (KLD), is a method for finding a basis that is able to represent the maximum energy content (or generally, the norm of the signal associated to the process) in an observed dynamical process represented, for instance, by a system of ordinary differential equations. In signal-processing literature the method was originally presented by Hotelling (Ref. [79]) as Principal Component Analysis (PCA) and the theory was further developed Kosambi (1943), Loève (1945), Karhunen (1946). The appealing property of POD consists of its optimality with respect to the energy distribution in the state-space. It is shown that, for a given N-dimensional process, the projection of the dynamics on the first Q elements of the POD basis extracts, on average, more energy than a projection on the first Q elements of any other orthonormal basis (Ref. [36]). This method was applied by Lumley (Ref. [80]) in 1967 to identify coherent structures in turbulent flows and has become a standard tool in turbulence studies. In the last ten years, POD is emerging as an experimental and analytical technique also in structural dynamics and vibrations where it can be used as a powerful tool for modal identification (see Refs. [40, 38]). In particular, it is demonstrated that for undamped structural systems, the Proper Orthogonal Modes (POMs) are equivalent to linear normal modes and this equivalence can be practically extended in weakly damped cases as well. If, as in aeroelasticity, the modal basis (namely, the system invariant subspaces) is generally complex and orthogonality does not apply, it is necessary a different approach to relate the dynamical invariant objects, in order to extend the relationship between invariant subspace (modal basis) and POD.

4.1   General issues on POD analysis

Let us consider an N dimensional state-space with a generic process $t \mapsto \mathsf{v}(t)$. The Proper Orthogonal Decomposition (POD) defines in such a space a set of $Q \leq N$ vectors $\{\mathsf{p}^i\}, i = 1, ..., Q$ which determine an *optimal* basis for the linear representation of the process $\mathsf{v} : \mathbb{R}^+ \mapsto \mathbb{R}^N$

$$\mathsf{v}(t) = \sum_{i=1}^{Q} \zeta(t)\mathsf{p}^i \tag{4.1}$$

where the $\zeta : \mathbb{R}^+ \mapsto \mathbb{R}$ are the dynamic components of the process referred to the POD basis. The optimality is defined by searching the unknown direction p such that the projection of $\mathsf{v}(t)$ on p be maximum in average on the time interval $\bar{I} = [0, T]$, $T \in \mathbb{R}^+$. Thus, imposing as constraint that the vector p has a unit magnitude, one has the constrained maximum problem

$$\lim_{T \to \infty} \frac{1}{T} \int_0^T [\mathsf{v}(t) \cdot \mathsf{p}]^2 \, dt - \sigma\, (\mathsf{p} \cdot \mathsf{p} - 1) = \max_{\mathsf{p} \in \mathbb{R}^N} \tag{4.2}$$

with

$$\mathsf{p} \cdot \mathsf{p} = 1 \tag{4.3}$$

The steady condition for this quadratic form yields (for all r and considering the Einstein convention):

$$0 = \frac{\partial}{\partial p_r} \left[\lim_{T \to \infty} \frac{1}{T} \int_0^T [v_i(t) p_i]^2 \, dt - \sigma p_i p_i \right] \tag{4.4}$$

Developing Eq. 4.4, one obtains

$$\lim_{T \to \infty} \frac{1}{T} \int_0^T v_r(t) v_i(t) dt \; p_i = \sigma p_r \tag{4.5}$$

or

$$\mathsf{R}\,\mathsf{p} = \sigma \mathsf{p} \tag{4.6}$$

where

$$\mathsf{R} := \lim_{T \to \infty} \frac{1}{T} \int_0^T \mathsf{v}(t) \otimes \mathsf{v}(t) dt \tag{4.7}$$

is the correlation matrix associated to the process $\mathsf{v}(t)$.

Equation 4.6 states that the POD-basis vectors p^i are the eigenvectors associated with the matrix R, whereas the eigenvalues σ_i represent the energy associated to with projection of

the process v along the direction p^i.

Let us consider the generic quadratic form associated to R, *i.e.*, $\forall\, \mathsf{x} \in \mathbb{R}^N$:

$$
\begin{aligned}
r^2(\mathsf{x}) := \quad \mathsf{x} \cdot \mathsf{R} \cdot \mathsf{x} \;=\; & \mathsf{x} \cdot \lim_{T\to\infty} \frac{1}{T} \int_0^T \mathsf{v}(t) \otimes \mathsf{v}(t)\; dt \cdot \mathsf{x} \;=\; \\
= \quad & \lim_{T\to\infty} \frac{1}{T} \int_0^T \mathsf{x} \cdot \mathsf{v}(t) \otimes \mathsf{v}(t)\; \cdot \mathsf{x}\, dt \;=\; \\
= \quad & \lim_{T\to\infty} \frac{1}{T} \int_0^T [\mathsf{v}(t) \cdot \mathsf{x}]\,[\mathsf{v}(t) \cdot \mathsf{x}]\; dt \;=\; \\
= \quad & \lim_{T\to\infty} \frac{1}{T} \int_0^T [\mathsf{v}(t) \cdot \mathsf{x}]^2\, dt > 0
\end{aligned}
\tag{4.8}
$$

From Equations 4.8 the positiveness of matrix R can be stated. Then, R is symmetric (by definition) and positive definite, this resulting in real-valued and positive eigenvalues (*Proper Orthogonal Values*) and real and orthogonal eigenvectors (*Proper Orthogonal Modes*).

4.2   Outline of the present POD application

Some remarks about the intermediate steps to carry out the outlined analysis can be further defined at this point. Typically, the state-space vector time-history $\mathsf{v}(t)$ is provided by simulations or by experimental data in POD applications. In the present case, however, it is interesting to evaluate the correlation matrix R using analytical solutions that express (linear case) or approximate (nonlinear case) the system evolution in the state-space. Since these solutions are herein both expressed as a linear combination of basis vectors with time dependent coefficients[1], *i.e.*,

$$
\mathsf{v}(t) = a_1(t)\,\mathsf{e}^1 + a_2(t)\,\mathsf{e}^2 + \ldots
\tag{4.9}
$$

it will be shown that the correlation matrix R can be then defined in terms of these basis vectors as well (the integral operator will obviously cancel out the time dependency), leading, under suitable hypothesis, to the general expression

$$
\mathsf{R} = \sum_{m=1}^{M} c_m^2\, \mathsf{e}^m \otimes \mathsf{e}^m
\tag{4.10}
$$

The above relationship, further specified for the linear case (see Eqs. 4.16 and 4.18) and for the nonlinear case (see Eq. 4.67), will be used to determine analytically the eigenvalues and eigenvectors of R, thus obtaining

$$
\mathsf{R}\mathsf{e}^i = \sigma\mathsf{e}^i,
\tag{4.11}
$$

---

[1]If this statement is trivial for linear systems, the nature of the chosen approximation for nonlinear systems is similar if perturbation methods are employed.

that indicates that the basis vector e^i is an eigenvector of R, whilst σ is its associated eigenvalue. Therefore, recalling Eq. 4.6, the basis vectors e^i and the scalars σ_i claim to be the proper orthogonal modes and the proper orthogonal values of the considered process, respectively. Thus, a relationship (namely, an equivalence) between vector basis e^i and proper orthogonal modes p^i will be established. However, the outlined scheme ceases to appear straightforward as soon as periodic solutions are considered that, indeed, constitute the true by interesting case (the energy content of the signal per unit time is constant). In this case, as a result of imaginary poles (linear case) or limit cycles (nonlinear case), Eq. 4.9 becomes

$$\mathsf{v}(t) = a_1(t)\,\mathsf{w}^1 + a_1^*(t)\,\mathsf{w}^{1*} + \dots \tag{4.12}$$

where the vector w^{*1} is the complex conjugate of the vector w^1 (the same applies for the scalars $a_1(t)$ and $a_1^*(t)$). Equation 4.12 rises the (crucial) issue relative to the fact that the proper orthogonal modes p^i are real by definition, whereas the basis vectors of the periodic solutions, *i.e.*, the pair $(\mathsf{w}^i, \mathsf{w}^{i*})$ are complex conjugate, motivating a key contribution to untangle this conflicting aspect. For this reason, in Section 4.3 the basis $(\mathsf{w}, \mathsf{w}^*)$ of the subspace where the periodic solution is embedded (for sake of clarity, the case of one couple of complex conjugated is here referred) will be first arranged to form a real basis $(\mathsf{w}_R, \mathsf{w}_I)$ spanning a real plane in the state-space. This basis, unfortunately, does not meet the additional requirement to be orthogonal, as prescribed by the POD analysis. This critical issue will be then considered in Section 4.3 as well, where a method to perform the orthogonalization, based on the contemporary rotation of both w_R and w_I, will provide a pair of orthogonal basis vector $(\mathsf{w}_{R_\perp}, \mathsf{w}_{I_\perp})$. As it will be clearer in the following sections, this real and orthogonal pair of vectors will provide the sought after result, that is, to unveil the origin of the proper orthogonal modes of the system process. This correspondence, in particular for a nonlinear system experiencing a Hopf bifurcation, constitutes the premise for the identification of the relevant and interacting modes.

4.3 POD analysis for marginally stable linear systems

Let us consider the process $\mathsf{v}(t)$ as a vector of the state-space of a $N-$dimensional unforced linear dynamical system described by the real matrix A

$$\begin{cases} \dot{\mathsf{v}} = \mathsf{A}\,\mathsf{v} \\ \mathsf{v}(0) = \mathsf{v}_0 \end{cases} \tag{4.13}$$

A standard eigenproblem can be associated to the matrix A

$$\mathsf{A}\mathsf{w} = \lambda \mathsf{w} \tag{4.14}$$

Note that in many physical problems like, for example, linear vibrations, the eigenvalues are typically *complex conjugate*, namely, they present pairs of complex conjugated eigenvalues and eigenvectors.

In the next Section, in order to clarify the nature of POMs, the relationship between the complex (conjugate) eigenvectors w and the associated eigenspaces in the state space will be investigated. In Section 4.3.1 the role of such a subspace in the description of the free response will be clarified. Finally in Section 4.3.2 the relation of this subspace with POMs is shown.

4.3.1 Free response and eigenspaces

The solution of Eq. 4.13 is generally given by

$$\mathsf{v}(t) = \sum_{n=1}^{N} c_n \mathsf{w}^n e^{\lambda_n t} = 2 \sum_{n=1}^{N/2} Re\left(c_n \mathsf{w}^n e^{\lambda_n t}\right) \tag{4.15}$$

with c_n suitable complex constants determined by the initial conditions.

Note that $N/2$ is the number of the subspaces $\mathcal{W}^n$, each one associated to the complex eigenvalues pairs. Note also that, since the initial conditions are prescribed, new complex eigenvectors $\tilde{\mathsf{w}}^n := c_n \mathsf{w}^n$ can be defined (see Sec. 1.3). Thus, Eq. 4.15 becomes

$$\mathsf{v}(t) = 2 \sum_{n=1}^{N/2} e^{\lambda_R t} \left(\cos(\lambda_I t)\tilde{\mathsf{w}}_R^n - \sin(\lambda_I t)\tilde{\mathsf{w}}_I^n\right) \tag{4.16}$$

that shows how the free response in the state space is obtained as a direct sum of $N/2$ distinct contributions belonging to different $\mathcal{W}^n$ invariant subspaces.

4.3.2 Systems with $M \leq N$ purely imaginary eigenvalues and $N - M$ eigenvalues with negative real part

If there are only M purely imaginary eigenvalue the Eq. 4.16, disregarding the contributions of the damped modes, yields

$$\mathsf{v}(t) \simeq 2 \sum_{n=1}^{M/2} \left(\cos(\lambda_I t)\tilde{\mathsf{w}}_R^n - \sin(\lambda_I t)\tilde{\mathsf{w}}_I^n\right) \tag{4.17}$$

Thus, considering the definition of the correlation matrix given by Eq. 4.7, one obtains

$$\mathsf{R} = \lim_{T \to \infty} \frac{4}{T} \sum_{m,n=1}^{M/2} \int_0^T Re\left(c_m \mathsf{w}^m e^{j\omega_m t}\right) \otimes Re\left(c_n \mathsf{w}^n e^{j\omega_n t}\right) dt \tag{4.18}$$

Developing Eq. 4.18, yields

$$\mathsf{R} = \sum_{m=1}^{M/2} 2\left|c_m\right|^2 \left[\mathsf{w}_R^m \otimes \mathsf{w}_R^m + \mathsf{w}_I^m \otimes \mathsf{w}_I^m\right] \tag{4.19}$$

Equation 4.19 implies that the rank of the obtained correlation matrix is equal to M if (and only if) all the coefficients $c_m \neq 0$, *i.e.*, all the M undamped marginal eigenvectors are excited by the given initial condition. This means that the space spanned by the POD basis has a dimension which is equal or less (if some c_n are equal to zero) to the dimension of the space spanned by the linear undamped marginal eigenvectors, belonging to the $M/2$ subspaces $\mathcal{W}^n$ defined in the Sec. 1.3.

A special case: $M = N$ purely imaginary eigenvalues in conservative systems

Let us consider a system of $N/2$ coupled free undamped oscillators, governed by the second order ordinary differential equation

$$\mathsf{I}\ddot{\mathsf{q}} + \mathsf{K}\mathsf{q} = 0 \tag{4.20}$$

with K semi-definite positive[2] . The associated generalized eigenproblem

$$\left(\mathsf{K} - \omega^2\mathsf{I}\right)\mathsf{z} = 0 \tag{4.23}$$

gives $N/2$ real and non-negative eigenvalues ω_n^2 and $N/2$ corresponding real and orthogonal eigenvectors z^n such that, once suitable normalized, satisfy the relation

$$\mathsf{z}^m \cdot \mathsf{z}^n = \delta_{mn}. \tag{4.24}$$

If Equation 4.20 is rewritten in a first order form, the state-space vector and the matrix of coefficients of Eq. 4.13 assume the following form

$$\mathsf{v}(t) = \left\{ \begin{array}{c} \mathsf{q}(t) \\ \dot{\mathsf{q}}(t) \end{array} \right\} \quad \text{and} \quad \mathsf{A} = \left[\begin{array}{cc} 0 & \mathsf{I} \\ -\mathsf{K} & 0 \end{array} \right] \tag{4.25}$$

Therefore, the standard eigenproblem given by Eq. 4.14 yields

$$\lambda_{n_{1,2}} = \pm j\omega_n \tag{4.26}$$

$$\mathsf{w}_{1,2}^n = \left\{ \begin{array}{c} \mathsf{z}^n \\ \pm j\omega_n\mathsf{z}^n \end{array} \right\} = \left\{ \begin{array}{c} \mathsf{z}^n \\ 0 \end{array} \right\} \pm j \left\{ \begin{array}{c} 0 \\ \omega_n\mathsf{z}^n \end{array} \right\} =: \mathsf{w}_R^n \pm j\mathsf{w}_I^n \tag{4.27}$$

---

[2]Note that if the mass matrix M is not equal to the identity one can use a suitable definition of state variables such as in this new state-space the system is in the form of Eq. 4.20. Let us consider a generic mechanical system of the form

$$\mathsf{M}\ddot{\hat{\mathsf{q}}} + \hat{\mathsf{K}}\hat{\mathsf{q}} = 0 \tag{4.21}$$

with M symmetric and definite positive and $\hat{\mathsf{K}}$ symmetric and non negative. Because the mass matrix $\hat{\mathsf{M}}$ is definite-positive, it is possible to define a new set of state variables q such that $\hat{\mathsf{q}} = \mathsf{M}^{-1/2}\mathsf{q}$. Substituting this new position in Eq. 4.21 one obtains a system of the form 4.20

$$\mathsf{I}\ddot{\mathsf{q}} + \mathsf{K}\mathsf{q} = 0 \tag{4.22}$$

where $\mathsf{K} = \mathsf{M}^{1/2}\hat{\mathsf{K}}\mathsf{M}^{-1/2}$ is still symmetric and non-negative.

This demonstrates that (see Eqs. 4.24 and 4.27):

- any w_R^n is orthogonal to the corresponding w_I^n, implying that $\mathsf{w}_R^n = \mathsf{w}_{R_\perp}^n$ and $\mathsf{w}_I^n = \mathsf{w}_{I_\perp}^n$ (see Fig. 1.1);

- any $\mathsf{w}_{R_\perp}^n$ and $\mathsf{w}_{I_\perp}^n$ are orthogonal to any $\mathsf{w}_{R_\perp}^m$ and $\mathsf{w}_{I_\perp}^m$ if $n \neq m$ (see Eq. 4.24).

This implies that any subspace (plane) $\mathcal{W}^n$ defined by the basis $(\mathsf{w}_R^n, \mathsf{w}_I^n)$ is orthogonal to any other one for $n = 1, ..., N/2$. As a consequence, using Eq. 4.19, one has

$$\mathsf{R}\,\mathsf{w}_{R_\perp}^n \;=\; \sum_{m=1}^{M/2} 2\,|c_m|^2 \left[\mathsf{w}_{R_\perp}^m \otimes \mathsf{w}_{R_\perp}^m + \mathsf{w}_{I_\perp}^m \otimes \mathsf{w}_{I_\perp}^m \right] \mathsf{w}_{R_\perp}^n \;=\; 2\,|c_n|^2\,\|\mathsf{w}_{R_\perp}^n\|\,\mathsf{w}_{R_\perp}^n \tag{4.28}$$

and also

$$\mathsf{R}\,\mathsf{w}_{I_\perp}^n \;=\; \sum_{m=1}^{M/2} 2\,|c_m|^2 \left[\mathsf{w}_{R_\perp}^m \otimes \mathsf{w}_{R_\perp}^m + \mathsf{w}_{I_\perp}^m \otimes \mathsf{w}_{I_\perp}^m \right] \mathsf{w}_{I_\perp}^n \;=\; 2\,|c_n|^2\,\|\mathsf{w}_{I_\perp}^n\|\,\mathsf{w}_{I_\perp}^n. \tag{4.29}$$

The above relations allow to state that

- the POMs p^n (see Eq. 4.6) are coincident with the modal eigenvectors $\mathsf{w}_{R_\perp}^n$ and $\mathsf{w}_{I_\perp}^n$;

- the POVs σ_n (see Eq. 4.6) are related to the energy associated to the oscillations, as shown by the following equations,

$$\sigma_{2n-1} \;=\; 2|c_n|^2\,\|\mathsf{w}_{R_\perp}^n\|^2 \tag{4.30}$$

$$\sigma_{2n} \;=\; 2|c_n|^2\,\|\mathsf{w}_{I_\perp}^n\|^2 \quad \text{for } n = 1, 2, ..., N/2 \tag{4.31}$$

where the dependence on the imposed initial conditions is contained in the coefficients $|c_n|^2$. The above results are equivalent to those obtained in Ref. [38] for systems of the form given by Eq. 4.20 and represents a generalization of them for systems written in the phase space.

A special case: $M = 2 < N$ purely imaginary eigenvalues and $N - 2$ eigenvalues with negative real part

If the system has only a pair of purely imaginary (marginal) conjugate eigenvalues ($M = 2$), the R matrix defined in Eq. 4.19 becomes (supposing that the purely complex pair is the p-th)

$$\mathsf{R} \;=\; 2\,|\,c_p\,|^2\,(\mathsf{w}_R^p \otimes \mathsf{w}_R^p + \mathsf{w}_I^p \otimes \mathsf{w}_I^p) \tag{4.32}$$

where $(\mathsf{w}_R^p, \mathsf{w}_I^p)$ is the basis of the subspace $\mathcal{W}^p$ associated with the purely imaginary conjugate eigenvectors. Considering the results of Sec. 1.3, it is possible to multiply the complex eigenvectors by the complex constant $e^{j\tilde{\theta}_\perp}$ given by Eq. 1.30 so that the real and imaginary

parts becomes mutually orthogonal (see Eq. 1.28 and 1.29). Thus, in the following we assume that $\mathsf{w}_R^p \equiv \mathsf{w}_{R_\perp}^p$ and $\mathsf{w}_I^p \equiv \mathsf{w}_{I_\perp}^p$ in the subspace $\mathcal{W}^p$.

Let us consider the following decomposition of the state-space

$$\mathbb{R}^N = \mathcal{W}^p \oplus \mathcal{W}^{p\perp} \tag{4.33}$$

where $\mathcal{W}^{p\perp}$ represents the orthogonal complement of $\mathcal{W}^p$

$$\mathcal{W}^{p\perp} = \{\mathsf{u} \in \mathbb{R}^N : \mathsf{u} \cdot \mathsf{v} = 0 \ \forall \mathsf{v} \in \mathcal{W}^p\}. \tag{4.34}$$

Thus, remembering that $\mathsf{w}_{R_\perp}^p \cdot \mathsf{w}_{I_\perp}^p$, one has

$$\mathsf{R}\,\mathsf{w}_{R_\perp}^p = 2\,|c_p|^2 \left[\mathsf{w}_{R_\perp}^p \otimes \mathsf{w}_{R_\perp}^p + \mathsf{w}_{I_\perp}^p \otimes \mathsf{w}_{I_\perp}^p\right] \mathsf{w}_{R_\perp}^p = 2\,|c_p|^2\,\|\mathsf{w}_{R_\perp}^p\|\,\mathsf{w}_{R_\perp}^p \tag{4.35}$$

$$\mathsf{R}\,\mathsf{w}_{I_\perp}^p = 2\,|c_p|^2 \left[\mathsf{w}_{R_\perp}^p \otimes \mathsf{w}_{R_\perp}^p + \mathsf{w}_{I_\perp}^p \otimes \mathsf{w}_{I_\perp}^p\right] \mathsf{w}_{I_\perp}^p = 2\,|c_p|^2\,\|\mathsf{w}_{I_\perp}^p\|\,\mathsf{w}_{I_\perp}^p \tag{4.36}$$

Furthermore, considering $N-2$ independent $\mathsf{u}^r \in \mathcal{W}^{p\perp}$, $r = 3, ..., N$ (see Eq. 4.34), one has

$$\mathsf{R}\,\mathsf{u}^r = 2\,|c_p|^2 \left[\mathsf{w}_{R_\perp}^p \otimes \mathsf{w}_{R_\perp}^p + \mathsf{w}_{I_\perp}^p \otimes \mathsf{w}_{I_\perp}^p\right] \mathsf{u}^r = 0 \tag{4.37}$$

The above relations show that

$$\sigma_1 = 2\,|c_p|^2\,\|\mathsf{w}_{R_\perp}^p\| \tag{4.38}$$

$$\sigma_2 = 2\,|c_p|^2\,\|\mathsf{w}_{I_\perp}^p\| \tag{4.39}$$

$$\sigma_r = 0 \qquad\qquad \forall r = 3, ..., N \tag{4.40}$$

Therefore, the rank of the correlation matrix is two and the *proper orthogonal modes* associated to a non-zero *proper orthogonal values* (namely, to non-zero energy) coincide with the only possible orthogonal basis of $\mathcal{W}^p$ associated to the critical complex eigenvectors (Eqs. 1.28, 1.29 and 1.30).

This approach is preliminary to the nonlinear analysis of Sec. 4.4, where results provided by the POD analysis are interpreted with respect to the approximate closed-form solution provided by a singular perturbation technique, namely Normal Form.

4.3.3 An introductory example on POD analysis for systems experiencing a bifurcation of equilibrium

To introduce the POD analysis of nonlinear systems, let us consider a simple introductory example concerning two coupled nonlinear oscillators (Ref. [50]):

$$\ddot{x} + x + \dot{x}[-\mu + c_1(x^2 + \dot{x}^2) + c_2(y^2 + \frac{1}{\omega_y^2}\dot{y}^2)] = 0 \tag{4.41}$$

$$\ddot{y} + \omega_y^2 y + \dot{y}[\delta - c_3(x^2 + \dot{x}^2)] = 0 \tag{4.42}$$

Equations 4.41 can be rewritten in a first order form:

$$\dot{z} = Az + f_{nl}(z) \qquad (4.43)$$

where $z^T = \{\dot{x}\ \dot{y}\ x\ y\ \}$ and

$$A = \begin{bmatrix} \mu & 0 & -1 & 0 \\ 0 & -\delta & 0 & -\omega_y^2 \\ 1 & 0 & 0 & 0 \\ 0 & 1 & 0 & 0 \end{bmatrix} \qquad (4.44)$$

$$f_{nl}(z) = \begin{Bmatrix} 0 \\ 0 \\ \dot{x}[c_1(x^2 + \dot{x}^2) + c_2(y^2 + \alpha^2\dot{y}^2)] \\ -\dot{y}[c_3(x^2 + \dot{x}^2)] \end{Bmatrix} \qquad (4.45)$$

The equilibrium solution of such a system is stable untill $\mu < 0$. If $\mu > 0$ a LCO arises. In particular assuming that

$$x(t) = X\cos(t + \phi_x),\ y(t) = Y\cos(\omega_y t + \phi_y) \qquad (4.46)$$

one obtains the bifurcation equations

$$X(-\mu + c_1X^2 + c_2Y^2) = 0 \qquad (4.47)$$
$$Y(\delta - c_3X^2) = 0 \qquad (4.48)$$

From Equations 4.47 it appears that for $\mu < 0$ the equilibrium solution is possible whereas for $\mu > 0$ a LCO appears with, assuming $Y = 0$ (see Ref. [50]), $X = \sqrt{\frac{\mu}{c_1}}$. It is clear that $\mu = 0$ represent a equilibrium bifurcation point for the considered dynamical system. Computing the correlation matrix R from Eq. 4.7 using Eqs. 4.46 and 4.47 one obtains:

$$R = \begin{bmatrix} X^2/2 & 0 & 0 & 0 \\ 0 & 0 & 0 & 0 \\ 0 & 0 & X^2/2 & 0 \\ 0 & 0 & 0 & 0 \end{bmatrix} \qquad (4.49)$$

Equation 4.49 shows that only two POVs are different from zero and that they are associated to the POMs $\{1, 0, 0, 0\}$ and $\{0, 0, 1, 0\}$ coinciding with the real and imaginary part of the critical mode of the state matrix of the linear part of Eq. 4.43. In general, this is true only after a suitable definition of the critical eigenvector (see Ref. [41]) but the subspace spanned by the significative POD basis and the real and imaginary part of the critical mode are the same as it will be shown in the next chapter. Recalling the results of Sec. 1.5.1

for $\mu > \mu_c = \frac{\delta c_1}{c_3}$ a new bifurcation appears and Y is no longer zero. Computing again the correlation matrix one has:

$$
\mathsf{R} = \begin{bmatrix} X^2/2 & 0 & 0 & 0 \\ 0 & Y^2/2 & 0 & 0 \\ 0 & 0 & X^2/2 & 0 \\ 0 & 0 & 0 & Y^2\omega_y^2/2 \end{bmatrix} \tag{4.50}
$$

where it is clear that now all the POMs are associated with non-zero energy. One can observe that now all the POMs are unique: in the previous example, $\mu < \mu_c$, only the first two were unique being all others vectors in the orthogonal complement of the subspace $Span\{\{1,\,0,\,0,\,0\},\{0,\,0,\,1,\,0\}\}$. The particular case analyzed introduces some of the general aspects that will be developed in the next Sections and which will bring to a comparison between the POD objects and the invariant manifolds.

4.4 POD analysis of nonlinear systems undergoing bifurcation of equilibrium

The aim of this section is to understand the results provided by the POD analysis as applied to differential nonlinear systems depending on a scalar parameter. The Normal Form method has been used to provide approximate closed-form solutions in the neighborhood of a Hopf bifurcation experienced by the system.

4.4.1 Limit Cycle Oscillation

Recalling the results of Sec. 2.2.1 one can find the analytical expression of the Limit Cycle Oscillations arising from a Hopf bifurcation. In particular, a system experiencing a Hopf bifurcation is characterized by a linearized system (evaluated in the studied equilibrium) with a pair of purely complex conjugate eigenvalues $\lambda_1 = \bar{\lambda}_2 = j\omega_1$ going to have positive real part. From the Normal Form point of view a Hopf bifurcation is associated with the presence of the following zero-divisors (see Ref. [16]):

$$
\lambda_i - \lambda_i = 0 \tag{4.51}
$$

$$
\lambda_1 + \lambda_2 + \lambda_j - \lambda_j = 0 \tag{4.52}
$$

The normal form equation is:

$$
\dot{\eta}_1 = j\omega_1\eta_1 + \epsilon[\alpha_{11}\eta_1 + (\gamma_{1121} + \gamma_{1211} + \gamma_{1112})\eta_1^2\eta_2] = \beta^{(1)}\eta_1 + \gamma^{(1)}\eta_1^2\bar{\eta}_1 \tag{4.53}
$$

$$
\dot{\eta}_2 = \bar{\dot{\eta}}_1 \tag{4.54}
$$

with

$$\alpha_{ij} = \sum_{s,p=1}^{4} U_{is}^{-1} A_{1sp} U_{pj} \tag{4.55}$$

$$\gamma_{islm} = \sum_{n,p,q,r=1}^{4} U_{jn}^{-1} c_{npqr} U_{ps} U_{ql} U_{rm} \tag{4.56}$$

where $\epsilon = \nu - \nu^*$, $\beta = -j\omega_1 - \epsilon\alpha_{11} = \beta_R + j\beta_I$, $\gamma = -\epsilon(\gamma_{1121} + \gamma_{1211} + \gamma_{1112}) = \gamma_R + j\gamma_I$.
Equation 4.53 can be rewritten as

$$\dot{\eta}_1 + \beta\eta_1 + \gamma\eta_1^2\bar{\eta}_1 = 0 \tag{4.57}$$

Finally, the stationary solution, on the modal basis, is:

$$\mathsf{v} = \sqrt{\epsilon}\left(a_1 e^{\phi(t)}\mathsf{w}^{(1)} + C.C.\right) + o(\epsilon^{3/2}) \tag{4.58}$$

where

$$a_1(t \to +\infty) = \sqrt{-\frac{\beta_R}{\gamma_R}} \tag{4.59}$$

$$\phi(t \to +\infty) = t\left(-\beta_I + \frac{\gamma_I\beta_R}{\gamma_R}\right) + \frac{\gamma_I}{\gamma_R}\ln(a_1) + \phi_0 \tag{4.60}$$

Observe that the solution is the same of Sec. 3.2.3 as expected, because the forced and unforced solutions coincide in absence of resonance load at the first perturbation order analysis.

4.4.2   The relationship between POMs and Normal Form

Using the Normal Form solution given by Eqs. 4.58, is possible to obtain an explicit form for the correlation matrix R in analogous way to what has been done in Sec. 4.3.2 for the linear case. Denoting perturbed quantities with the superscript symbol $(\check{\cdot})$, the dependence on the perturbation parameter ϵ can be highlighted as

$$\check{\mathsf{R}} = \epsilon\mathsf{R}_1 + \epsilon^2\mathsf{R}_2 + o(\epsilon). \tag{4.61}$$

Equation 4.61 gives an ϵ-expansion for the correlation matrix related to the free response of a nonlinear system. The POD is obtained again from the ϵ-perturbed eigenproblem associated with $\check{\mathsf{R}}$:

$$\check{\mathsf{R}}\check{\mathsf{p}} = \check{\sigma}\check{\mathsf{p}} \tag{4.62}$$

Observing the structure of the correlation matrix and considering the energy interpretation of the σ_i, $i = 1, ..., N$, we can assume this form of POVs and POMs in the perturbation

parameter[3]:

$$\check{p} \;=\; p_0 + \epsilon p_1 + \epsilon^2 p_2 + \mathcal{O}(\epsilon^3) \tag{4.63}$$

$$\check{\sigma} \;=\; \epsilon \sigma_0 + \epsilon^2 \sigma_1 + o(\epsilon) \tag{4.64}$$

Hence, considering terms up to the order ϵ^3, we have at the orders ϵ^2 and ϵ^3 respectively:

$$R_1 p_0 \;=\; \sigma_0 p_0 \tag{4.65}$$

$$(R_1 - \sigma_0 I) p_1 \;=\; \sigma_1 p_0 - R_2 p_0 \tag{4.66}$$

The ϵ term is given by the standard eigenproblem 4.65. The ϵ^2 order correction follows from Eq. 4.66: note that the left-hand side is singular, so that it admits solutions if and only if the right-end side is orthogonal to the left eigenvector of R_1 corresponding to σ_0. Thus, imposing this condition, the N sought after σ_1^i, $i = 1, ..., N$ can be determined. Once the σ_1^i are known, the N vectors p_1^i can be evaluated by Eq. 4.66 but an additional condition, given by $p_1^i \cdot p_0^i = 0$, is required to avoid the presence of an arbitrary component.

Substituting Eq. 4.58 in the definition of the correlation matrix given by Eq. 4.7, truncating the expansion to the first order and considering, without loss of generality (see Sec. 1.3), the critical eigenvector to be such that $w_{R_\perp} \cdot w_{I_\perp} = 0$, one has

$$\check{R} \;=\; \epsilon R_1 + \mathcal{O}\left(\epsilon^2\right) \;=\; 2\epsilon \left(-\frac{\beta_R}{\gamma_R}\right) [w_{R_\perp} \otimes w_{R_\perp} + w_{I_\perp} \otimes w_{I_\perp}] + o(\epsilon) \tag{4.67}$$

Thus, considering Eq. 4.67 and the definition of POMs and POVs (Eq. 4.6), one achieves the following relations

$$\check{R} w_{R_\perp} \;=\; 2\epsilon \left(-\frac{\beta_R}{\gamma_R}\right) [w_{R_\perp} \otimes w_{R_\perp} + w_{I_\perp} \otimes w_{I_\perp}] w_{R_\perp} + o(\epsilon) =$$

$$\;=\; 2\epsilon \left(-\frac{\beta_R}{\gamma_R}\right) \|w_{R_\perp}\|^2 w_{R_\perp} + o(\epsilon) \tag{4.68}$$

$$\check{R} w_{I_\perp} \;=\; 2\epsilon \left(-\frac{\beta_R}{\gamma_R}\right) [w_{R_\perp} \otimes w_{R_\perp} + w_{I_\perp} \otimes w_{I_\perp}] w_{I_\perp} + o(\epsilon) =$$

$$\;=\; 2\epsilon \left(-\frac{\beta_R}{\gamma_R}\right) \|w_{I_\perp}\|^2 w_{I_\perp} + o(\epsilon) \tag{4.69}$$

$$\check{R} u \;=\; o(\epsilon) \quad \forall u \in \mathcal{W}^\perp \tag{4.70}$$

which shows that:

- the orthogonalized pair $w_{R_\perp}$ and $w_{I_\perp}$ coincide with the two POMs p associated with non-zero energy (to non-zero POVs) at the ϵ order, namely, they are the p_0 contribution in Eq. 4.65;

---

[3]Indeed, since the LCO amplitude is of $\sqrt{\epsilon}$ order, the associated energy, *i.e.*, the greater POVs, are of order ϵ.

• the POVs σ are given by (at the ϵ order see Eq. 4.65)

$$\sigma_{1_0} = 2\epsilon\left(-\frac{\beta_R}{\gamma_R}\right)\|\mathsf{w}_{R_\perp}\|^2 \tag{4.71}$$

$$\sigma_{2_0} = 2\epsilon\left(-\frac{\beta_R}{\gamma_R}\right)\|\mathsf{w}_{I_\perp}\|^2 \tag{4.72}$$

$$\sigma_{r_0} = 0 \quad r = 3, ..., N \tag{4.73}$$

The above result indicates that the dimension of the significant POD basis is strongly related to the *dimension* of the center manifold, *i.e.*, the dimension of the tangent subspace. Considering a higher-order perturbation, the rank of R increases and analogously the number of the non-zero POVs. However the largest part of the energy will be still contained in the first two POVs until the other modes give a significant contribution.

Chapter 5

POD analysis for bifurcated systems

In this Chapter the POD behavior in the neighborhood of bifurcation is analyzed. In particular, we will discuss how the POD objects, namely POMs, relate with the intrinsic geometry of nonlinear systems represented by the nonlinear manifolds. The POD generates an orthonormal basis collecting the largest part of the response energy. If, as in aeroelasticity, the modal basis (namely, the system invariant subspaces) is generally complex and orthogonality does not apply, it is necessary a different approach is needed to relate invariant subspaces (modal basis) and POD. The proposed approach is based on the fact that the complex modes can be equivalently represented by the subspace spanned by their real and imaginary part (Ref. [44]). Moreover, in nonlinear systems the concept of linear modes is still locally significant in the neighborhood of an equilibrium point. Indeed, these modes represent the tangent spaces to the invariant manifolds. In presence of an equilibrium bifurcation, like a Hopf bifurcation, the solution can be locally built starting from the center invariant subspace (Center Manifold Theorem, see Ref. [42]).

In Chapter 4, we worked out a few relevant cases available in literature for linear systems and by using the perturbative solution given by the Normal Form (see Refs. [30, 74, 81]), we showed that the significant POD-basis spans the critical subspace, *i.e.*, the center subspace, with only a small correction due to higher order terms defined in the perturbation process. It is important to stress that since the main interest is on the proper dynamical features of the process, we will analyze by POD only free responses of the dynamical. In this Chapter, the accuracy of the theoretical results obtained in Chapter 4 will be assessed against numerical applications on linear and nonlinear aeroelastic and structural systems.

5.1 Numerical results on nonlinear aeroelastic systems

Two typical aeroelastic applications are herein considered: the linear and nonlinear response of a wing section in an unsteady potential flow (Sec. 5.1.1), and the nonlinear oscillations of a vibrating panel in a supersonic flow (Sec. 5.1.5).

5.1.1 A typical section from critical to post-critical regime

A three-degree-of-freedom aeroelastic typical section with a trailing-edge control surface, shown in Fig. 5.1, is modeled including nonlinear springs for the control surface hinge elastic moment. The POD is then applied to the system free response evaluated numerically via the Runge-Kutta algorithm. Thus, the correlation matrix is computed using the time-discrete form given by Eq. 4.7. Specifically, the parameters governing the system are chosen so that the system experiences a supercritical Hopf bifurcation, that is, a stable LCO arises after the flutter speed. In the following, the mathematical model describing the typical section behavior is first addressed. In Section 5.1.1 the linearized system in the neighborhood of the stability margin is then analyzed. In Sec. 5.1.2 and 5.1.3 the POD analysis for both the linear and nonlinear system is shown. Finally, some specific issues about POD related to the system observability are also presented in 5.1.4.
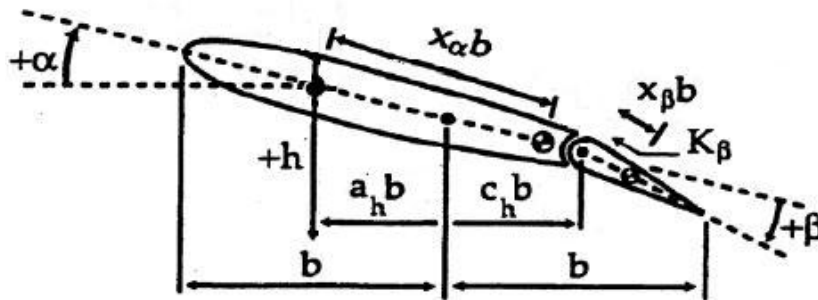

Figure 5.1: 3-d.o.f. aeroelastic typical section.

Governing equations

Consider a 3-dof airfoil, elastically supported by a linear plunge spring and a linear torsional spring (Fig. 5.1). It is equipped with a control surface (flap), constrained to the wing with a nonlinear torsional spring. Using standard notation, the plunging deflection is denoted by

h, positive in the downward direction, α is the pitch angle about the elastic axis, positive with nose up, and β is the flap angle, positive when the trailing edge (TE) surface is moved down. The elastic axis is located at a distance $a_h b$ from the mid-chord, where b is half the chord, while the wing mass center is located at a distance $x_\alpha b$ from the elastic axis. The axis of rotation for the flap is located at a distance $c_h b$ from the mid-chord, whereas the flap mass center is located at a distance $x_\beta b$ from the flap hinge. All the previous distances are positive when measured towards the TE of the airfoil.

The linear equations of motion of the typical section ideally immersed in a potential flow were found by Theodorsen in 1935 (Ref. [82]). The typical-section equations are

$$\ddot{\xi} + x_\alpha \ddot{\alpha} + x_\beta \ddot{\beta} + \frac{\Omega_1^2}{U^2} = p, \tag{5.1a}$$

$$\frac{x_\alpha}{r_\alpha^2}\ddot{\xi} + \ddot{\alpha} + [r_\beta^2 + (c_h - a_h)x_\beta]\frac{1}{r_\alpha^2}\ddot{\beta} + \frac{1}{U^2}M_\alpha(\alpha) = r, \tag{5.1b}$$

$$\frac{x_\beta}{r_\beta^2}\ddot{\xi} + \ddot{\beta} + [1 + (c_h - a_h)\frac{x_\beta}{r_\beta^2}]\ddot{\alpha} + \frac{\Omega_2^2}{U^2}M_\beta(\beta) = s, \tag{5.1c}$$

where

$$M_\alpha(\alpha) = c_{1\alpha}\alpha \tag{5.1d}$$

$$M_\beta(\beta) = c_{1\beta}\beta + c_{3\beta}\beta^3. \tag{5.1e}$$

In the above equations, the overdot denotes differentiation with respect to the dimensionless time τ, defined as $\tau = Vt/b$, $\xi = h/b$ is the dimensionless plunge displacement of the elastic axis, $r_\alpha = \sqrt{J_\alpha/mb^2}$ is the reduced radius of gyration about the elastic axis, $r_\beta = \sqrt{J_\beta/mb^2}$ is the reduced radius of gyration about the flap hinge and $\mu = \sqrt{\pi\rho b^2/m}$ is the mass ratio. The symbols Ω_1 and Ω_2 are defined as $\Omega_1 = \omega_\xi/\omega_\alpha$ and $\Omega_2 = \omega_\beta/\omega_\alpha$, where ω_ξ, ω_α and ω_β are the uncoupled plunging, pitching and flapping natural frequencies, respectively, which depend on the parameter U. Moreover, $M_\alpha(\alpha)$ represents the overall contribution of the torsional spring moment of the wing section, whereas $M_\beta(\beta)$ represents the overall contribution of the torsional spring moment of the wing section including both the linear and nonlinear parts. The coefficients of the unknowns in Eqs. 5.1 depend on the system control parameter $U = V/b\omega_\alpha$, i.e., the reduced flow velocity, where V is the dimensional speed. The sysmbols p and r denote the lift and the pitch aerodynamic moment for the wing, respectively, whereas s is the pitching moment acting on the flap. Assuming an incompressible two-dimensional

flow, the expressions of the forces in the time domain are given by (Refs. [82], [4]):

$$p = -\frac{1}{\mu}\left[\dot{\alpha} + \ddot{\xi} - a_h\ddot{\alpha} - (T_4/\pi)\dot{\beta} - (T_1/\pi)\ddot{\beta} + 2u(w_{3/4})\right] \tag{5.2}$$

$$r = -\frac{1}{\mu r_\alpha^2}[\bar{a}_h\dot{\alpha} + (1/8 + a_h^2)\ddot{\alpha} - a_h\ddot{\xi} + (T_4/\pi + T_{10}/\pi)\beta + (T_1/\pi - T_8/\pi \tag{5.3}$$

$$- (c_h - a_h)T_4/\pi + 1/2(T_{11}/\pi))\dot{\beta} - (T_7/\pi + (c_h - a_h)T_1/\pi)\ddot{\beta}$$

$$- 2(a_h + 1/2)u(w_{3/4})]$$

$$s = -\frac{1}{\mu r_\beta^2}[(-2T_9/\pi - T_1/\pi - \bar{a}_hT_4/\pi)\dot{\alpha} + 2(T_{13}/\pi)\ddot{\alpha} + (T_5/\pi^2 - T_4T_{10}/\pi^2)\beta$$

$$- (T_4/\pi)(T_{11}/\pi)\dot{\beta} - (T_3/\pi^2)\ddot{\beta} - (T_1/\pi)\ddot{\xi} + (T_{12}/\pi)u(w_{3/4})] \tag{5.4}$$

where the circulatory part of the lift and of the pitching moments is denoted with $u(w_{3/4})$ (Ref. [83]) and the expressions of the coefficients T_i are the same as defined in Ref. [82]. Using a finite-state approximation for the circulatory part of the aerodynamics forces, the problem is recast (Ref. [84]) as a system of eight first-order differential equations, *i.e.*,

$$\dot{\mathsf{v}} = \mathsf{A}(U)\mathsf{v} + \mathsf{g}(\mathsf{v},\mathsf{U}) \tag{5.5}$$

where $\mathsf{v}^T = \{\xi, \alpha, \beta, u, \dot{\xi}, \dot{\alpha}, \dot{\beta}, \tilde{u}\}^T$ is the state-space vector, $\mathsf{A}(U)$ and $\mathsf{g}(\mathsf{v},\mathsf{U})$ are the linear and nonlinear part of the equations of motion, respectively. In general, it is possible to use P aerodynamic states to model the unsteady part of the aerodynamic operator but, in the present case, only two augmented states, denoted as u and $\tilde{u}$, were sufficient for the present scope (Ref. [4]).

Stability analysis and bifurcation scenarios

The values of the coefficients in Eqs. 5.1-5.4 were the same already used by Edwards in Ref. [85] and, for the reader convenience, are listed in Tab. 5.1. The corresponding evaluated

a_h	-0.4	c_h	0.6
m	40	Ω_1	0.5
Ω_2	3.0	$c_{1\alpha}$	1
$c_{1\beta}$	1	$c_{3\beta}$	50
x_α	0.2	x_β	0.0125
r_α^2	0.125	r_β^2	0.00625

Table 5.1: Airfoil parameters.

flutter speed is $U_F = 3.0246$ and, beyond this value, the nonlinear system exhibits a supercritical Hopf bifurcation. The bifurcation diagram obtained via both numerical integration

and Normal Form perturbation analysis is depicted in Fig. 5.2, where the LC amplitude is plotted as a function of U (the continuous line is obtained by Multiple Time Scaling analysis, whereas the markers represent the numerical integration results). After the critical value U_F,
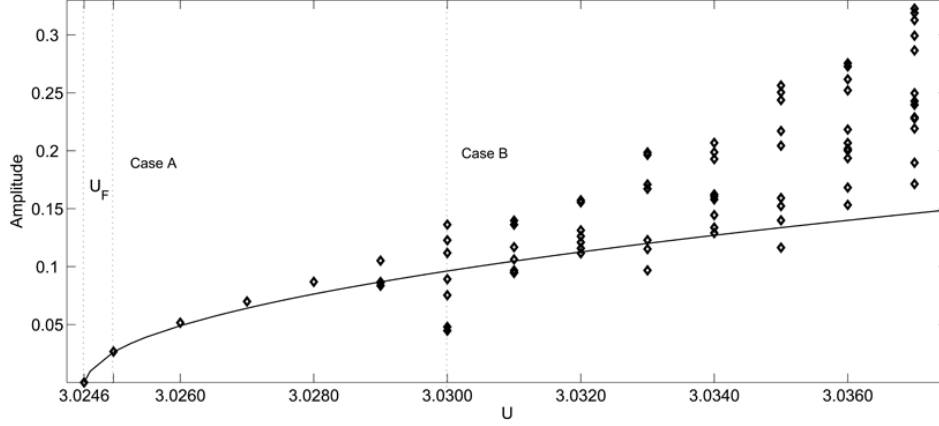
Figure 5.2: Bifurcation diagram. - Normal Form; ◇ Numerical Integration.

the free response is harmonic and represented by a single oscillation amplitude. However, for $U > 3.029$, it keeps to be periodic but more than one harmonic component appears in its time-history, as reported by the multiple points for each flight speed which indicate the local maximum peak in a period. In this case, the perturbation solution needs to include more than first-order terms to be satisfactorily described. With respect to the presented scenario, a numerical validation of the analytical achievements regarding the relation between the POD basis and the critical eigenvectors will be proposed. In particular, the *modal assurance criterion parameter* (MAC) will be used to check the parallelism between the POMs and the real and imaginary part of the critical mode (transformed through Eq. 1.27), defined as

$$\text{MAC}(\mathsf{a}, \mathsf{b}) = \frac{(\mathsf{a} \cdot \mathsf{b})^2}{\|\mathsf{a}\|^2 \|\mathsf{b}\|^2} \tag{5.6}$$

where a and b are the considered vectors. Note that $\text{MAC}(\mathsf{a}, \mathsf{b}) = 1$ if a and b are parallel and $\text{MAC}(\mathsf{a}, \mathsf{b}) = 0$ if they are orthogonal.

5.1.2 POD analysis: Linear case

The analysis is first performed for the linear case, to which the dynamical system is reduced if $c_{3\beta} = 0$ in Eqs. 5.1. Moreover, let us assume the system to be marginally stable, by setting $U = U_F$. The correlation matrix R (see Eq. 4.7 is evaluated with an initial condition given by the vector $\mathsf{v}_0^T = \{0, 0, 0.3, 0, 0, 0, 0, 0\}^T$ and a observation time window T of $1.8 \cdot 10^4$ dimensionless time units after removal of the transient. R (Eq. 4.7) gives only two significant

	p_1	p_2
w_R	0.0000	1.0000
w_I	1.0000	0.0000

Table 5.2: MAC between linear mode and significant POD basis. Marginally stable linear case.

	p_1	p_2
w_R	$2 \cdot 10^{-4}$	0.9997
w_I	0.9997	$2 \cdot 10^{-4}$

Table 5.3: MAC between critical linear mode and POD significant basis. Nonlinear case, $U = 3.0250$.

POVs accounting for all the response energy. As expected, their analytical estimated values (see Eqs. 4.38-4.40) present a very small difference with respect to the numerical ones (relative difference is equal to -0.01% and 0.02%), mainly due to numerical approximations in the evaluation of the correlation matrix R. Table 5.2 shows the MAC values obtained comparing the significant POMs (numerically obtained) and the orthogonalized real and imaginary part of the critical mode (Eqs. 1.28 and 1.29). This result numerically assesses the coincidence between the significant POMs and the critical mode in flutter condition as predicted by the developed theory.

5.1.3 POD analysis: Nonlinear case

The previous task is carried out again for the nonlinear case, *i.e.*, with the system experiencing a Hopf bifurcation. Because of the more complicated scenario, the relation between the POMs and the tangent critical eigenvectors (w_R, w_I) (recall Eqs. 4.68, 4.69 and 4.70 in Sec. 4.4.2) will be validated for two different values of the parameter U.

A first postcritical case: $U = 3.0250$ (Case A, Fig. 5.3)

In this case, the system is slightly beyond the linear flutter speed ($U - U_F = 0.0004$). The LCO is simply harmonic (see Fig. 5.3) as predicted by the Normal Form analysis. Like the marginally-stable linear system, all the energy is associated with the first two POMs, as shown by the corresponding POVs covering almost the 100% of the sum of all the eigenvalues. Also, in this case the orthogonalization procedure (see Eqs. 1.28 and 1.29) of the real and the imaginary parts of the critical mode allows to obtain real-valued vectors in full agreement with the first and the second POMs, as shown in Tab. 5.3.

Second postcritical case: $U = 3.03$ (Case B, Fig. 5.4)
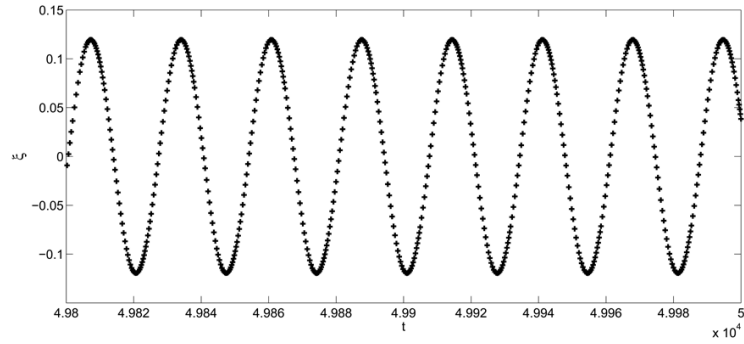
(a) Plunge
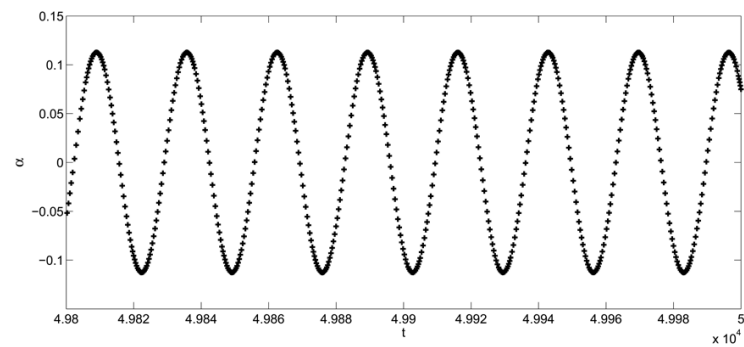
(b) Pitch
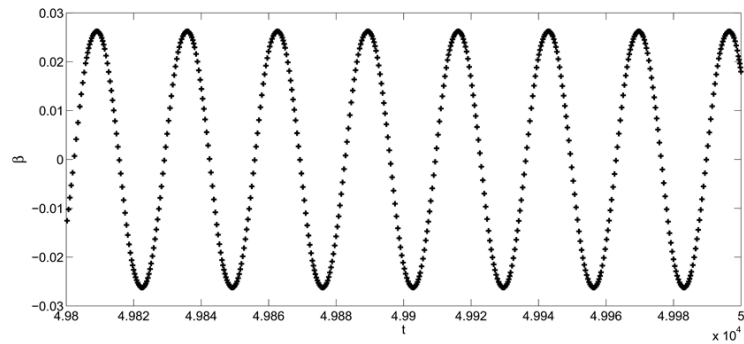
(c) Flap

Figure 5.3: Limit Cycle Oscillation at $U = 3.0250$ (CASE A).

In this second case ($U - U_F = 0.0054$), the effect of the nonlinear terms is emphasized but the equivalence between the significant POMs and the critical mode is still essentially valid, although minor differences arise. From the inspection of the time histories of h, α and β (see Fig. 5.4), it is possible to realize that the nonlinearities affect the oscillation depending on the considered state-space variable. Indeed, especially considering the flap response, the presence of multiple harmonics is evident. In this particular case, the carried out Normal Form

	p_1	p_2
w_R	$5 \cdot 10^{-4}$	0.9951
w_I	0.9957	$1 \cdot 10^{-4}$

Table 5.4: MAC between critical linear mode and POD significant basis. Nonlinear case, $U = 3.030$.

analysis is not able to follow satisfactorily the solution because the presence of the mentioned harmonics requires at least the inclusion of more terms in the perturbation expansion or even a higher-order solution. However, the critical eigenvectors still play a relevant role in accounting the system dynamics on a time-averaged perspective. In fact, the first two POVs collect 99.82% of the overall signal energy. The relation between the center subspace and POD basis is investigated with the MAC in Tab. 5.4, that confirm the fact that the POD basis is still related to the center subspace. In addition to the case already considered, the dependence of the percentage energy content associated with the first two POMs with respect to the inflow velocity U varying in a neighborhood of the critical value is analyzed in Fig. 5.5, confirming the previous observations also for other values of U. As shown before, this energy percentage is expressed as the POV value normalized with respect to the sum of all the POVs. Similarly, the correspondence between the critical mode $w = w_{R_\perp} + jw_{I_\perp}$ and the significant POD basis p^n, $n = 1, 2$ is further analyzed for different values of U using the MAC (see Fig. 5.6). It is apparent that the link between the critical mode and the POMs keeps to be relevant even when nonlinear effects are significant, with MAC values rather close to one even if slightly lower than in the linear case. The POMs and their associated energy are global properties of the observed process and, in this perspective, the Normal Form approach seems to be still able to capture these general features. Indeed, the value of the generic POV depends on the approximation order of the Normal Form solution: thus, it is not surprising that, when the Normal Form approximation becomes inaccurate (*e.g.*, moving away from the critical value of the parameter, U_F), the Normal Form prediction of the POVs values (see Eqs. 4.71 and 4.72) are also inaccurate as well. These remarks allow to explain the results shown in Fig. 5.7, where the values of the first POV computed analytically and numerically are compared (a similar trend has been also obtained for the second POV). Moreover, considering Tabs. 5.3 and 5.4, where the MAC distribution of the considered nonlinear cases are shown, one can observe that increasing the difference $U - U_F$ (and hence, the effect of nonlinearities) the couples $(w_{R_\perp}, w_{I_\perp})$ and (p_1, p_2), that at the stability margin are coincident, differ by a rigid rotation in the same plane (or, subspace) that increases (see Fig. 5.8) with $U - U_F$, *i.e.*, the nonlinearities effect.
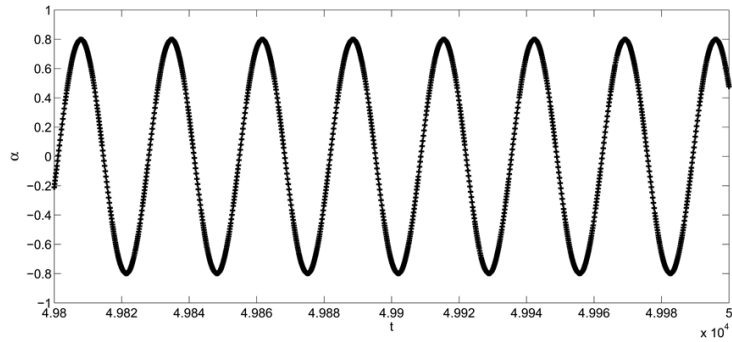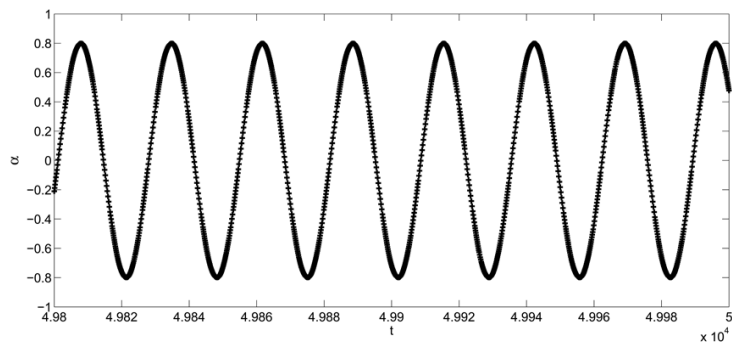
(a) Plunge

(b) Pitch
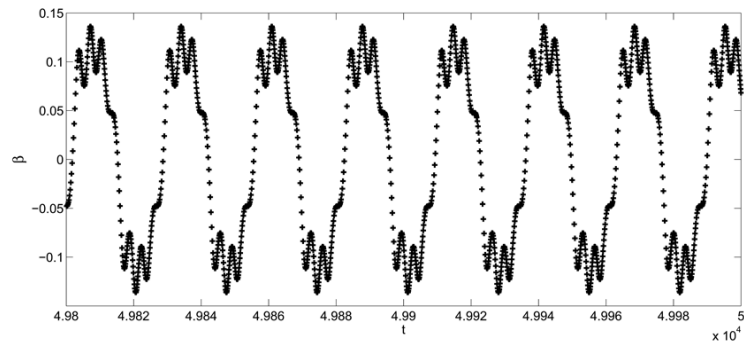
(c) Flap

Figure 5.4: Limit Cycle Oscillation at $U = 3.030$ (CASE B).

5.1.4 Some remarks on system observability

The POMs and the POVs are evaluated using a correlation matrix R that is built considering the contribution of all the space-state variables, including the aerodynamic states u and $\tilde{u}$ along with $\dot{h}, \dot{\alpha}, \dot{\beta}$. Indeed, the aerodynamic states are not directly observable, whereas velocities are related to displacements. However, our results remain valid also in the case of a POD analysis based only on generalized displacements, as it will briefly discussed.
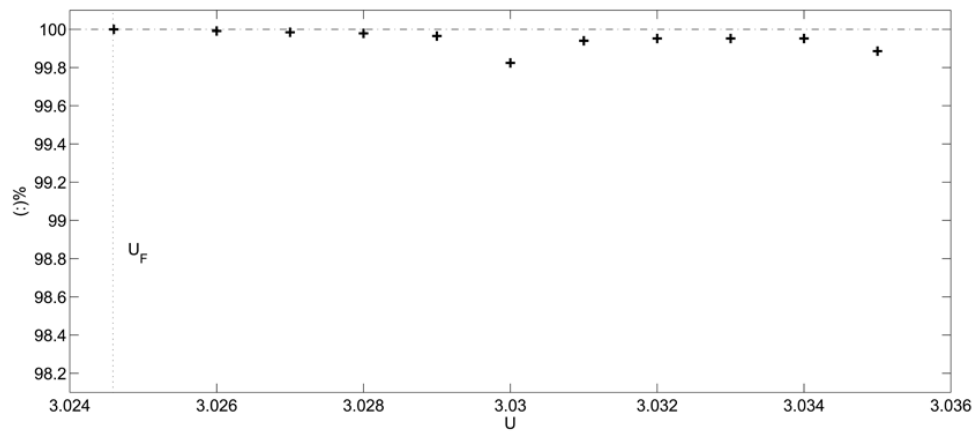
Figure 5.5: Percentage of energy in the first two POVs varying the U from the critical value.
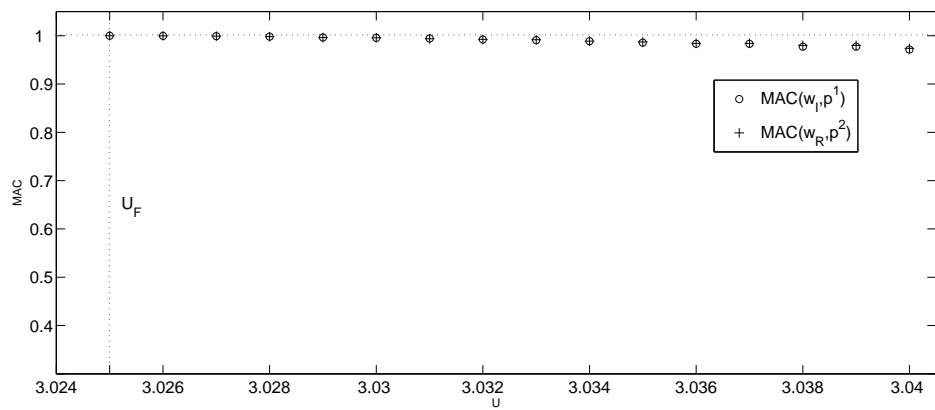
Figure 5.6: Modal Assurance Criterion (MAC) vs U.
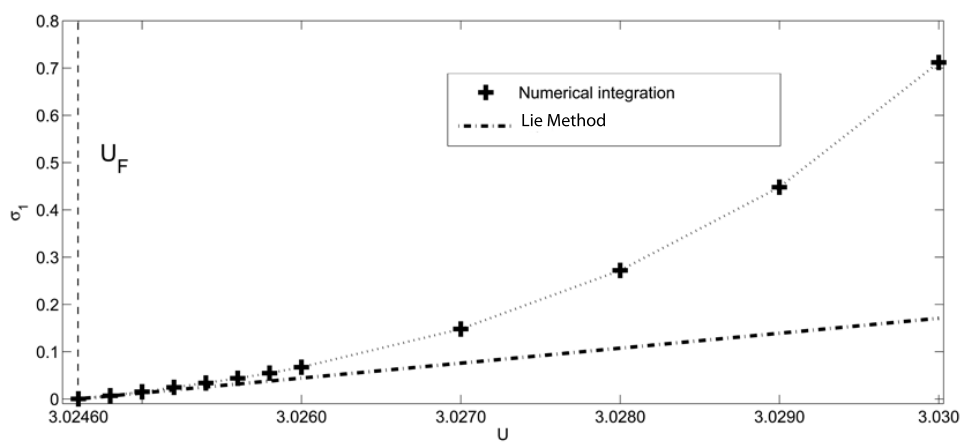
Figure 5.7: Comparison between the first POV analytically and numerically computed.
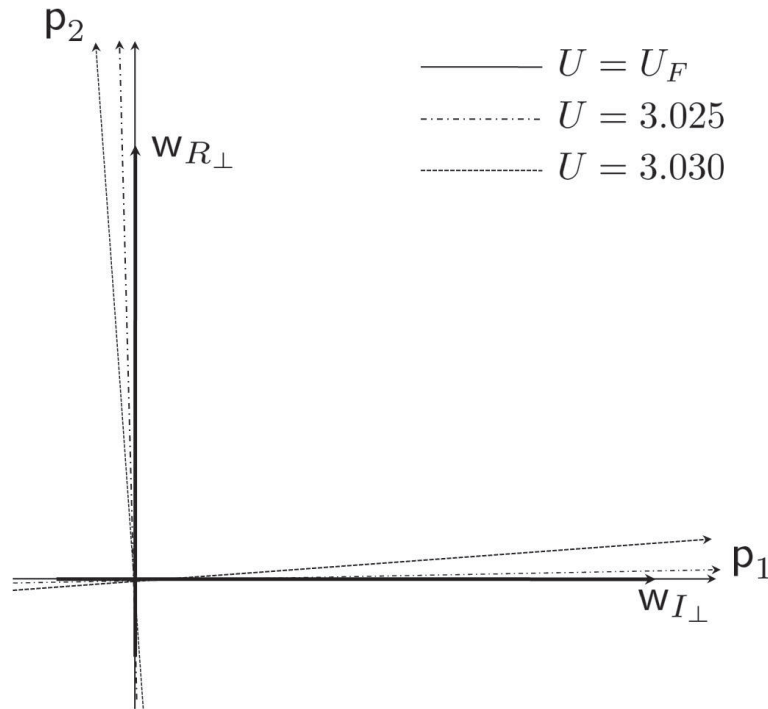
Figure 5.8: Rotation between POD significant basis and orthogonalized critical mode.

	p_1	p_2
w_R	$5.0 \cdot 10^{-3}$	0.9705
w_I	0.9708	$2.0 \cdot 10^{-3}$

Table 5.5: MAC between critical linear mode and POD significant basis. Nonlinear case, $U = 3.030$.

This issue is typically related to the real collection of information about the dynamical behavior performed by an on-board measurement system. Without recalling the steps of the underlying procedure, the nonlinear case with $U = 3.03$ is considered again without accounting for the aerodynamic states in the computation of R. The first two POVs do collect practically the 100% of the energy of the restricted signal and Table 5.5 shows that the corresponding POMs are still practically equivalent to the critical eigenvector.

5.1.5   The panel flutter model: from LCO to chaos

In the present section, the analysis already carried out for the case of a space-discrete aeroe-lastic system in Sec. 5.1.1 is also applied to a space-continuous systems, *i.e.*, a panel vibrating in a supersonic flow (see Ref. [6]). This application has given the opportunity to extend the results to a space-continuous model (Ref. [5]) that exhibits an even more various response scenario than the one investigated in Sec. 5.1.1. This system has two driving parameters that influence its structural stability, beyond the linear stability. Different choices of such parameters yield a free response that can be simply harmonic or even evolving to chaotic so-lutions (see Ref. [2]). For this application, it will be possible to compare the results obtained with POD analysis, and to discuss them in relation with the system nonlinear behavior.

Governing equations

Let us consider a simply supported panel (Fig. 5.9) immersed in a supersonic flow with speed U_∞ and with the dimension transverse to the flow direction (spanwise direction) larger than the panel length in the flow direction x^* (chordwise direction). The equation of motion is, see Ref. [81]:
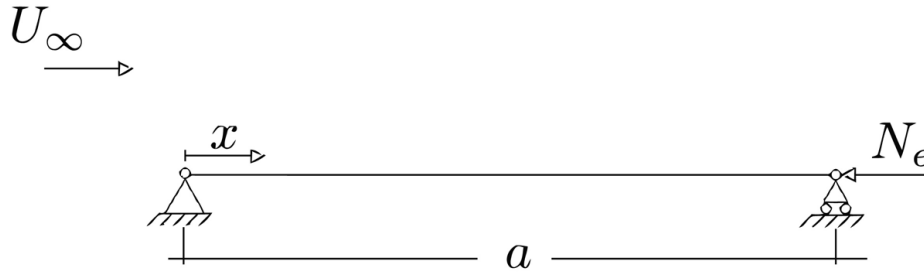
Figure 5.9: Vibrating panel supported to the ends in a flux with speed U_∞ and compression load N_e.

$$\rho_m \frac{\partial^2 v}{\partial t^2} + Lv + D\zeta \frac{\partial^5 v}{\partial t \partial^4 x^*} + N_{nl}(v)\frac{\partial^2 v}{\partial^2 x^*} + p(v) - p_\infty = 0 \tag{5.7}$$

$$\text{with} \quad L(\cdot) := D\frac{\partial^4(\cdot)}{\partial^4 x^*} + N_e \frac{\partial^2(\cdot)}{\partial^2 x^*}$$

where $v(x^*, t)$ is the vertical displacement, D is the bending stiffness, ζ is the viscoelastic damping coefficient, N_e is the compression load, and

$$N_{nl}(v) = -\frac{Eh}{2a}\int_0^a (\frac{\partial v}{\partial x^*})^2 dx^* \tag{5.8}$$

is the nonlinear load induced by the deformation, ρ_m is the material density of the panel, h is the panel thickness, a is the panel length and the differential pressure load $p(v) - p_\infty$ is

given by

$$p(v) - p_\infty = \rho_\infty U_\infty^2 (\frac{\partial v}{\partial x^*} + \frac{\partial v}{\partial t}/U_\infty)/\sqrt{M_\infty^2 - 1} \tag{5.9}$$

where ρ_∞ e M_∞ are the air density and the Mach number of the undisturbed flow, respectively.

Using the Galerkin approach with N_M orthonormal functions $\{\phi^n\} = \{sin\left(\frac{n\pi x^*}{a}\right)\}$ (namely, the eigenfunctions of the structural operator L), $n = 1, ..., N_M$, one has:

$$v(x,t) = \sum_{m=1}^{N_M} z_m(t) sin\left(\frac{m\pi x^*}{a}\right) = \sum_{m=1}^{N_M} z_m(t)\phi^m(x); \quad x = \frac{x^*}{a} \tag{5.10}$$

After projecting Eq. 5.7 on the basis functions $\{\phi^n\}$ and introducing a dimensionless time $\tau := t\left(D/\rho_m h a^4\right)^{1/2}$, one obtains

$$\ddot{z}_n + d_n \dot{z}_n + \Omega_n^2 z_n + \bar{q} \sum_{p=1}^{N_M} e_{np} z_p + g_n = 0 \quad n = 1, 2, ..., N_M \tag{5.11}$$

where the overdots denote the derivative with respect to the dimensionless time τ and

$$\theta_1 := \sqrt{\rho_\infty a\bar{q}/\sqrt{M_\infty^2 - 1}\rho_m h} \qquad \theta_2 := \pi^4 \zeta \sqrt{D/\rho_m h a^4}$$

$$N := \frac{N_e a^2}{D\pi^2} \qquad\qquad\qquad \Omega_n^2 := \pi^4(n^4 - n^2 N)$$

$$\bar{q} := \frac{\rho_\infty U_\infty^2 a^3}{D\sqrt{M_\infty^2 - 1}} \qquad\qquad d_n := \theta_1 + n^2 \theta_2$$

$$e_{np} := \frac{np}{n^2 - p^2}[1 - (-1)^{(n+p)}]$$

whereas the term g_n collects the nonlinear cubic terms

$$g_n := \sum_{p,q,r=1}^{N_M} c_{npqr} z_p z_q z_r \tag{5.12}$$

with

$$c_{npqr} := 3(1 - \nu^2)\pi^4(np)^2 \delta_{nq}\delta_{pr} \tag{5.13}$$

The continuous solution expanded in N_M terms, see Equation 5.10, can be localized, at any time, in N_p physical spatial points with coordinate x_i with $i = 1, ..., N_p$

$$v(x_i, \tau) = \sum_{m=1}^{N_M} z_m(\tau)\phi^m(x_i) \tag{5.14}$$

$$\frac{\partial v}{\partial \tau}(x_i, \tau) = \sum_{m=1}^{N_M} \dot{z}_m(\tau)\phi^m(x_i) \tag{5.15}$$

which can be rewritten in matrix form as

$$\mathsf{v}(\tau) = \mathsf{C}\bar{\mathsf{r}}(\tau) \tag{5.16}$$

with

$$\mathsf{C}_{ij} = \phi^j(x_i) \quad i = 1, ..., N_p, \quad j = 1, ..., N_M \tag{5.17}$$

$$\bar{\mathsf{r}}^T(\tau) = \{z_1(\tau), z_2(\tau), ..., z_{N_M}(\tau)\}$$

$$\mathsf{v}^T = \{v(x_1, \tau), v(x_2, \tau), ..., v(x_{N_p}, \tau)\}$$

The system can be rewritten in first order form as

$$\dot{\mathsf{r}} = \mathsf{A}\mathsf{r} + \begin{bmatrix} \mathbf{0} \\ \mathsf{I} \end{bmatrix} \mathsf{g}(\mathsf{r}) \tag{5.18}$$

where the unknown is $\mathsf{r}^T = \{\bar{\mathsf{r}}^T, \dot{\bar{\mathsf{r}}}^T\}$, the matrix A is the linear part of the dynamical system, $\mathsf{g}(\mathsf{r})$ is the vector of the nonlinear terms defined with Eq. 5.12.

The time-marching integration of Eq. 5.18 provides the solution of the panel-flutter equation (see Eq. 5.7) via the coordinate transformation given by Eq. 5.16, that represents the discretized form of the continuous solution for the displacement v, see Eq. 5.10. This solution allows to perform the POD analysis for the space continuous system, leading to solve the eigenproblem associated to the integral operator

$$P(\cdot) = \int_{\mathcal{V}} R(x, y)(\cdot) d\,y \tag{5.19}$$

where $R = R(x, y) = \lim_{T \to +\infty} \frac{1}{T} \int_0^T v(x, t)\, v(y, t)\, dt$.

Equation 5.19 defines the space-continuous proper orthogonal modes $\boldsymbol{\varphi}^s$ and proper orthogonal values σ_s as

$$P(\varphi) = \sigma \varphi. \tag{5.20}$$

Note that, by choosing N_p points on the panel the discretized form of the integral operator P (Eq. 5.19) gives a $N_p \times N_p$ correlation matrix R similar to the one already considered for the POD analysis of discrete systems.

In an analogous way, the eigenproblem associated to the space-discretized system of Eq. 5.18, *i.e.*,

$$\mathsf{A}\,\mathsf{w} = \lambda\,\mathsf{w}, \tag{5.21}$$

provides the eigenvectors w^q. The generic q-th aeroelastic eigenfunction $\boldsymbol{\chi}^q$, $q = 1, ..., 2N_M$, can be expanded with respect to the basis of $\{\phi^n\}$ to yield:

$$\chi^q(x) = \sum_{n=1}^{N_M} \mathsf{w}_n^q \phi^n(x) \tag{5.22}$$

where the complex numbers w_n^q represents the n-th component of the q-th eigenvector w^q. The $2N_M$ obtained eigenfunctions are independent and, generally, they appear in complex conjugate pair. Thus, without loss of generality, one can consider N_M independent couples (χ_R^p, χ_I^p), with $p = 1, 2, ..., N_M$, ordered as:

$$\begin{aligned} \chi^{2p-1} &:= \chi_R^p + j\chi_I^p \\ \chi^{2p} &:= \chi_R^p - j\chi_I^p \end{aligned} \tag{5.23}$$

where

$$\chi_R^p := \sum_{n=1}^{N_M} w_{nR}^p \phi^n(x) \quad \chi_I^p := \sum_{n=1}^{N_M} w_{nI}^p \phi^n(x) \tag{5.24}$$

Once the continuous POMs and the aeroelastic eigenfunctions are introduced, it is possible to define the critical eigenfunction so that its real and imaginary parts be orthogonal. Repeating the steps already illustrated in the Sec. 4.4.2, one can reach the same conclusions obtained for the case of discrete systems:

- complex conjugate eigenfunctions are directly related to the subspace $\mathcal{W}$ of the state-space spanned by their real and imaginary parts χ_R and χ_I;

- it is possible to orthogonalize the vectors χ_R and χ_I on the subspace $\mathcal{W}$ by multiplying the correspondent complex eigenfunction by a suitable complex constant so as to obtain an orthogonal basis $(\chi_{R_\perp}, \chi_{I_\perp})$ of $\mathcal{W}$;

- considering simply stable linear systems in the presence of only one marginal eigenfunction, its orthogonalized real and imaginary parts $\chi_{R_\perp}$ and $\chi_{I_\perp}$ are coincident with the first two POMs that are the only ones associated with non-zero energy, namely, to non-zero POVs;

- using a perturbation approach to express the solution, the above issue can be extended to nonlinear systems exhibiting a supercritical Hopf bifurcation.

Once it is assumed that there exists a relationship (see Eq. 5.10) between the continuous displacement function $v(x, t)$ and the vector of its modal components $\mathsf{r}^T = \{z_1, z_2, ..., z_{N_M}, \dot{z}_1, \dot{z}_2, ..., \dot{z}_{N_M}\}^T$ (the orthogonal basis $\{\phi^n\}$ ensures this issue), then there is also a direct correspondence between the obtained eigenfunctions χ^p and the eigenvectors w^p, between the continuous POMs φ^p and their discrete form, i.e., the vectors p^p, and between the space-continuous variable $v(x, t)$ and its space-discrete form $\mathsf{v}(t)$.

Stability analysis

Two control parameters are considered in the panel flutter analysis: $\bar{q}$, that accounts for the inflow, and the compression load N. There are three main dynamic scenarios (see Fig. 9 in Ref. [5]) depending on the choice of such parameters:

- aeroelastic dynamical instability without compression load ($N = 0$, $\bar{q} \neq 0$)

- structural static instability due to compression load ($\bar{q} = 0$, $N \neq 0$)

- instability with compression load and aerodynamic combined effects ($\bar{q} \neq 0$, $N \neq 0$)

Next, four qualitatively different conditions will be analyzed with the POD analysis. Three cases imply harmonic responses (limit cycles), and one case exhibits a chaotic behavior. The response time-history of the vertical displacement is built retaining the contribution of $N_M = 4$ and is evaluated ats 10 equally spaced points ($N_p = 10$) on the panel. This implies that, performing a direct numerical time-integration of Eq. 5.18 and using Eq. 5.16, a 10×10 dimensional correlation matrix R was built and the consequent POVs and POMs evaluated. For all the results considered in the following, the evaluated POMs (namely, the φ) will be compared with the corresponding aeroelastic LMs (namely, the $\chi_{R_\perp}$ and $\chi_{I_\perp}$). The comparison between POMs and LMs will be done through the definition of a modal assurance criterion parameter (MAC) here redefined in functional spaces as

$$\text{MAC}(\vartheta, \psi) = \frac{<\vartheta, \psi>^2}{<\vartheta, \vartheta><\psi, \psi>} \tag{5.25}$$

where $\vartheta(x)$ and $\psi(x)$ are bounded functions in I and $<\vartheta, \psi> := \int_I \vartheta(x) \cdot \psi(x)\, dx$. For the evaluation of the correlation matrix, a time-window of 18000 dimensionless time units is used.

POD analysis

Next, the POD analysis of the different regimes is carried out. The different cases give the possibility to correlate POD basis with the aeroelastic modal contribution to the free response.

<u>Simple-harmonic limit cycle</u>

Let us consider the case defined by the following choice of the parameters

$$N = 0, \quad \theta_1 = 1, \quad \theta_2 = 0, \quad \bar{q} = 344. \tag{5.26}$$

	φ_1	φ_2
χ_R	0.0000	1.0000
χ_I	1.0000	0.0000

Table 5.6: MAC for the simply-harmonic case.

The system is beyond the linear flutter stability margin and the presence of a limit cycle having a purely harmonic oscillation is shown in Fig. 5.10, where the phase diagram (velocity vs displacement) of the oscillation at $x^*/a = 3/4$ is presented. The first two POVs collect
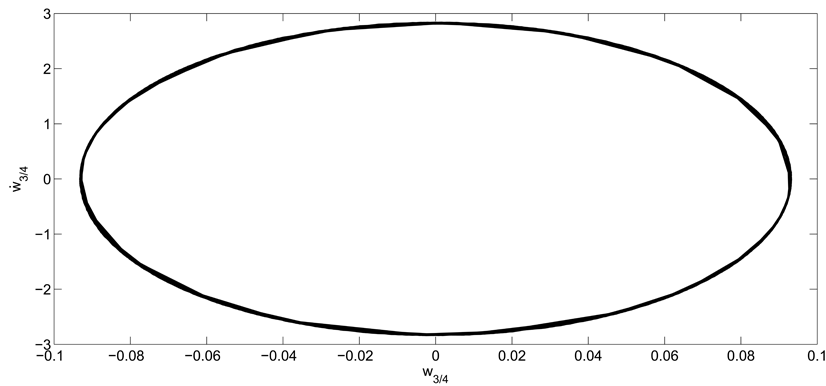
Figure 5.10: Simply harmonic limit cycle, $N = 0$, $\bar{q} = 344$.

about the 99.95% of the energy associated to the process. The application of the MAC between the significant POMs and the real and imaginary part of the critical orthogonalized eigenvectors is shown in Tab. 5.6. The MAC analysis, calculated by evaluating $\chi_{R_\perp}$ and $\chi_{I_\perp}$) and φ in 10 equispaced location on the panel, confirms a full equivalence between the significant POMs and the critical mode, in a similar way to what has been already presented for the discrete aeroelastic system (see Sec. 5.1.1, Tab. 5.3).

Non-simple-harmonic limit cycle-Case A

Let us consider another case given by the following parameter choice:

$$N = 3.5, \quad \theta_1 \quad = 1, \quad \theta_2 = 0, \quad \bar{q} \quad = 170.4. \tag{5.27}$$

The phase diagram at $x^*/a = 3/4$ of the free response is shown in Fig. 5.11, where a non-simple-harmonic nature appears to be evident. After a POD analysis one has that the first two POVs include again most of the energy, namely, the 99.93%. The MAC between the significant POMs and the orthogonalized real and imaginary part of the critical mode is shown in Tab. 5.7. Though the energy distribution is the same as the simply harmonic
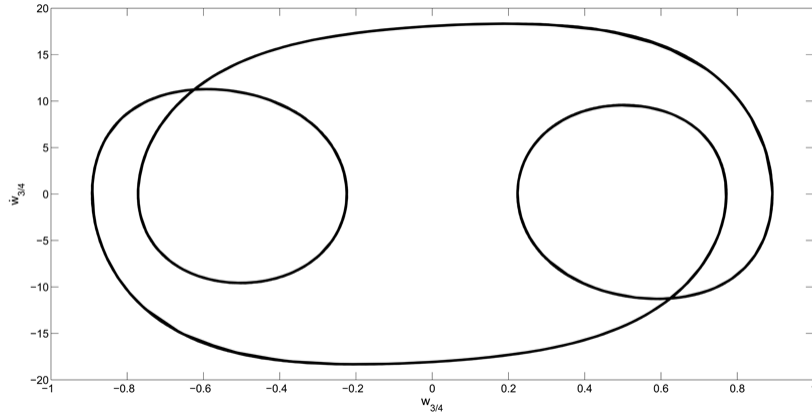
Figure 5.11: Pseudo harmonic limit cycle, $N = 3.5$, $\bar{q} = 170.4$.

	φ_1	φ_2
χ_R	0.0494	0.9504
χ_I	0.9499	0.0492

Table 5.7: MAC for the non-simply-harmonic case. Case A.

response, there is now a weakening of the correspondence between the significant POMs and the critical mode. Anyway, the cross-correspondence of the MAC coefficient in Tab. 5.7 shows that the subspace spanned by the χ_R and χ_I and the subspace spanned by φ_1 and φ_2 are practically coincident.

Non-simple-harmonic limit cycle-Case B

By increasing the value of the compression load, it is possible to observe that a real eigenvalue becomes positive. For the following set of the parameters:

$$N = 8.7, \quad \theta_1 \ = 1, \quad \theta_2 = 0, \quad \bar{q} \ = 170.4, \tag{5.28}$$

the linearized system presents a couple of complex conjugate eigenvalues with positive real part, and it is no longer the onset of a positive real eigenvalue. Figure 5.12 shows the phase diagram of the observed limit cycle. Regarding the energy distribution, the first two POVs collect only the 97.71% of the total energy, a result slightly but significantly different from the previously considered cases, that demands for a changed modal participation to the system dynamics. The correspondence between the critical mode and the first two POMs keeps to be still remarkable as the MAC distribution in Tab. 5.8 shows. For a slightly increased value of the compression load, $N = 9$, one obtains three system eigenvalues with positive real parts, *i.e.*, one pair of complex conjugate eigenvalues and a purely real eigenvalue. Figure
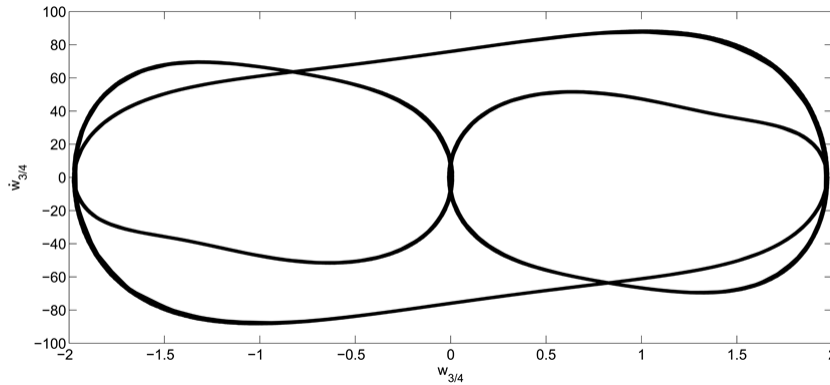
Figure 5.12: Pseudo harmonic limit cycle, $N = 8.7$, $\bar{q} = 170.4$.

	φ_1	φ_2
χ_R	0.1158	0.8644
χ_I	0.7904	0.1345

Table 5.8: MAC for the non-simple-harmonic case with a real pole marginally stable. Case B.

5.13 shows the phase space of the observed limit cycle, suggesting that the dimension of the center manifold should be increased from two to three, as also indicated by the first two POVs that collect about the 97.50%. It is worth to note that if one adds the contribution of
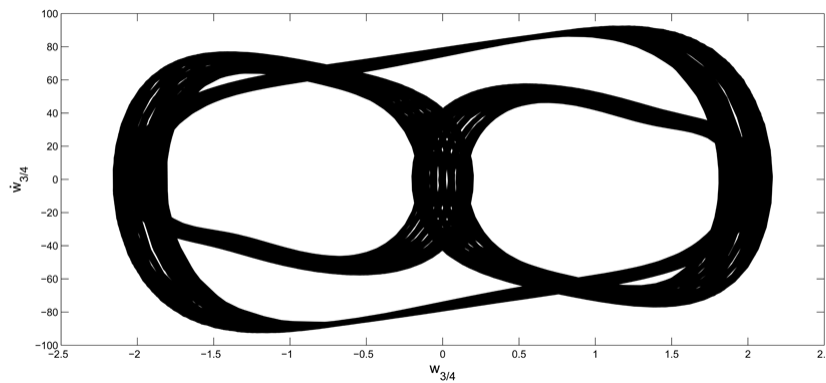
Figure 5.13: Pseudo harmonic limit cycle, $N = 9$, $\bar{q} = 170.4$.

the third eigenvalues, the percentage of the energy collected by the first three POMs raises to the 99.99%. Thus, it seems reasonable to conclude that the relevant POD basis is augmented with respect to the previous cases. Observing the MAC matrix in Tab. 5.9, it is apparent the relation between the POD significant basis (now composed by three orthogonal vectors) and the tangent space of the center manifold spanned by the three eigenfunctions $\chi^1_{R_\perp}$, $\chi^1_{I_\perp}$,

	φ_1	φ_2	φ_3
χ_R^1	0.0953	0.7775	0.1271
χ_I^1	0.8557	0.1336	0.0106
χ^2	0.1589	0.1265	0.7134

Table 5.9: MAC for the non-simple-harmonic case with a instable real pole. Case B.

and χ^2. Indeed, these results are still in line with the developed theory. In fact, the new included mode is real and almost orthogonal to the subspace associated to the unstable complex conjugate pair of modes. This implies that the evaluated POMs basis is still closely related to the eigenfunctions describing the tangent subspace at the equilibrium point.

Chaotic oscillation

The model representing the panel flutter can exhibit a chaotic behavior for special choices of the compression load and the flow speed. In particular, if one takes:

$$N = 4 \quad , \theta_1 \quad = 1, \quad \theta_2 = 0, \quad \bar{q} \quad = 120, \tag{5.29}$$

the response appears to be chaotic, as shown in Fig. 5.14, where the phase diagram of the oscillation at $x^*/a = 3/4$ is shown. In this case, the first two POVs collect about the 99.95%
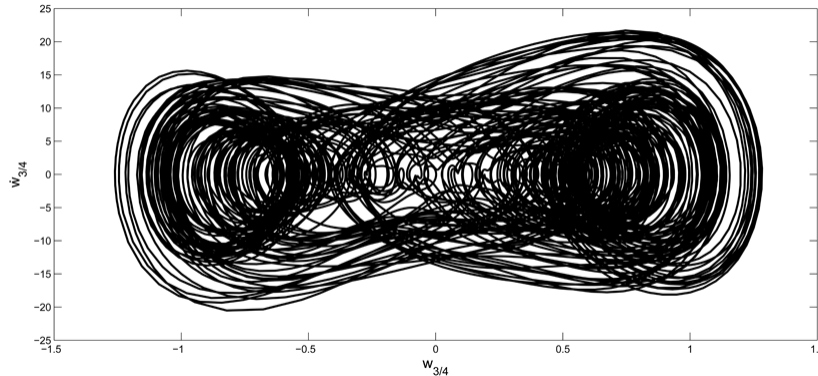
Figure 5.14: Chaotic solution, $N = 4$, $\bar{q} = 120$.

of the energy in a way very similar to the simply harmonic case. The MAC between the significant POD basis and the real and imaginary part of the critical orthogonalized eigenvectors is reported in Tab. 5.10 and shows that the POM basis and the critical mode are two distinct orthogonal basis in the same 2-dimensional subspace: however, in this case, they are not coincident as shown in the previous cases. Though lying on the same plane, the rotation between these orthogonal basis may be considered as a measure of complexity (or chaoticity)

	φ_1	φ_2
χ_R	0.1869	0.8130
χ_I	0.8129	0.1868

Table 5.10: MAC for the chaotic case.

of the nonlinear dynamics exhibited by the system (indeed, in this case the nonlinearities are relevant during all the period of oscillation and not only when the amplitude is high). Moreover, the energy distribution shows that there is not a new modal contribution to the response. Finally, starting form the MAC distribution of Tabs. 5.6, 5.7 and 5.10, one can conclude that the nonlinearities cause a rigid rotation in the same subspace between (φ_1, φ_2) with respect to $(\chi_{R_\perp}, \chi_{I_\perp})$. Indeed, the nonlinearities effect, if the modal contribution do not change (see Tabs. 5.8 and 5.9), is to rotate the POD significant basis with respect to the modal critical one. Moreover, observe that this is in agreement with the observations of Sec. 5.1.1 where a space-discrete system has been considered.

5.1.6   POD analysis in the neighborhood of a Hopf Bifurcation: concluding remarks

POD analysis have been performed and discussed for the free responses of linear and non-linear aeroelastic systems experiencing Hopf bifurcations and other more complex dynamic behaviors.

   In the neighborhood of an equilibrium solution, the POD analysis generates an orthogonal basis that has been analytically related to the invariant tangent subspaces. In order to show this issue, the eigenspaces related to the linearized problem around the equilibrium solution and corresponding to a complex conjugate pairs of eigenvalues, have been represented considering their real and imaginary parts in the state-space. Therefore, any generic pair of complex conjugate eigenvalues of the linearized system can be associated with the subspace of the state-space spanned by the real and imaginary parts of the corresponding complex eigenvector (namely, a plane). This has allowed to establish a straightforward relationship between the POMs and such a subspace. Specifically, for simply stable systems with only one pair of marginal (purely complex) eigenvalues it has been shown that, among the arbitrary complex constants multiplying the critical complex eigenvector, the only one able to make orthogonal its real and imaginary parts in the state-space makes also the resulting orthogonal vectors coincide with the correspondent POMs. Namely, such an orthogonal pair of vectors represents the POD energy-significant basis for linear and/or linearized systems in the aforementioned hypothesis.

Furthermore, starting from the previous issue and considering a singular perturbation approach around the equilibrium solution of a nonlinear system (Lie Transform Method) in a neighborhood of a Hopf bifurcation, it has been demonstrated that the energy content of the simply-harmonic limit-cycle response is embedded only in the first two POMs that are equivalent to (the real and imaginary part of) the critical mode. These results, initially obtained for finite-dimensional systems, have been extended to space-continuous systems as well.

These theoretical issues have been confirmed through numerical investigations of the free response of a typical aeroelastic section and of the free response of a panel in a supersonic flow undergone to a nonlinear kinematics.

As obtained via numerical simulation on nonlinear systems, once the level of nonlinearities increases, the POD (orthogonal) basis and the critical-mode (orthogonalized) basis do not coincide anymore but they differ for a rigid rotation in the same subspace. Therefore, this effect could be considered as an indirect and qualitative measure of the nonlinearities necessary to represent the response.

Moreover, in the case of a chaotic response, it has been numerically shown that the energetically significant POD basis does not change significatively with respect to non-chaotical regimes, *i.e.*, periodic motion with one or more spectrum frequencies. Nevertheless, though no more coincident, the POD basis and the orthogonalized eigenbasis span the same space.

5.2 Some issues about POD analysis in the neighborhood of a pitchfork bifurcation

The relation between the linearized modes, *i.e.*, the eigenfunction of the linear part of the structural operator, and the Proper Orthogonal Modes in the neighborhood of a Hopf bifurcation has been analyzed in Ref. [41]. In particular, the possibility to identify modes via POD analysis has been studied. In this Section, the relation between POD modes and linearized modes has been analyzed for a forced pitchfork bifurcation extending the cited results to a static bifurcation with a harmonic load. In this Section, the above observations are done considering a forced structural system experiencing a pitchfork bifurcation. In particular, the problem of a forced buckled beam presented in Sec. 3.1. It is relevant to observe the need to consider a forcing load in the considered case. Indeed, the considered bifurcation is static and the long-term behavior is represented by a new fixed point: to work efficiently the POD requires a persistent motion and sufficiently large time window.

Considering the results of Sec. 3.1 one can conclude that the forced response of the hinged beam can be represented as N oscillations along N different orthogonal directions

in the generalized displacement space. In particular, if we filter out the static part of the response the oscillations are about the origin. Then the displacement can be written as:

$$u(x,t) = \sum_{i,n=1}^{N} q_n(t) u_i^n \phi^i(x) \tag{5.30}$$

where the set of vectors $\mathbf{u}^n$ represent the eigenvectors of the linear part of the discretized system. The generalized displacements that are orthogonal can be chosen as the canonical base in $\mathbb{R}^N$:

$$u(x,t) = \sum_{i,n=1}^{N} q_n(t) e_i^n \phi^i(x) = \sum_{i,n=1}^{N} q_n(t) \delta_{ni} \phi^i(x) =$$
$$= \sum_{i=1}^{N} q_i(t) \phi^i(x) \tag{5.31}$$

The POD operator for space-continuous systems is:

$$\mathbf{P}(\cdot) = \int_V \mathsf{R}(\mathbf{x},\mathbf{y})(\cdot) dV \tag{5.32}$$

where:

$$\mathbf{R}(\mathbf{x},\mathbf{y}) = \lim_{T \to +\infty} \frac{1}{T} \int_0^T u(\mathbf{x},t) u(\mathbf{y},t) dt \tag{5.33}$$

is the correlation matrix and the eigenvectors and eigenvalues of the POD-operator give the Proper Orthogonal Modes (POMs) $\{\boldsymbol{\varphi}\}$ and Proper Orthogonal Values (POVs) $\{\sigma\}$ respectively:

$$\mathbf{P}(\boldsymbol{\varphi}) = \sigma \boldsymbol{\varphi} \tag{5.34}$$

The displacement in the neighborhood of a harmonically forced pitchfork bifurcation can be written as (filtering the static response):

$$u(x,t) = \epsilon\sqrt{\epsilon} \sum_{i=1}^{N} q_i(t) \phi^i(x) + o(\epsilon^{3/2}) \tag{5.35}$$

assuming the order interaction of above Sections. In the present case $q_i(t)$ are harmonic functions with the same frequency of the load component (see Sec. 3.1.5) in the direction of the i-th mode, then Eq. 5.33 becomes:

$$\mathbf{R}(x,y) = \lim_{T \to +\infty} \frac{1}{T} \int_0^T u(x,t) u(y,t) dt =$$
$$= \epsilon^3 \sum_{p,s=1}^{N} \alpha_{ps} \phi^s(x) \phi^p(y) + o(\epsilon^3) \tag{5.36}$$

If one supposes that every modal component of the load has a different frequency

$$\alpha_{ps} = 0 \Rightarrow p \neq s \tag{5.37}$$

$$\alpha_{ps} = \lim_{T \to +\infty} \frac{1}{T} \int_0^T q_p(t)q_s(t)dt \Rightarrow p = s \tag{5.38}$$

Then substituting, the Eqs. 5.36 in Eq. 5.33, we have:

$$\mathbf{R}(x,y) = \sum_{p=1}^{N} \alpha_p \phi^p(x)\phi^p(y) + o(\epsilon^3) \tag{5.39}$$

Therefore, from the definition of the space-continuous POD given by Eqs. 5.32 and 5.34 one obtains that, if the structural operator is self-adjoint (as in the considered examples), the POMs are the eigenfunctions of the structural operator and the POVs are the α_{pp} coefficients. Indeed, in the analyzed case, it is possible to state the equivalence between POD-modes (energetical behavior of the system) and eigenfuncions (intrinsic geometry of the analyzed problem). In general the correspondences between POD-modes and eigenfunctions is affected by the geometry of the problem. The POD analysis gives always a orthogonal basis, thus, it is not able to fit a non-orthogonal basis exactly but only in a minimum squares sense. This means that in the presence, for example, of a non self-adjoint structural operator it is not possible to find a direct correspondence except in a particular case as a permanent motion along a mode. A first example is a LCO arising after a Hopf bifurcation (example analyzed in Ref. [41]) or the same example of this paper but with a non self-adjoint structural operator with a dominant load component along only one mode. In this case Eq. 5.39 can be written as:

$$\mathbf{R}(x,y) \cong \alpha_{rr}\phi^r(x)\phi^r(y) \tag{5.40}$$

where r is fixed and corresponding to the dominant mode. From Equation 5.40 it is clear that the first POD-mode will correspond to the excited mode. The 1-mode approximation of the beam equation is included in the cases where Eq. 5.40 is valid. Indeed, the oscillation is possible only along the first structural mode (by hypothesis), which will correspond to the only one energetically significant (associated with non-zero energy) POD-mode.

Let us consider Eq. 3.5 approximated with four structural modes, and let us analyze the correlation between the POD energetically significant basis and the approximation modes. The POD is evaluated observing the time response at twenty points along the beam with a time of observation of 2000 dimensionless time units, filtering the transient phase. Of course, only the first four modes will be in general associated to non-zero energy. The comparison between POMs and structural modes is made using the Modal Assurance Criterion (MAC) defined in functional spaces as

$$MAC(\vartheta, \psi) = \frac{<\vartheta, \psi>^2}{<\vartheta, \vartheta><\psi, \psi>} \tag{5.41}$$

	φ_1	φ_2	φ_2	φ_2
χ_1	1.00	0.00	0.00	0.00
χ_2	0.00	1.00	0.00	0.00
χ_3	0.00	0.00	1.00	0.00
χ_4	0.00	0.00	0.00	1.00

Table 5.11: MAC between POMs and structural modes.

where $\vartheta(x)$ and $\psi(x)$ are bounded functions in the considered domain and $< \vartheta, \psi >:= \int_I \vartheta(x) \cdot \psi(x) \, dx..$

The assigned parameters, in this case, are:

$$N = 1.1 \quad \Omega_1 = 0.5 \quad \Omega_2 = 1 \quad \Omega_3 = 2 \quad \Omega_4 = 3 \quad \delta = 1$$

$$f_i = 1 \quad i = 1, ..., 4$$

The time response at $x = 0.75$ is shown in Fig. 5.15. Every load component has a different
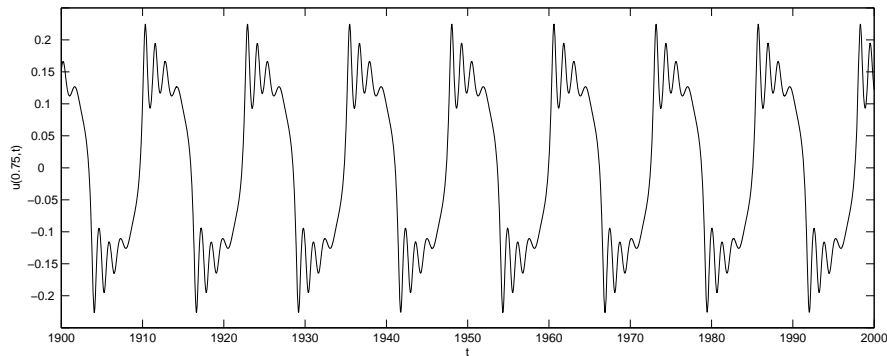
Figure 5.15: Time response of the vertical displacement at $x = 0.75$.

frequency, thus the matrix of the MACs between POD-modes and eigenmodes coincides, as expected, with the unit-matrix, see Tab. 5.11. The energy is effectively collected only by the first mode with the 99.998%.

Let us consider the case of a load with every components at the same frequency without a dominant one:

$$N = 1.1 \quad \Omega_1 = \Omega_2 = \Omega_3 = \Omega_4 = 1 \quad \delta = 1$$

$$f_i = 1 \quad i = 1, ..., 4$$

The time response at $x = 0.75$ is shown in Fig. 5.16. The first POD-mode still collects the larger part of the total energy (the 99.998%), but the shape of the correlation matrix is no
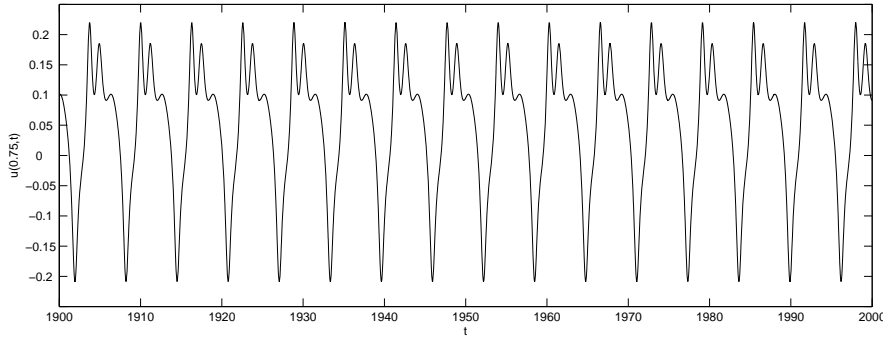
Figure 5.16: Time response of the vertical displacement at $x = 0.75$.

	φ_1	φ_2	φ_2	φ_2
χ_1	1.00	0.00	0.00	0.00
χ_2	0.00	0.97	0.02	0.00
χ_3	0.00	0.03	0.60	0.38
χ_4	0.00	0.00	0.38	0.62

Table 5.12: MAC between POMs and structural modes.

longer similar to the one of the unit matrix, see Tab. 5.12: In the two previous examples the energy distribution seems to be very similar. The amount of energy is the same for both the examples (the load is the same in magnitude) but it changes the correlation between the components of the response. Indeed, in the first example the POD operator (being the coefficients $\alpha_{nm} = \delta_{nm}$) is diagonal if expressed on the basis of the structural eigenfunctions whereas in the second one this is not true.

Finally, it is interesting to consider the same frequency for the components of the load when there is one of the components that is dominant in magnitude:

$$N = 1.1 \quad \Omega_1 = \Omega_2 = \Omega_3 = \Omega_4 = 1 \quad \delta = 1$$
$$f_1 = 100 \quad f_i = 1 \, i = 2, 3, 4$$

The time response at $x = 0.75$ is shown in Fig. 5.17. In this case the first POM collect practically the 100% of the energy. The correlation matrix is given in Table 5.13, which shows that the presence of a dominant load force the POD basis to coincide to the basis of the structural eigenfunction. In the first example, Table 5.11, it is the decorrelation between harmonic signals that causes the diagonal structure of the POD operator over the structural eigenbasis. Instead, in the latter example, see Table 5.13, the presence of a dominant component of the load 'forces' the correlation between the POD basis and the eigenfunction basis.
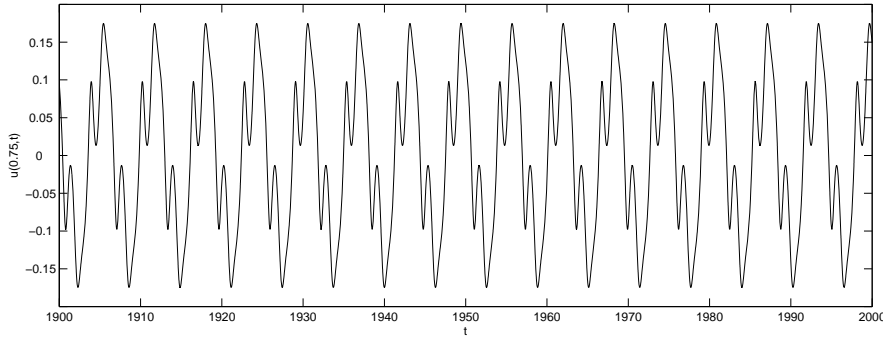
Figure 5.17: Time response of the vertical displacement at $x = 0.75$.

	φ_1	φ_2	φ_2	φ_2
χ_1	1.00	0.00	0.00	0.00
χ_2	0.00	0.97	0.03	0.00
χ_3	0.00	0.03	0.82	0.15
χ_4	0.00	0.00	0.15	0.85

Table 5.13: MAC between POMs and structural modes.

5.2.1 POD analysis in the neighborhood of a Pitchfork Bifurcation: concluding remarks

The behavior of the POD basis in the neighborhood of a harmonically forced static bifurcation has been analyzed comparing the Proper Orthogonal Modes and the modes of the linearized system. In particular, some conditions about the observability of linearized modes via Proper Orthogonal Decomposition are given. It has been demonstrated that in presence of a self-adjoint linear part of the partial differential operator and uncorrelated frequency of the modal load, the Proper Orthogonal Modes and the linear modes are coincident. Otherwise, the first Proper Orthogonal Mode associated with the larger amount of energy will tend to coincide with the mode with higher load, whereas the other Proper Orthogonal Modes will lay in the complementary orthogonal space of such functional direction.

5.3   POD vs Small divisors: general interpretation

The solution of the nonlinear problem has been written as an asympotic series of the form:

$$\mathsf{v} = \sqrt{\epsilon}\mathsf{v}_0 + \sqrt{\epsilon}\epsilon\mathsf{v}_1 \tag{5.42}$$

Let us consider a system experiencing a Hopf bifurcation, which gives the most interesting results for its complex observed behavior. Considering Eq. 2.22 and Eq. 4.58 one has:

$$\mathsf{v}(t) = \sqrt{\epsilon}(a(t)\mathsf{w} + a^*(t)\mathsf{w}^*) + \epsilon\sqrt{\epsilon}\mathsf{U}\left(\sum_{s=1}^{N} \frac{\eta_s}{\lambda_s - \lambda_n} + \sum_{p,q,r=1}^{N} \frac{\eta_p\eta_q\eta_r}{\lambda_p + \lambda_q + \lambda_r - \lambda_n}\right) \quad (5.43)$$

where U represents the matrix of eigenvectors of the linearized system and w the critical mode. Evaluating the correlation matrix from Eq. 5.43 one obtains an expansion series of the form

$$\check{\mathsf{R}} = \epsilon\mathsf{R}_1 + o(\epsilon) = 2\epsilon\left(-\frac{\beta_R}{\gamma_R}\right)[\mathsf{w}_{R_\perp} \otimes \mathsf{w}_{R_\perp} + \mathsf{w}_{I_\perp} \otimes \mathsf{w}_{I_\perp}] + o(\epsilon) \quad (5.44)$$

being the first term of expansion embedded in the space spanned by the critical eigenvectors. Moreover, in presence of a LCO the time-response is such that the first term of Eq. 5.44 is diagonal in the base $\{\mathsf{w}_{R_\perp}, \mathsf{w}_{I_\perp}\}$. If the response change its geometrical properties, for example, it is no longer represented by an ellipse in the phase-space, then also the structure of the matrix R_1 will change and in general it will be no longer diagonal in the basis $\{\mathsf{w}_{R_\perp}, \mathsf{w}_{I_\perp}\}$ assuming a general form:

$$\mathsf{R}_1 = c_1\mathsf{w}_{R_\perp} \otimes \mathsf{w}_{R_\perp} + c_2\mathsf{w}_{R_\perp} \otimes \mathsf{w}_{I_\perp} + c_3\mathsf{w}_{I_\perp} \otimes \mathsf{w}_{R_\perp} + c_4\mathsf{w}_{I_\perp} \otimes \mathsf{w}_{I_\perp} \quad (5.45)$$

The form of the first term of the solution in Eq. 5.42 depends on the zero divisor conditions which characterized the observed bifurcation (see for example Sec. 4.4). If some small divisors appears the time-response can be such that R_1 is no longer diagonal on the critical eigenvector basis: its eigenvectors associated to nonzero energy are a combination of $\{\mathsf{w}_{R_\perp}, \mathsf{w}_{I_\perp}\}$. This means that the rotation observed in the numerical experiments can be related to the necessity to include more resonance conditions (see Ref. [16]). Observing Eq. 5.43 it appears that if there is some mode activation, the embedding space of the first term of asympotic expansion increases and then the rank of correlation matrix: the number of energetically significant POD mode can be related to the number of active modes.

Conclusions

Il est aisé d'être *profond*:
on a qu'à se laisser submerger par ses propres tares.

Syllogismes de l'amertume, Emil Cioran.

The modern engineering must deal with applications of high complexity. Mathematical complexity means a large number of degrees of freedom and nonlinearities in the equations describing the process. Two levels of simplification can be considered in approaching this problem. The first level is a physical reduction where the real problem is represented by mathematical models that are treated in order to be studied and their solution computed. Here we can find all the discretization techniques like Galerkin projection or Finite Element Methods. The second level is a simplification of the original problem in order to study it in an easier way by adopting a reduced order model.

Two different methodologies to obtain reduced order models of nonlinear systems has been studied and compared:

1. Lie Transform Method.

2. Proper Orthogonal Decomposition.

The first approach, based on Normal Form Theory, consists in the identification of a transformation of coordinates which simplify the original problem by reducing the nonlinearities and identifying an essential dynamics (of a lower dimension with respect to the original one) driving the whole process. The second, Proper Orthogonal Decomposition, consists in a statistical analysis which determines an energetically significant subspace of the state space determining the most energetically significant basis to represent the studied problem (with lower dimension with respect to the original one).

The Lie Transform procedure has been used in order to obtain analytical solution for forced nonlinear systems experiencing bifurcation of equilibrium. In particular, the behavior of Von Kármán beam and finite panel has been studied. From such analytical solutions same issues about the physical interpretation of zero and small divisors have been discussed. The

small divisors are the main issues related to the integrability of nonlinear systems and there is no general theory about them considering nonconservative systems like the aeroelastic ones. In the present work, this problem is considered and some physical parameters are related to such conditions determining qualitatively what small means for a divisor relatively to a perturbation parameter. In particular, it has been identified what means *small* in terms of order of magnitude of the perturbation parameter. Moreover, it has been shown which parameters are relevant to evaluate in order to obtain a good assessment of the system behavior considering weakly loaded bifurcated systems. Indeed, it appears that if it is considered a weak forcing load the bifurcation process do not depend on the external loads. This comes from the fact that the hypotheses of weak load means that the forcing terms do not influence the eigengeometry of the studied systems and can be treated as a linear perturbation.

Using the analytical results obtained via Normal Form, the POD behavior in a neighborhood of a bifurcation has been studied. In particular, extending the previous results in literature, the equivalence between POD and linearized modes has been demonstrated in presence of a Hopf bifurcation. The POD generate an orthonormal basis collecting the largest part of the response energy. If, as in aeroelasticity, the modal basis (namely, the system invariant subspaces) is generally complex and orthogonality does not apply, it is necessary a different approach to relate the dynamical invariant objects, in order to extend the relationship between invariant subspace (modal basis) and POD. The proposed approach is based on the fact that complex modes can be equivalently represented by the subspace spanned by their real and imaginary part. Moreover, in nonlinear systems, the concept of linear modes is still locally significant in the neighborhood of an equilibrium point. Indeed, these modes represent the tangent spaces to the invariant manifolds. In presence of an equilibrium bifurcation, like a Hopf bifurcation, the solution can be locally built starting from the center invariant subspace. Moreover, some conditions of equivalence are addressed also in presence of static bifurcations with forcing loads. Finally, it has been observed that, if the modal contribution is fixed, increasing the nonlinearities in the response causes a rigid rotation between the critical eigenvector and the POD energetically significant POD basis. From the nature of the solution as predicted by Normal Form, this rigid rotation has been put in relation with the problem of small divisors.

Appendix A

Modal discretization and POD behavior

The Proper Orthogonal Decomposition (POD) provides a direct-energy based decomposition on the phase state-space of a dynamical system as shown in the previous Chapters. In particular, it has been demonstrated that (see Chapter 4 and 5 and Ref. [41]) the significant POD-basis coincides with the critical subspace , with only a small correction due to higher order terms. Moreover, it seems that once the nonlinearities contribution increases, the POD basis and the critical-mode (always represented by real and imaginary parts), that at the stability margin coincide, do not coincide anymore but they differ for a rigid rotation in the same space. This could be explained as an effect of the participation of the nonlinearities along the motion. Therefore, this effect could be considered as an indirect and qualitative measure of nonlinearity. The typical aeroelastic systems of a panel vibrating in a supersonic flow as in Chapter 5 has been considered. In this Appendix the attention is put on the energy distribution of the system response and, in particular, the effect of the modal approximation has been studied for the same examples considered in Chapter 5. Indeed, if the analysis is carried out through a modal approximation of the system the information content, the maximal embedding space of the system, is fixed a priori. The effect of this assumptions on the energy distribution on the state-space is analyzed by performing the POD on the system response directly calculated through a time/space integration of the corresponding PDE equations and than comparing the two energy distribution. Moreover, the energy distribution along POVs, i.e. the dimension of the energy-significant POD basis, is related to the modal participation.The same examples of Sec. 5.1.5 of Chapter 5 will be considered, and, in order to study the energy distribution, some of the geometrical results repeated.

A.1 Effect of modal approximation on energy distribution

The well-known mathematical model of a vibrating panel in a supersonic flow (see Ref. [6]) has been presented in Chapter 5 where the modal approximation has been used in order to obtain the time responses used to calculate the POD objects, namely, POMs and POVs. The modal discretized analysis is based on a strong assumption: the number of modal component N_M is fixed *a priori*. In the following Sec. A.2, some results of POD analysis and the energetic distribution obtained via modal representation and via direct space/time integration of the PDE model for the same cases considered in Chapter 5 will be compared. Being interested in a direct time integration of the PDE equation the PDE model presented in Sec. 5.1.5 is here written in an dimensionless form.

A.1.1 Panel dimensionless PDE model

The dimensional PDE model governing the nonlinear behavior of an axially loaded panel is, (Ref. [6]):

$$\rho_m \frac{\partial^2 v^*}{\partial t^2} + Lv^* + D\zeta \frac{\partial^5 v^*}{\partial t \partial^4 x^*} + N_{nl}(v^*)\frac{\partial^2 v^*}{\partial^2 x^*} + p(v^*) - p_\infty = 0 \tag{A.1}$$

$$\text{with} \quad L(\cdot) := D\frac{\partial^4(\cdot)}{\partial^4 x^*} + N_e \frac{\partial^2(\cdot)}{\partial^2 x^*}$$

where $v^*(x^*, t)$ is the vertical displacement, D is the bending stiffness, ζ is the viscoelastic damping coefficient, N_e is the compression load, and

$$N_{nl}(v^*) = -\frac{Eh}{2a}\int_0^a (\frac{\partial v^*}{\partial x^*})^2 dx^* \tag{A.2}$$

is the nonlinear load induced by the deformation, ρ_m is the material density of the panel, h is the panel thickness, a is the panel length and the differential pressure load $p(v^*) - p_\infty$ is given by

$$p(v^*) - p_\infty = \rho_\infty U_\infty^2 \left(\frac{\partial v^*}{\partial x^*} + \frac{\partial v^*}{\partial t}/U_\infty\right)/\sqrt{M_\infty^2 - 1} \tag{A.3}$$

where ρ_∞ e M_∞ are the air density and the Mach number of the undisturbed flow, respectively.

Defining the following dimensionless quantity and introducing the dimensionless time $\tau := t\left(D/\rho_m h a^4\right)^{1/2}$,

$$x := \frac{x}{a} \qquad\qquad v = \frac{v^*}{h}$$

$$\theta_1 := \sqrt{\rho_\infty a\bar{q}/\sqrt{M_\infty^2 - 1}\rho_m h} \qquad \theta_2 := \zeta\sqrt{D/\rho_m h a^4}$$

$$N := \frac{N_e a^2}{D} \qquad\qquad \bar{q} := \frac{\rho_\infty U_\infty^2 a^3}{D\sqrt{M_\infty^2 - 1}}$$

$$\Theta = 6(1 - \nu^2)$$

one obtains:

$$\frac{\partial^2 v}{\partial \tau^2} + \bar{L}v + \theta_2 \frac{\partial^5 v}{\partial t \partial x^4} - \Theta \left[\int_0^1 \left(\frac{\partial v}{\partial x} \right)^2 dx \right] \frac{\partial^2 v}{\partial x^2} + \theta_1 \frac{\partial v}{\partial \tau} + \bar{q} \frac{\partial v}{\partial x} = 0 \qquad \text{(A.4)}$$

$$\text{with} \quad \bar{L}(\cdot) := \frac{\partial^4(\cdot)}{\partial x^4} + N \frac{\partial^2(\cdot)}{\partial x^2}$$

It will presented a numerical scheme to obtain a direct calculation of the solution of Equation A.4 whereas the discretizzation process can be applied as in Sec. 5.1.5.

A.1.2   PDE model: direct time/space discretization integration

The Equation A.4 that governs the panel flutter behavior can be integrated through a finite-difference scheme with N_T time-discretization points and N_s space-discretization points. In particular, using a second order scheme in space and time (see Ref. [86]), one obtains the following system of algebraical equations (for the expression of the matrix see Appendix **A**):

$$\mathsf{A}\mathsf{v}^{n+1} + (\mathsf{B} + \mathsf{N}^n)\mathsf{v}^n + \mathsf{C}\mathsf{v}^{n-1} = 0 \qquad \text{(A.5)}$$

where the matrix N^n represent the nonlinear terms at the time $n\Delta\tau$ and $n = 1, ..., N_T$. Moreover,

$$\mathsf{v}_m^n = v_m^n = v(x_m, \tau_n) = v(m\Delta x, n\Delta\tau) \quad \text{m} = -1, ..., \text{Ns} + 2 \qquad \text{(A.6)}$$

Observing the Eq. A.6 it is evident the presence of two auxiliary nodes: $m = -1$ and $m = N_s + 2$. They are necessary because of the presence of the fourth partial derivative in the panel equation. Being the panel simply supported the second derivative of the solution is zero at $m = 0$ and $m = N_s + 1$: this boundary condition can be used to compute the value of the vertical displacement field in the auxiliary nodes. The direct integration gives the time histories in the discretization points that through the Eq. 4.7 can be used to compute the correlation matrix and than the POD analysis. The direct integration will provide a POD energetic analysis independent from the number of chosen modes to approximate the solution. The POD results performed on the modal solution will be compared with this to study how the modal approximation affects the energy distribution in the embedding space.

A.2   Numerical results

In Section A.2.1 the numerical scheme presented in Sec. A.1.2 is validated. In the Section A.2.2 POD analyses are conducted via both PDE direct and modal integration.

A.2.1   Numerical Scheme Validation

The relevant parameter,$\bar{q}$ and N, values of the system A.4 are those defining the stability margins. The static margin is not dependent on the discretization of the domanin and can be analytically evaluated: $N_{cr} = 1$ given the possibility to directly validate statically the linear part of numerical scheme. The dynamical margin depends on the aerodynamic terms in the Eq. A.4 that are not diagonalizable with the projection of the structural eigenfunction basis: the flutter dynamical pressure $\bar{q}_F$ depends on the number of modes used in the representation of the process and on the damping coefficients. We assume the following values for the damping coefficients:

$$\theta_1 = 1, \quad \theta_2 = 0 \tag{A.7}$$

Figure A.1 shows the comparison between the value of $\bar{q}_F$ computed through direct numerical integration and through modal one ($1/N_M$ is the convergence parameter depicted in abscissa). As it is possible to observe the modal analysis converges to the direct numerical validating the scheme also for the dynamical linear part. In particular $\bar{q}_F = 343.68$. To
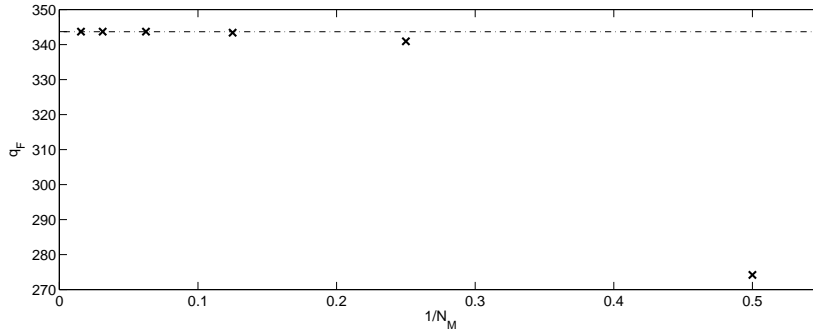

Figure A.1: Comparison between dynamical flutter pressure computed through direct $(- \cdot -)$ and modal integration $(\times)$

validate the number of integration point a static convergence analysis has been conducted and presented in Fig. A.2 where the buckling maximal displacement at $x = 0.5$ for a compressure load $N = 1/\pi^2 + 1$ is represented. Note that this analysis do not depend on the damping coefficients being static. This choice for N_p is assumed for all the following results. Figure A.2 shows the convergence of the scheme for $N_p \to \infty$. In particular, from Fig. A.2 we assume in the following $N_p = 100$ which is sufficiently high to give a good representation of the nonlinear terms.
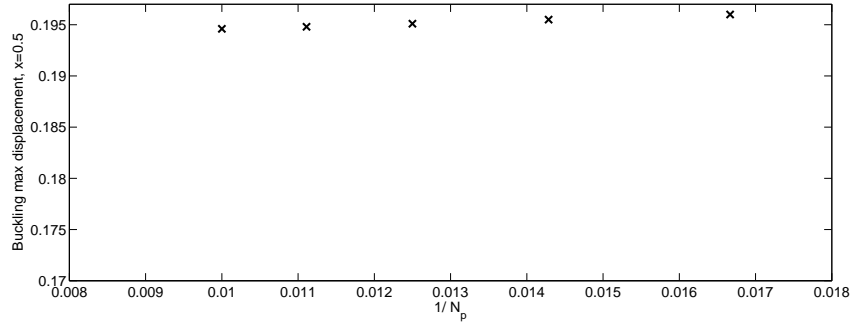
Figure A.2: Max buckling displacement vs number of discretization points

A.2.2   Simply harmonic (LCO) and multi-frequency solution

The same dynamical scenarios considered in Chapter 5 are considered. To study the effect of discretization on the energetic distribution is presented also the energy-distribution among POD obtained through the direct integration of Eq. A.4 with the time/space discretization scheme given by Eq. A.5.

Simple-harmonic limit cycle

Let us consider the case defined by the following choice of the parameters

$$N = 0, \quad \theta_1 = 1, \quad \theta_2 = 0, \quad \bar{q} = 344. \tag{A.8}$$

The system is beyond but very close its linear flutter stability margin and the presence of a limit cycle having a purely harmonic oscillation is shown in Fig. A.3 for $x^*/a = 3/4$. Considering the modal integration the first two POVs collect about the 99.95% of the energy
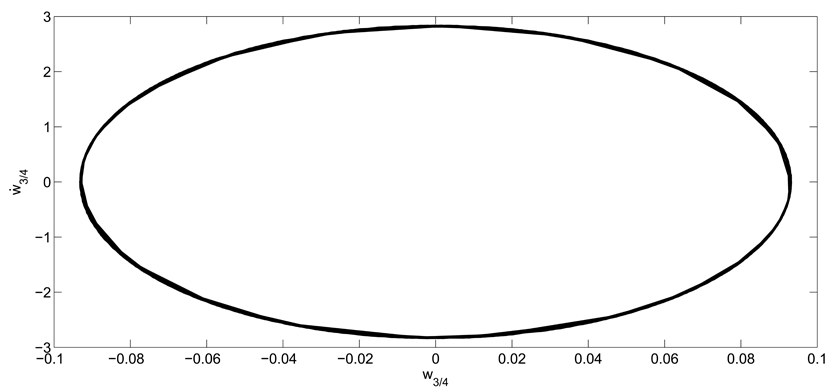

Figure A.3: Simply harmonic limit cycle, $N = 0$, $\bar{q} = 344$.

associated to the process in perfect agree with the POD obtained by direct PDE integration

which identifies practically the 100% of the energy content two POMs. As shown in Chapter 5 in the considered case the eigengeomtery is directly identified by the POD approach (see Tab. 5.6). This follows from the fact that the systems is practically at its stability margin and the our perturbation approach works optimally.

Non-simple-harmonic limit cycle-Case A

Let us consider:

$$N = 3.5, \quad \theta_1 = 1, \quad \theta_2 = 0, \quad \bar{q} = 170.4. \tag{A.9}$$

The phase diagram at $x^*/a = 3/4$ shows the non-simple-harmonic nature of the response. After a POD analysis one has that the first two POVs include again most of the energy,
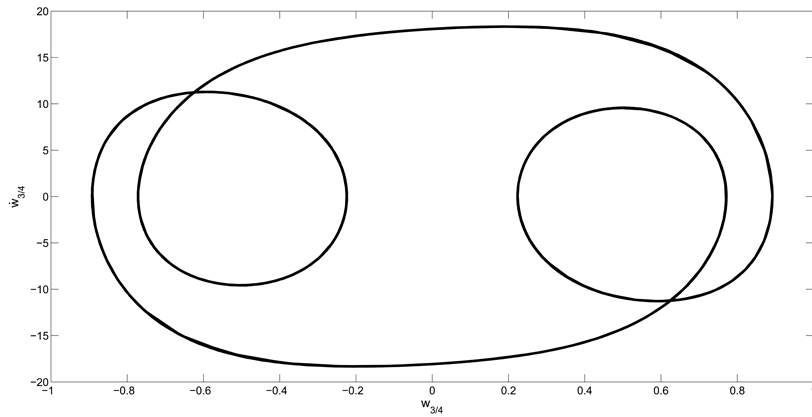

Figure A.4: Non-simple-harmonic limit cycle, $N = 3.5$, $\bar{q} = 170.4$.

namely, the 99.93% whereas the energy distribution obtained by the PDE direct integration shows that the first two POVs collect the 99.93% of the total energy, confirming the four-modes approximation analysis. It is worth to note that in this case the POMs identify only the subspace spanned by the critical eigenvector (see Chapter 5) and not the eigenvector itself.

Non-simple-harmonic limit cycle-Case B

If the compression load is increased it is possible to observe that a real eigenvalue becomes positive. For the following set of the parameters:

$$N = 8.7, \quad \theta_1 = 1, \quad \theta_2 = 0, \quad \bar{q} = 170.4, \tag{A.10}$$

the linearized system presents a couple of complex conjugated eigenvalues with positive real part and it is no longer the onset of a positive real eigenvalue. Figure A.5 shows the phase
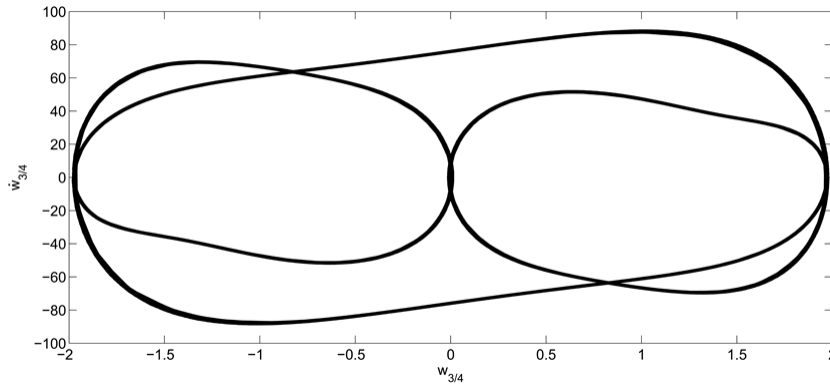
Figure A.5: Non-simple-harmonic limit cycle, $N = 8.7$, $\bar{q} = 170.4$.

diagram of the observed limit cycle. Regarding the energy distribution, the first two POVs collect only the 97.71% of the total energy, a result slightly but significantly different from the previous considered cases, that demands for a changed modal participation to the system dynamics. Considering the energetic distribution obtained through the POD analysis performed by the PDE direct integration one obtains that the first two POMs collect the 99.22% of the total energy whereas the first three modes collect the 99.98%. This results is quantitatively different from the one obtained considering the four-modes approximated system but qualitatively it agrees with the approximated one.

It is worth to point out that in this case, even if the energy distribution is similar the motion obtained by direct integration of the PDE model and by modal approximation are different at all. Figure A.6 shows a comparison by the two obtained solution: the four-modes
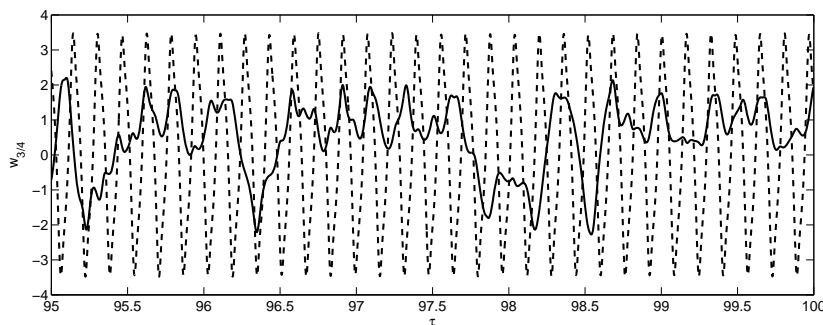

Figure A.6: - direct integration, – four-modes approximation

approximation is more regular, periodic, with respect to the exact solution. Thus, the four-modes approximation is able to give the right energy distribution in the state-space but it is not able to reconstruct the real complex behavior of the system: it is evident the filter

effect of such an approximation and, in the meanwhile, the well-know properties of the first modes to contain the great part of the energy signal. It is interesting to note that in this case even if the linearized systems predict only a dominant subspaces of dimension two the POD shows a greater driving dynamics. In this case we can conclude that the POD gives more information that the simple linearization of the systems equations.

<u>Chaotic oscillation</u>

The chaotic behavior for the following choice of the equations parameters

$$N = 4 \quad , \theta_1 \quad = 1, \quad \theta_2 = 0, \quad \bar{q} \quad = 120, \tag{A.11}$$

is shown in Fig. A.7 for $x^*/a = 3/4$ (response obtained with a four-modes numerical simulation). In this case, the first two POVs collect about the 99.95% of the energy in a way
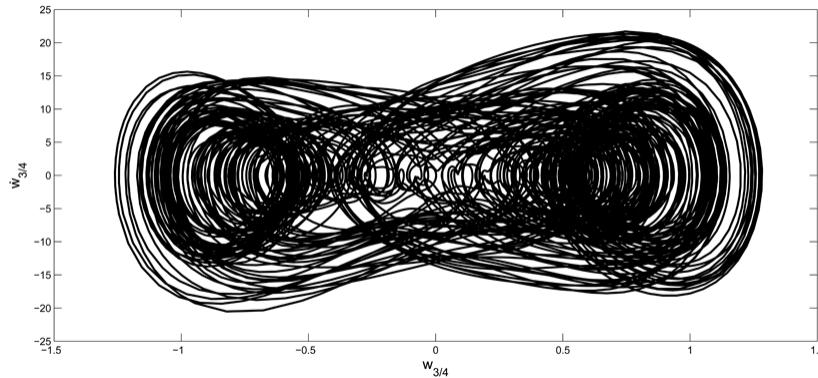

Figure A.7: Chaotic solution, $N = 4$, $\bar{q} = 120$.

very similar to the simply harmonic case. Considering now, the energetic distribution on the state-space following from the direct PDE integration, one obtains that the first two POMs collect the 99.96% of the total energy, a value practically equal to the one obtained by the modal representation of the process. This means that even within an approximation depending on N_M, the intrinsic dynamical properties are well described also with four modes. In particular, the shown comparison stress the relevance of the conclusion of Sec. 5.3. Indeed, also in the full PDE model the response is very well embedded in the tangent space to the Center Manifold underlining that the observed rigid rotation is due to small divisors acting in this subspace and not to some slave modes activation.

A.3 Concluding remarks

The relations between POD objects and intrinsic dynamical invariants has been studied through numerical experiments following a direct approach (finite difference PDE integra-

tion) and a modal approximated one. Using as starting point that the energetically significant POD basis has a dimension (the number of non-zero POVs) related to the nature of the bifurcation (the dimension of the center manifolds) and that the POMs are linked with the intrinsic geometry induced by the dynamics on the state-space, *i.e.*, with the eigenspaces and invariant manifold, the effect on the energy distribution on the state-space has been investigated comparing the one obtained by four-modes approximation and the one following from a POD analysis based on the direct integration of the POD model. This comparison showed that the four-modes approximation seems to be able to depict the qualitative intrinsic dynamics, *i.e.*, , the energetic distribution, even if the quantitative nature of the solution can not different from the exact one. Moreover, in some cases, it has been observed that POD approach can give deeper information about the local dynamics than the linearized systems stressing its useful contribution in the study of nonlinear systems.

Appendix B

Numerical Scheme Matrices

The matrices of Eq. A.5 are reported:

$$
A = \begin{bmatrix}
0 & 0 & \cdots & 0 \\
0 & 0 & \cdots & 0 \\
\mathsf{a} & 0 & \cdots & 0 \\
0 & \mathsf{a} & \cdots & 0 \\
\vdots & \vdots & \ddots & \vdots \\
0 & 0 & \cdots & \mathsf{a} \\
0 & 0 & \cdots & 0 \\
0 & 0 & \cdots & 0
\end{bmatrix}
\tag{B.1}
$$

where

$$
\mathsf{a} = \left\{ \begin{array}{ccccc}
\dfrac{\theta_2}{2\Delta t \Delta x^4} & -\dfrac{4\theta_2}{2\Delta t \Delta x^4} & \dfrac{1}{\Delta t^2} + \dfrac{6\theta_2}{2\Delta t \Delta x^4} + \dfrac{\theta_1}{2\Delta t} & -\dfrac{4\theta_2}{2\Delta t \Delta x^4} & \dfrac{\theta_2}{2\Delta t \Delta x^4}
\end{array} \right\}
\tag{B.2}
$$

$$
B = \begin{bmatrix}
0 & 0 & \cdots & 0 \\
0 & 0 & \cdots & 0 \\
\mathsf{b} & 0 & \cdots & 0 \\
0 & \mathsf{b} & \cdots & 0 \\
\vdots & \vdots & \ddots & \vdots \\
0 & 0 & \cdots & \mathsf{b} \\
0 & 0 & \cdots & 0 \\
0 & 0 & \cdots & 0
\end{bmatrix}
\tag{B.3}
$$

where

$$
\mathsf{b} = \left\{ \begin{array}{ccccc}
\dfrac{1}{\Delta x^4} & -\dfrac{4}{\Delta x^4} - \dfrac{N}{\Delta x^2} - \dfrac{\bar{q}}{2\Delta x} & -\dfrac{2}{\Delta t^2} + \dfrac{6}{\Delta x^4} + \dfrac{2N}{\Delta x^2} & -\dfrac{4}{\Delta x^4} - \dfrac{N}{\Delta x^2} + \dfrac{\bar{q}}{2\Delta x} & \dfrac{1}{\Delta x^4}
\end{array} \right\}
\tag{B.4}
$$

$$
C = \begin{bmatrix} 0 & 0 & \cdots & 0 \\ 0 & 0 & \cdots & 0 \\ c & 0 & \cdots & 0 \\ 0 & c & \cdots & 0 \\ \vdots & \vdots & \ddots & \vdots \\ 0 & 0 & \cdots & c \\ 0 & 0 & \cdots & 0 \\ 0 & 0 & \cdots & 0 \end{bmatrix}
\tag{B.5}
$$

where

$$
c = \left\{ \begin{array}{ccccccc} -\frac{\theta_2}{2\Delta t \Delta x^4} & \frac{4\theta_2}{2\Delta t \Delta x^4} & -\frac{1}{\Delta t^2} - \frac{6\theta_2}{2\Delta t \Delta x^4} - \frac{\theta_1}{2\Delta t} & \frac{4\theta_2}{2\Delta t \Delta x^4} & -\frac{\theta_2}{2\Delta t \Delta x^4} \end{array} \right\}
\tag{B.6}
$$

Moreover,

$$
N^n = (Su^n)^T (Su^n) D
\tag{B.7}
$$

with

$$
S = \begin{bmatrix} 0 & 0 & \cdots & 0 \\ 0 & 0 & \cdots & 0 \\ s & 0 & \cdots & 0 \\ 0 & s & \cdots & 0 \\ \vdots & \vdots & \ddots & \vdots \\ 0 & 0 & \cdots & s \\ 0 & 0 & \cdots & 0 \\ 0 & 0 & \cdots & 0 \end{bmatrix}
\tag{B.8}
$$

$$
s = \left\{ \begin{array}{ccccc} 0 & -\frac{1}{\Delta x} & 0 & \frac{1}{\Delta x} & 0 \end{array} \right\}
\tag{B.9}
$$

and

$$
D = \begin{bmatrix} 0 & 0 & \cdots & 0 \\ 0 & 0 & \cdots & 0 \\ d & 0 & \cdots & 0 \\ 0 & d & \cdots & 0 \\ \vdots & \vdots & \ddots & \vdots \\ 0 & 0 & \cdots & d \\ 0 & 0 & \cdots & 0 \\ 0 & 0 & \cdots & 0 \end{bmatrix}
\tag{B.10}
$$

with

$$\mathsf{d} = \left\{ \begin{array}{ccccc} 0 & \frac{1}{2\Delta x^2} & -\frac{2}{\Delta x^2} & \frac{1}{2\Delta x^2} & 0 \end{array} \right\} \tag{B.11}$$

Bibliography

[1] T. Von Karman. The Engineer Grapples with Nonlinear Problems. *Bulletin of the American Mathematical Society*, 46, 1940.

[2] E. H. Dowell. *A Modern Course in Aeroelasticity*. Kluwer Academic Publishers, Boston, 1995.

[3] E.H. Dowell, M. Ilgamov. *Studies in Nonlinear Aeroelasticity*. Springer-Verlag, 1988.

[4] Y.C. Fung. *An Introduction to the Theory of Aeroelasticity*. Wiley, 1955.

[5] Earl H. Dowell. Nonlinear oscillations of a fluttering plate. *AIAA Journal*, 1966.

[6] V.V. Bolotin. *Nonconservative Problems of the Theory of Elastic Stability*. The MacMillan Company, New York, 1963.

[7] F. Mastroddi L. Morino. Introduction to Theoretical Aeroelasticity for the Aircrat . Sapienza Università di Roma.

[8] R.Piva L.Morino. Boundary Integral Methods Theory and Applications. *Boundary Integral Methods Theory and Applications (Proceedings of the IABEM Symposium held in Rome)*, 1990.

[9] A.V. Balakrishnan. *Aeroelasticity. The Continuum Theory.* Springer, 2012.

[10] R.H. Scanlan, R. Rosenbaum. *Introduction to the Study of Aircraft Vibration and Flutter.* The Macmillan Company, 1951.

[11] R.L. bisplinghoff, H. Ashley, R.L. Halfman. *Aeroelasticity.* Addison-Wesley Publishing Comapny, 1955.

[12] R.L. bisplinghoff, H. Ashley. *Principles of Aeroelasticity.* John Wiley and Sons, 1962.

[13] H. Ashley, J. Dugundji, A.G. Rainey. *Notebook for Aeroelasticity.* AIAA Professional Seminar Series, 1969.

[14] A. Petre. *Theory of Aeroelasticity. Vol. I Statics.* Publishing House of the Academy of the Socialist Republic of Romania, 1966.

[15] A. Petre. *Theory of Aeroelasticity. Vol. II Dynamics.* Publishing House of the Academy of the Socialist Republic of Romania, 1966.

[16] L. Morino, F. Mastroddi, M. Cutroni. Lie transformation method for dynamical system having chaotic behavior. *Nonlinear Dynamics*, 7:403–4281, 1995.

[17] G. Iooss, M. Adelmeyer. *Topics in Bifurcation Theory and Applications.* World Scientific, 1992.

[18] C. Elphick, E. Tirapegui, M.E. Brachet, P. Coullet, G. Iooss. A simple global characterization for normal forms of singular vector fields. *Physica D 29, 95-127*, 1987.

[19] V.I. Arnold. *Geometrical Methods in the Theory of Ordinary Differential Equations.* Springer-Verlag, New York, Heidelberg, Berlin, 1982.

[20] P. Manneville. *Dissipative structures and weak turbulence.* Academic Press, 1990.

[21] A.H. Nayfeh. *Method of Normal Forms.* Wiley-Interscience Publication, 1993.

[22] M.A. Lieberman, A.J. Lichtenberg. *Regular and Stocastic Motion.* Springer, 1983.

[23] M. Tabor. *Chaos and Integrability in nonlinear dynamics.* Wiley, New York, 1989.

[24] A.A. Kamel. Perturbation Method in the Theory of Nonlinear Oscillations. *Celestial Mechanics*, 3:90–106, 1970.

[25] A. Deprit. Canonical transformation depending on a small parameter. *Celestial Mechanics*, 1:12–30, 1969.

[26] W. Gröbner. *Die Lie-Reihen und ihre Anwendungen.* Springer, 1960.

[27] A.H. Nayfeh. *Perturbation Methods.* Wiley-Interscience Publication, 1973.

[28] G. Sandri. The foundations of nonequilibrium statistical mechanics, i. *Annals of Physics, Volume 24*, 1963.

[29] J. Cole, J. Kevorkian. *Uniformly Valid Asymptotic Approximation for Certain Nonlinear Differential Equations.* Academic Press, 1963.

[30] A.H. Nayfeh. *Method Normal Forms.* J. Wiley, New York, 1993.

[31] D.S. Broomhead, G.P. King. Extracting qualitative dynamics from experimental data. *Physica D 20*, page 217Ű236, 1986.

[32] A.M. Albano, J. Muench, C. Schwartz. Singular-value decomposition and the grassberger-procaccia algorithm. *Physical Review*, A 38 (6):3017Ű3026, 1988.

[33] S. Volkwein K. Kunisch. Galerkin proper orthogonal decomposition methods for parabolic problems. *Numerische Mathematik*, 90(1):117–148, 2001.

[34] A. Dür. On the optimality of the discrete karhunen-loève expansion. *SIAM Journal of Control and Optimization*, 36(6):1937–1939, 1998.

[35] B.F. Feeny. On proper orthogonal coordinates as indicators of modal activity. *Journal of Sound and Vibration*, 255(5):805–817, 2002.

[36] J.L. Lumey P. Holmes and G. Berkooz. *Turbulence, Choerent Structures, Dynamical Systems and Symmetry*. Cambridge, New York, 1996.

[37] Z.W. Lin, K.H. Lee, P. Lu, S.P. Lim, Y.C. Liang. On the physical interpretation of proper orthogonal modes in vibrations. *Journal of Sound and Vibration*, 211(4):607–616, 1998.

[38] J.C. Golinval G. Kerschen. Physical interpretation of the proper orthogonal modes using the singular value decomposition. *Journal of Sound and Vibration*, Volume 249(Issue 5):849Ű865, 2002.

[39] U.Iemma, M.Diez, and L.Morino. An extended Karhunen-Loève decomposition for modal identification of inhomogeneous structures. *Journal of Vibration and Acoustics*, 1989.

[40] R.Kappagantu B.F.Feeny. On the physical interpretation of proper orthogonal modes in vibrations. *Journal of Sound and Vibrations*, Volume 211(Issue 4):607Ű616, 1998.

[41] F. Mastroddi, D. Dessi, M. Eugeni. Pod analysis for free response of linear and nonlinear marginally stable aeroelastic dynamical systems. *Journal of Fluid and Structures*, 33:85–108, 2012.

[42] J. Guckenheimer, P. Holmes. *Nonlinear Oscillations, Dynamical Systems, and Bifurcations of Vector Fields*. Springer-Verlag, applied mathematical sciences vol. 42 edition, 1983.

[43] M. W. Hirsch, S. Smale. *Differential equations, dynamical systems and linear algebra*. Academic Press, 1974.

[44] V.I. Arnold. *Ordinary Differential Equations*. M.I.T. Press, Cambridge, MA, 1973.

[45] P. Hartman. *Ordinary Differential Equations*. Wiley, New York, 1964.

[46] M. Braum. *Differential Equations and Their Apllications*. Springer-Verlag, New York, Heidelberg, Berlin, 1978.

[47] R.M. Rosenberg. The normal modes of nonlinear n-degree-of-freedom systems. *Journal of Applied Mechanics*, 29:7–14, 1962.

[48] S. Shaw C. Pierre, D. Jiang. Nonlinear normal modes and their application in structural dynamics. *Mathematical Problems in Engineering*, 26:1–15, 2006.

[49] A.F. Vakakis. Non-linear normal modes and their applications in vibration theory: an overview. *Mechanical Systems and Signal Processing*, 11(1):3–22, 1997.

[50] D. Dessi, M. Eugeni, F. Mastroddi. Slave-modes analysis beyond a bifurcating dynamical system. In *European Nonlinear Oscillation Conference*, 24-29 July 2011, Rome, Italy, 2011.

[51] D. Dessi, F. Mastroddi, L. Morino. Normal-form analysis of hopf bifurcations beyond the center-manifold approximation. In *Euromech Colloquium 457 on Nonlinear Normal Modes,*, St. Raphael, France, 2004.

[52] V.I. Arnold. *Catastroph Theory*. Springer, Berlin, Heildelberg, 1984.

[53] A.J. Lichtenberg, M.A. Lieberman. *Regular and Stocasic Motion*. Springer, New York, 1983.

[54] V.I. Arnold. *Mathematical Methods of Classical Mechanics*. Springer, New York, 1978.

[55] L.N. Virgin. *Vibration of Axially Loaded Structures*. Cambridge University Press, 2009.

[56] R.H. Plaut L.N. Virgin. Effect Of Axial Load On Forced Vibrations Of Beams. *Journal of Sound and Vibration*, 168:395–405, 1993.

[57] S.T. Santillan, L.N. Virgin, R.H. Plaut. Post-buckling and vibration of heavy beam on horizontal or inclined rigid foundation. *Journal of Applied Mechanics*, Volume 73:664–671, 2006.

[58] R.H. Plaut, L.N. Virgin. Vibration and snap-through of bent elastica strips subjected to end rotations. *Journal of Applied Mechanics*, Volume 76:041011, 2009.

[59] S. Neukirch, J. Frelat, A. Goriely, C. Maurini. Vibrations of post-buckled rods: The singular inextensible limit. *Journal of Sound and Vibrations*, Volume 331(3):704–720, 2012.

[60] A. Lazarus, J.T. Miller, P.M. Reis. Continuation of equilibria and stability of slender elastic rods using an asymptotic numerical method. *Journal of the Mech. and Phys. of solids*, Volume 61(8):1712–1736, 2013.

[61] W. Szemplinska-Stupnika, J. Bajkowski. The 1/2 subharmonic resonance and its transition to chaotic motion in a nonlinear oscillator. *International Journal of Non-Linear Mechanics*, 21:401–419, 1986.

[62] V. Pata M. Coti Zelati, C. Giorgi. Effect Of Axial Load On Forced Vibrations Of Beams. *Mathematical Models and Method in Applied Science*, 20:43–58, 2010.

[63] V. Pata M. Coti Zelati, C. Giorgi. On the extensible viscoelastic beam. *Nonlinearity*, 21:713–733, 2008.

[64] I. Bochicchio, C. Giorgi, E. Vuk. Steady states stability and exponential stability of an extensible thermoelastic system. *Communication to ISMAI Congress ISSN 1827-9015*, 3:232–244, 2009.

[65] A.H. Nayfeh, S.A. Emam. Exact solution and stability of postbuckling configurations of beams. *Nonlinear Dynamics*, 54:395–408, 2008.

[66] A. Eden, A. J. Milani. Exponential attractors for extensible beam equations. *Nonlinearity*, 6:457–479, 1993.

[67] C. Giorgi, M.G. Naso, V. Pata, M. Potomkin. Global attractors for the extensible thermoelastic beam system. *Journal of Differential Equations*, 246:3496–3517, 2009.

[68] Bochicchio, E. Vuk. Buckling and longterm dynamics of a nonlinear model for the extensible beami. *Mathematical and Computer Modelling*, 51:833–846, 2010.

[69] A. M. Abou-Rayan, A. H. Nayfeh, D. T. Mook, M. A. Nayfeh. Nonlinear response of a parametrically excited buckled beam. *Nonlinear Dynamics*, 4:499–525, 1993.

[70] A.H. Nayfeh. *Introduction to Perturbation Methods*. J. Wiley, New York, 1973.

[71] F. Pellicano, F. Mastroddi. Nonlinear dynamics of a beam on elastic foundation. *Nonlinear Dynamics*, 14:335–355, 1997.

[72] T. Smelova-Reynolds, E.H. Dowell. The role of higher modes in the chaotic motion of the buckled beam-part 2. *International Journal of Non-Linear Mechanics*, 31:941–950, 1996.

[73] T. Smelova-Reynolds, E.H. Dowell. The role of higher modes in the chaotic motion of the buckled beam-part 1. *International Journal of Non-Linear Mechanics*, 31:931–940, 1996.

[74] A. H.Nyfeh, B. Balachandran. *Applied Non Linear Dynamics*. Wiley-Interscience Publicatin, 1995.

[75] H. Ashley, G. Zartarian. Piston theory- a new aerodynamic tool for the aeroelastician. *Journal of the Aeronautical Sciences, Vol. 23, No. 12, 1109-1118.*, 1956.

[76] L. Smith, L. Morino. Stability analysis of nonlinear differential autonomous systemswith applications to flutter. *AIAA Journal, Vol. 14, 333Ű341*, 1976.

[77] V.V. Bolotin. Nonlinear flutter of plates and shells. *Inzhenerny Sbornik, Vol. 29, 55-75*, 1960.

[78] M. Eugeni, E.H. Dowell, F. Mastroddi. Post-buckling longterm dynamics of a forced nonlinear beam: perturbation and pod approaches. *In preparation*, 2013.

[79] H. Hotelling. Analysis of a complex of statistial vairables into principal components. *J. Edu. Psychology*, 1933.

[80] J.L. Lumey. *Stochastic Tools in Turbulence*. Academic Press, New York, 1970.

[81] L. Morino L. Smith. Stability analysis of nonlinear differential autonomous system with applications to flutter. *AIAA Journal*, 14(3), 1976.

[82] Theodore Theodorsen. General theory of aerodynamic instabiity and the mechanism of flutter. *NACA tecnichal Report*, Volume 46, 1936.

[83] F. Mastroddi D. Dessi. Limit-cycle stability reversal via singular perturbation and wing-flap flutter. *Journal of Fluids and Structures*, 19:765–783, 2004.

[84] F. Mastroddi L. Morino, D. Dessi. Limit-cycle stability reversal near a hopf bifurcation with aeroelastic applications. *Journal of Sound and Vibration*, 2002.

[85] J. Breakwell J.W. Edwards, H. Ashley. Unsteady Aerodynamic Modelling for Arbitrary Motions. *AIAA*, 17(4):365–374, 1979.

[86] J. C. Strikwerda. *Finite Difference and Partial Differential Equations*. Chapman and Hall/CRC, 1989.